Investigation of Parameters Affecting Copper Recovery from Brass Melting Dross

S. Basit, M. N. Sarıdede

Abstract—Metal amounts of copper based compounds in the various wastes have been recovered successfully by hydrometallurgical treatment methods in the literature. X-ray diffraction pattern of the brass melting slag demonstrate that it contains sufficient amount of recoverable copper. Recovery of copper from brass melting dross by sulfuric acid leaching and the effect of temperature and acid and oxidant concentration on recovery rate of copper have been investigated in this study. Experiments were performed in a temperature-controlled reactor in sulfuric acid solution in different molarities using solid liquid ratio of 100 g/L, with leaching time of 300 min. Temperature was changed between 25°C and 80°C and molarity was between 0.5 and 3M. The results obtained showed that temperature has important positive effect on recovery whereas it decreases with time. Also copper was recovered in larger amounts from brass dross in the presence of H_2O_2 as an oxidant according to the case that oxidant was not used.

Keywords—Brass dross, copper recovery, hydrogen peroxide, leaching.

I. INTRODUCTION

HIGH-grade copper ores decrease on the earth crust that new sources are needed to produce high purity copper which demand on it increases day by day. Slag amount and hence environmental problems also inevitably increases depending on copper extraction and consumption. Secondary sources mean wastes and residues containing copper sufficiently is a significant solution for the problem that the sector is facing. Both economy and environmental facts recovery of copper from secondary sources is very crucial [1], [2].

Several hydrometallurgical processes with or without oxidizing agent have been improved for base metal extraction from melting slags and drosses. The sulfuric acid leaching of copper and zinc from brass slag in the presence of hydrogen peroxide (H_2O_2) as oxidizing agent was studied by [1]. They reported that the zinc recovery was rapid and increased with increasing concentration of sulfuric acid. They also demonstrated chemically controlled shrinking core model in their work. Olubambi *et al* [2] studied to analyze the effect of hydrogen peroxide as an oxidant agent. They conducted the leaching of copper and zinc from sulfide ore in acidic media with sulfuric acid. It was determined that the leaching rate of

S. Basit is with the Metallurgical and Materials Engineering Department, Yildiz Technical University, Istanbul 34210 TURKEY (corresponding author to provide phone: +90-536-817-2431; fax: +90-212-383-4660 e-mail: sercanbst@gmail.com).

M.N. Sarıdede is with the Metallurgical and Materials Engineering Department, Yildiz Technical University, Istanbul 34210 TURKEY (e-mail: msaridede@gmail.com).

zinc and copper increased with increasing hydrogen peroxide concentration. Also they reported that because of promoting decomposition of hydrogen peroxide, stirring speed had a negative leaching effect. Researchers in [3] conducted leaching experiments to examine the effect of hydrogen peroxide utilizing high grade Nigerian chalcopyrite in the presence of sulfuric acid. They demonstrated that copper dissolution was enormously raised by adding hydrogen peroxide in sulfuric acid leaching. Hydrometallurgical treatment method to recycle base metals including copper, zinc and lead from dross of brass by using acidic and alkali leaching agents was enhanced by Nesbit and Xue [4]. A study was performed to recover copper from both copper smelter dust and copper smelter dross by hydrometallurgical process [5]. Researchers showed that nearly 80% of copper in the dross could be dissolved at 80°C with 200 kg/m³ sulfuric acid using 150 kg solid/m³ and 4-6 h leaching time in the oxidizing media. Besides the leaching of copper in the smelter dust was easier than dross. In reference [6], it is reported that hydrogen peroxide (H_2O_2) is stronger oxidizing agent than oxygen for sulfide minerals. It is noticed that while wet grinding was applied sphalerite begin to oxidize with H_2O_2. Therefore they suggest that H_2O_2 rather than oxygen is the main reason of oxidation.

According to another study [7], copper, zinc, and lead could be successfully recovered using different acid and alkali solutions by hydrometallurgical ways. This method used hydrogen peroxide to develop recovery of these metals. The study demonstrated that mineral acids could leach almost all metals in hot media. It is reported that the yield value of dissolution for the acidic media from large to small is nitric, hydrochloric and sulfuric acid respectively. According the analysis the maximum yield value of 98% was measured. Guy *et al.* [8] who researched leaching of complex ore contained copper, zinc and lead utilizing cupric chloride, suggested a selective method to recover copper, zinc and lead from brass waste. In the method while lead recovered insoluble salt form, zinc and copper was obtained as a soluble salt with leachates. High temperature pressure acid leaching was studied by Yunjiao *et al.* [9] as a method to facilitate slag cleaning and dissolution of base metals for economic extraction. Antonijevic *et al.* [10] studied kinetics of chalcopyrite in sulfuric acid and they reported that increasing the acid concentration resulted in increased chalcopyrite oxidation.

The aim of this study was to investigate recovery of copper from brass melting dross by sulfuric acid leaching and to study the effect of temperature and concentration of acid and oxidant on the recovery rate of copper.

II. EXPERIMENTAL

A. Materials

Brass dross used in this work is provided from a brass manufacturing plant in Turkey. Procedures applied to brass melting residues are shown in Fig.1. Fine fraction was used in this study. The chemical composition of brass dross determined by ICP-OES is given in Table I.
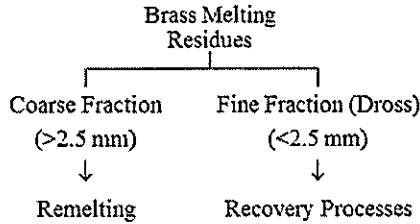
```
                  Brass Melting
                   Residues
        ┌─────────────────┴─────────────────┐
  Coarse Fraction              Fine Fraction (Dross)
    (>2.5 mm)                      (<2.5 mm)
        ↓                              ↓
    Remelting                  Recovery Processes
```

Fig. 1 Procedures applied to brass melting residues

Main components of the dross are zinc and copper. The other major elements are Si, Ca, and Al.

TABLE I
CHEMICAL COMPOSITION OF BRASS MELTING DROSS

Zn	Cu	Ca	Al	Mg	Na	K	S	Cl	Si
53.92	22	5.84	3.4	0.31	0.30	0.35	0.32	0.35	12.17

Mineralogical analysis of the sample was determined by XRD (Fig. 2). It can be seen from the peaks in Fig.2 that the dross sample consists of Cu, CuO, and ZnO substantially.
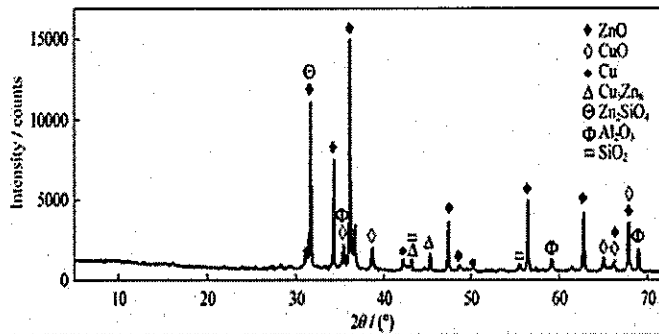

Fig. 2 XRD analysis of brass melting dross

B. Leaching

All leaching experiments were done in a temperature-controlled reactor (Fig. 3) with sulfuric acid leach solution of 1, 2, and 3M using solid liquid ratio of 100 g/L, during 300 min. Temperature was changed between 25°C and 80°C. H_2O_2 was used as an oxidant in all group of tests. Solution samples of 20 ml were taken and is filtered through filter paper for 10, 20, 30, 40, 60, 120, 180, 240, and 300 minute leaching time in each tests.
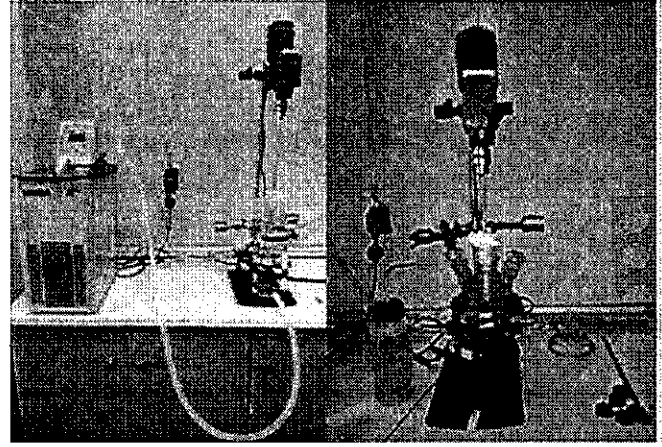

Fig. 3 Temperature-controlled reactor for leaching tests

After necessary dilutions, these samples were analyzed by atomic absorption spectrometry (AAS800). Recovery rate of copper was calculated according to (1).

$$Recovery\ rate\ of\ copper(\%) = \frac{Copper\ in\ the\ leach\ solution}{Copper\ in\ the\ dross} \times 100 \tag{1}$$

III. RESULTS AND DISCUSSION

A. Effect of temperature

In order to investigate the effect of temperature on the copper recovery rate, experiments were carried out under the conditions of 1 M sulfuric acid, 100 g/L solid liquid ratio and in the range of 10-300 minutes. The results was shown in Fig. 4. It can be seen from the figure that recovery rate of copper are relatively high at higher temperature. Lower recovery rates obtained at low temperature because of weaker reactivity of dross at low temperature. For instance, recovery of copper was 1.3% at 25°C whereas it reached to 20.3% at 80°C in 10 minutes. In addition, recovery rate of copper decreased by progressing time for 60 and 80°C but it remained constant for 25 and 40°C during dissolution time. Dissolution ratio under all temperature and time conditions could not reach noteworthy results because important amounts of copper exist in metallic state in the dross.

B. Effect of acid concentration with/without H_2O_2

The experiments in which the effect of sulfuric acid concentration on copper dissolution with and without hydrogen peroxide was carried out in the range of 1M-3M at fixed temperature of 60°C during 300 min. The results are showed in Fig. 5 and proved that higher molarities give lower recovery rates. The highest recovery rate (7.3%) was attained at 1M H_2SO_4 in 15 min. Besides, dissolution ratio of copper decreased from the beginning to the end of tests for all test groups.
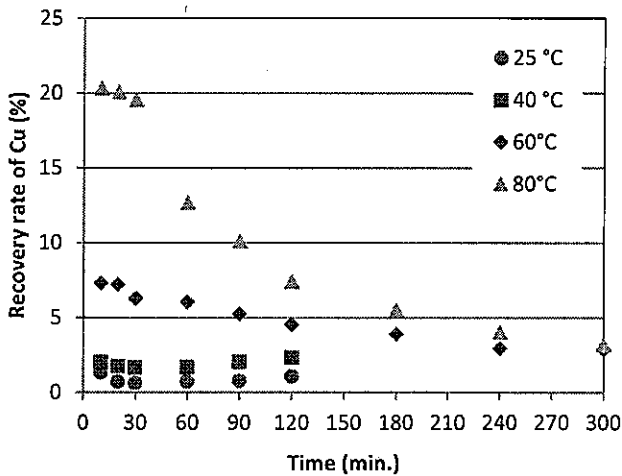
Fig. 4 Effect of temperature on the recovery rate of copper

It can be said that leaching of copper in high acidity medium causes an increase in the viscosity of the solution thus hinders the extraction process [1]. Possible formation of silica gel at the same time causes the increase in viscosity and thereby decrease in the dissolution rate [11].
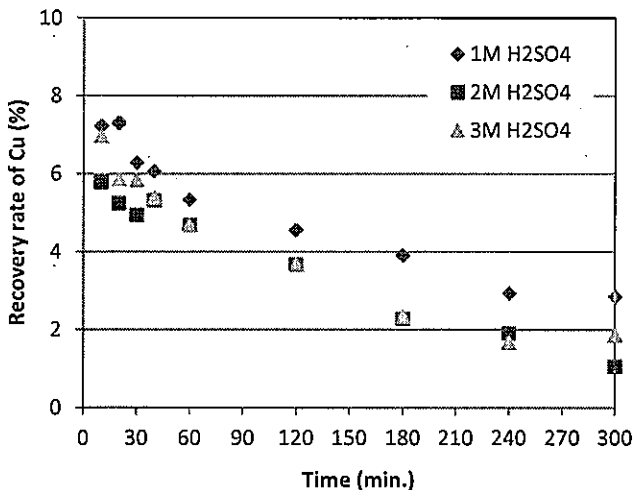

Fig. 5 Effect of sulfuric acid concentration on the recovery rate of copper

Addition of 1M hydrogen peroxide (H_2O_2) in various molarities into the sulfuric acid solution (0.5M - 3M) led to remarkable increase in the dissolution of copper (Fig. 6). Maximum recovery rate of copper of 32.2% was obtained in 3M H_2SO_4 concentration in these tests. H_2O_2 is more effective when it is added to higher molarities of sulfuric acid. Since H_2O_2 is strong oxidant, it oxides metallic copper causing to pass into the solution. Similar to previous experiments, the recovery values decreased by time from the first 10 minutes but there was no sharp decrease in the recovery values throughout the test period. It is estimated that decreasing of dissolution rate of copper by time is because of zinc in the solution which precipitate the copper [12].
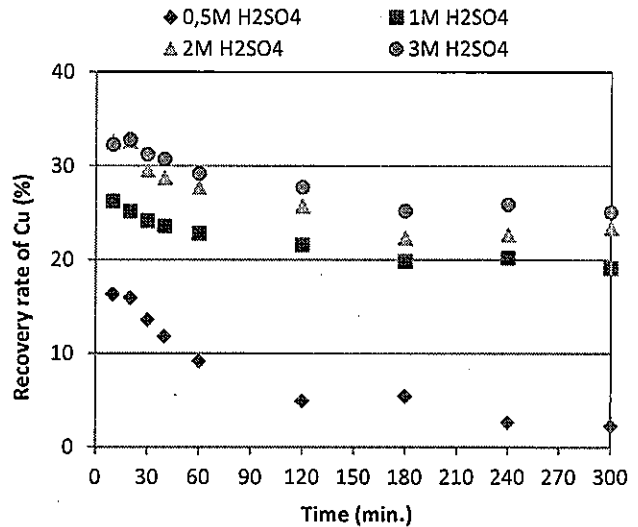

Fig. 6 Effect of sulfuric acid concentration on the recovery rate of copper (H_2O_2: 1M, T: 60°C)

IV. CONCLUSION

Based on the results of this study, the following conclusions can be presented:

Copper solubility is directly related to temperature. The recovery rate of copper is increased with increasing temperature.

Recovery rate of copper is inversely proportion with concentration of solution. Possible reason for this is the increasing viscosity of solution when the copper dissolution raises.

H_2O_2 is an effective oxidant causing to increase in copper dissolution rate significantly.

ACKNOWLEDGMENT

REFERENCES

[1] I. M. Ahmed, A.A. Nayl, J.A. Daoud, "Leaching and recovery of zinc and copper from brass slag by sulfuric acid," Journal of Saudi Chemical Society (in press), http://dx.doi.org/10.1016/j.jscs. 2012.11.003

[2] P. A. Olubambi, J.O. Borode, S. Ndlovu, "Sulphuric acid leaching of zinc and copper from Nigerian Complex Sulphide Ore in the presence of hydrogenperoxide," The Journal of The Southern African Institute of Mining and Metallurgy, 106, 2006, pp. 765-770.

[3] A. O. Adebayo, K.O. Ipinmoroti, O.O. Ajayi, "Dissolution Kinetics of chalcopyrite with Hydrogen peroxidein sulphuric acid medium," Chemical and Biochemical Engineering Quarterly, vol, 17, no.3, 2003, pp. 213-218.

[4] C. Nesbit, S. Xue, "Recycling of Base Metals from Metal Wastes of Brass Foundries," Treatment and Minimization of Heavy Metal-containing Wastes Conf., Las Vegas, NV, USA, 12-16 February 1995, pp. 43-56.

[5] T. Shibaski, N. Hasegawa, "Combined Hydrometallurgical Treatment of Copper Smelter Dust and Lead Smelter Copper Dross," Hydrometallurgy, 30, 1992, pp.45-57

[6] A. J Nooshabadi, H. R. Kota, *"Formation of hydrogen peroxide by sphalerite"* International Journal of Mineral Processing, 125, 2013, pp. 78-85.

[7] S. M. Abdel Baser, M.A Rabah, *"Hydrometallurgical recovery of metal values from brass melting slag,"* Hydrometallurgy 53, 1999, pp. 31-44.

[8] S. Guy, C. P. Broadbent, G. J. Lawson, *"Cupric Chloride Leaching of Complex Copper/Zinc/Lead Ore"* Hydrometallurgy, 10, 1983, pp. 243-255

[9] L. Yunjiao, I. Predery, V.G. Papangelakis, *"Cleaning of waste smelter slags and recovery of valuable metals by pressure oxidative leaching,"* J. Hazard. Mater. 152, pp. 607-615.

[10] M. M. Antonijevic, Z.D. Jankoviç, M.D. Dimirijevic, *"Kinetics of chalcopyrite dissolution by hydrogen peroxide in sulphuric acid,"* Hydrometallurgy 71, 2004, pp. 329-334.

[11] A. N. Banza, E. Gock, K. Kongolo, *"Base metals recovery from copper smelter slag by oxidizing leaching and solvent extraction,"* Hydrometallurgy 67, 2002, pp. 63-69.

[12] S. Aydoğan, *"Dissolution kinetics of sphalerite with hydrogen peroxide in sulphuric acid medium,"* Chemical Engineering Journal 123, 2006, pp. 65–70.

S. Basit was born in Turkey in 1988. He started his undergraduate education at Karadeniz Technical University (KTU), Trabzon, Turkey in 2007. He transferred from KTU to Yildiz Technical University (YTU) in 2008 and he completed his BSc in YTU, Istanbul, Turkey in 2012. Same year he began his master of science. His department is Metallurgical and Materials Engineering. He works in YTU on behalf of Ahi Evran University, Kırşehir, Turkey as research assistant and he continue MSc in this university. He interested in hydrometallurgy and separation science.

Grid Tied Photovoltaic Power on School Roof

Yeong-cheng Wang, Jin-Yinn Wang, Ming-Shan Lin, Jian-Li Dong

Abstract—To universalize the adoption of sustainable energy, the R.O.C. government encourages public buildings to introduce the PV power station on the building roof. Whereas most old buildings did not include the considerations of photovoltaic (PV) power facilities in the design phase. Several factors affect the PV electricity output, temperature is the key one, different PV technologies have different temperature coefficients. Other factors like PV panel azimuth, panel inclination from the horizontal plane, and row to row distance of PV arrays, mix up in the beginning of system design. The goal of his work is to maximize the annual energy output of a roof mount PV system. Tables to simplify the design work are developed, the results can be used for engineering project quote directly.

Keywords—Optimal inclination, array azimuth, annual output.

I. INTRODUCTION

IN order to promote the energy conservation buildings in Taiwan area, the R.O.C. government awards the intelligent building logo to those buildings satisfying several reviewing indices of building automation. One index for labeling the grade of intelligence is the sustainable energy harvest. Meanwhile, to facilitate the introduction of this labeling activity, public buildings are encouraged to apply for the logo of intelligent building in the first phase. The photovoltaic electricity is of course a sustainable energy, vast area is the feature of providing photovoltaic power, the roof of school classroom is a better site than those ordinary condominium top, because of large roof area available. The Jian-Gong elementary school, a public school, latitude 24.8°N, longitude 121.0°E, UTC/GMT +8, located in suburban Xin-Zhu City with broad open neighborhood has the geographic advantage for deploying PV panels to generate electricity. There are three buildings are eligible to mount PV panels, they all have the features of being tall and free of shade. The first thing for an engineering proposal searching for city government financial support is the cost estimation. While, the major components of PV power system are PV modules and inverters, here a simple procedure to conceptually estimate the numbers of system component is proposed. The best azimuth to arrange a PV array in Northern Hemisphere, on the basis of maximum annual energy output, is facing south. However, the roof of buildings may sit in different azimuths referring to south, may be irregular in shape for laying

Yeong-cheng Wang is with the Vanung University, Zhong-Li City, Taiwan 32061, R.O.C. (corresponding author, phone: +886-3-451-5811; fax: +886-3-462-1348; e-mail: starwang@mail.vnu.edu.tw).

Jin-Yinn Wang is with the Vanung University, Zhong-Li City, Taiwan 32061, R.O.C. (e-mail: jywang@mail.vnu.edu.tw).

Ming-Shan Lin and Jian-Li Dong are with the Bureau of Standards, Metrology & Inspection, M.O.E.A., R.O.C. (e-mail: ms.lin@bsmi.gov.tw, jianli.dong@bsmi.gov.tw).

This work was made possible in part by the BSMI under Contract No. 1D151031201-117, grant from BSMI, M.O.E.A., R.O.C.

down the PV panels, and may not be flat but with various roof slopes, several tables are developed in this work to make the design simpler, to break the complicated calculations into parts.

II. SYSTEM DESIGN

Quite commonly seen specifications of a single PV module are listed in Table I [1]. A 20kW inverter can accommodate several modules connected in series, even the better, it is very easy to find a manufacturer carrying 20kW inverter in the Internet. As a result, the 240Wp PV modules match with the 20kW inverter very well.

TABLE I
TYPICAL SPECIFICATIONS OF A POLYCRYSTALLINE PV MODULE

Power Output (W)	Vmpp (V)	Impp (A)	Temp Coef. of Pmpp	Dimensions(mm) H × W × D
240	30.2	7.96	-0.45%	1650 × 992 × 40

Having the specifications of those two components, an initial suggestion of the PV power system is portrayed in Fig. 1. Six serial strings of fourteen modules are fed into the inverter, the AC output of the inverter is 380V which is widely used in local substation. The inverter is chosen to be three phase AC output, for the full loaded case, the inverter output current is

$$I_{3\phi} = \frac{(14 \times 240W) \times 75\% \times 6}{380V \times \sqrt{3}} = 23A \tag{1}$$
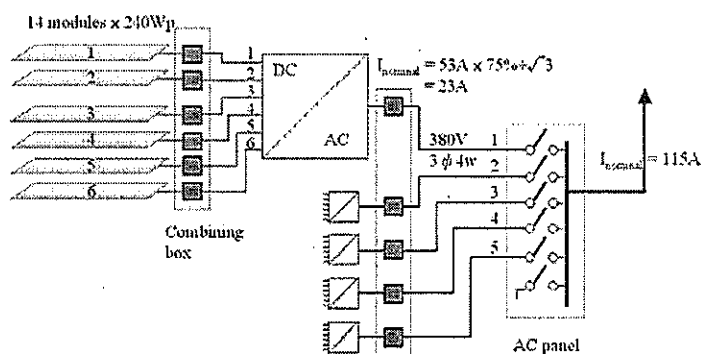
where a system loss of 1-75% = 25% is assumed.

Fig. 1 The initial design of the PV power generating system.

A. Available Roof Area

The roof plan of the first building, as an example, is shown in Fig. 2. The top view shows the roof has two different zones, one is made of concrete and the other is made of standing seam, summing up the area separately reserves the capability for different panel installing schemes. The available area in the irregular roof is marked piece by piece and then summed up in the second line of Table II. The available area of standing seam roof in Table II is the net idle area of Fig. 2 by deducting the

roof area from skylight, HVAC(Heating, Ventilation and Air Conditioning), access walkway, gutter, and the zone outside the fall arrest. Of course, site survey helps the calculations a lot if necessary.
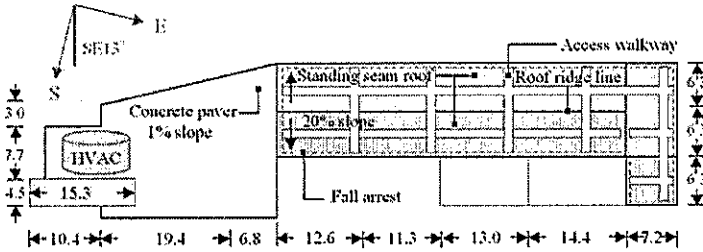

Fig. 2 Top view of the classroom building no. 1, the unit is meter.

The total available installation roof area for the three buildings is thus summarized Table II.

TABLE II
THE AREA AVAILABLE FOR PANEL DEPLOYMENT

Building	Roof area (m^2)	Available standing seam roof (m^2)	Available concrete roof (m^2)
No. 1	1511.35	337.63	495.94
No. 2	1486.03	0	1221.48
No. 3	878.4	444.04	0

The electricity output of the photovoltaic power system depends on a variety of factors, the azimuth of the PV arrays, the inclination of the PV panels, the arrangement of PV arrays, and the material that the PV cells are made of. Some factors affect the system output are discussed in the followings:

B. Temperature

The operating temperature of a solar cell erected in an angle steeper than 10° is assumed to be 46°C(115°F), or it is at its nominal operating cell temperature(NOCT). On the other hand, the operating temperature of solar cell in plane with the roof surface is assumed to be 55°C(131°F) due to its poor air convection for heat dissipating. The typical temperature coefficient of output power is -0.2%/K for thin film technology, -0.405%/K for polycrystalline module, and -0.45%/K for monocrystalline module, respectively. Table III illustrates the temperature effect of the module power output.

TABLE III
TEMPERATURE LOSS

	Thin film -0.2%/K	Poly-crystalline -0.405%/K	Mono-crystalline -0.45%/K
Panel temperature			
55°C (in plane with the roof surface)	6.0% loss	12.2% loss	13.5% loss
46°C (inclined at an steeper angle)	4.2% loss	8.5% loss	9.5% loss

C. Miscellaneous Integration Loss

Some other factors that reduce the solar system output are [2] :

(a) Production tolerance: as a usual, +/-5% of the module rating power is assumed, to be conservative, the lower bound of the output is used as a rating power, discount the ideal output by 95%, or 5% loss.

(b) Dirt and dust: a typical annual dust reduction factor is 93%, or 7% power loss. In a windy city like Xin-Zhu, the PV panels need to be cleaned more frequently.

(c) Module mismatch and wiring losses:' a reasonable reduction factor is 95%, or 5% loss.

(d) DC to AC conversion losses: In actual field condition, measured conversion efficiency is 90% to 94%, a good compromise is 92%, or we can say 8% loss.

Therefore, the ratio of AC power delivered to the utility network is

$$\eta_{sys} = \text{(temperature residue)} \times 95\% \times 93\% \times 95\% \times 92\%$$
$$= \text{(temperature residue)} \times 0.77 \quad (2)$$

The realistic expectation of the system output for different module technologies are listed in Table IV

TABLE IV
SYSTEM EFFICIENCY FOR DIFFERENT INCLINATIONS

	Thin film -0.2%/K	Poly-crystalline -0.405%/K	Mono-crystalline -0.45%/K
Panel temperature			
55°C (in plane with the roof surface)	72.6%	67.8%	66.8%
46°C (inclined at an steeper angle)	74.0%	70.6%	69.9%
Optical-electrical conversion rate	9.0%	15.7 %	16.7%

D. Panel Azimuth

To maximize the annual energy output the best azimuth in Northern Hemisphere of PV arrays is south facing. However, the building does not align with this north-south line. As a result, the PV panels can be arranged in either directing to north-south line, as shown in Fig 3(a), or parallel to roof corrugating lines, as shown in Fig. 3(b).
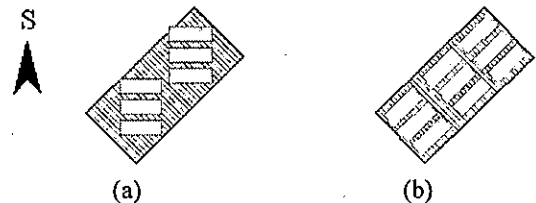

Fig. 3 PV panels are arranged in (a) aligned to north-south line; (b) parallel to roof corrugating lines.

The first approach depicted in Fig. 3(a) wastes at least ten percent available area for PV deployment, it is not compatible with the orientations of HVAC equipment as well as skylight, is thus difficult to lay down the maintenance path, furthermore, lacks of aesthetics. A numerical simulation shows that the PV facing due South outperforms the PV arrangement of paralleling to roof line, SW 45°, by a factor of 102%, but, don't forget, the available area for PV deploying may lose at least 10%, it does not compensate the azimuth gain. The arranging

approach of Fig. 3(a) is thus discarded and the PV arrays along the roof corrugating line is assumed in this work.

E. Panel Inclination

The PV panels can be in plane with the roof surface, or tilted to an optimal radiation receiving angle which is dependent on the latitude of the project site and the array azimuth, the simulation results with the help of RETScreen® are shown in Table V.

TABLE V
THE OPTIMAL INCLINATION FOR PANEL AT LATITUDE 24°N

Building azimuth	SE25°	SE13°	South	SW45°
Optimal panel inclination	22°	22°	23°	19°
Average peak solar hour (PSH), h/day	5.39	5.42	5.43	5.30
Roof utilization rate	58.75%	58.75%	55.74%	59.76%

The best radiation receiving period over a whole day is 9:00 to 15:00[3], the array should be arranged in such a way that the panel suffers no shade in this period. Fig. 4 shows two possible panel arrangements on the roof, 4(a) is horizontally fixed, while 3(b) is tilted to the optimal inclination. The panel arrangement along the horizontal plane leaves no problem of front-back light blocking, as shown in Fig. 4(a), to add 20% access space to the roof[2], the roof utilization rate is 1/120% = 83.3%. For a SW 45° oriented panel, the optimal inclination angle shown in column 5, Table V, is 19°, applying the light ray coming from West at 15:00, winter solstice, or 24.1°[4], to Fig. 4(b), the roof utilization rate is apparently reduced to 59.76%, the unused area is just enough for the access path and reserved for future maintenance use. The calculations show that Fig. 4(b) is preferred due to its higher electricity output on a unit PV area, which is explained in the next section.
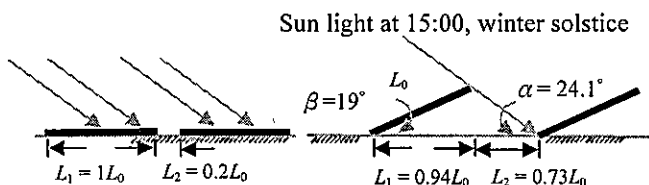
Sun light at 15:00, winter solstice

Fig. 4 PV panels are (a) in plane with the roof surface, 20% area is added for the access space to the system, or 83.3% roof utilization rate; (b) tilted to the optimal inclination, 19°, L1 + L2 = 1.67L0, indicates a 59.76% roof utilization rate.

III. RESULTS AND DISCUSSIONS

The annual energy output of the concrete part of building 1 under two different panel arranging approaches, see Fig. 4, is given in TABLE VI. The results of Fig. 4(a) are shown in row two of the Table, the data are in contrast with the third row, Fig. 4(b), mounted in the optimal inclination. The installed PV area in row 2 is larger than row 3, however, the unit PV area output of the horizontally mounted panel, row 2 of TABLE VI, is 199.4kWh/m², which performs worse than the optimal panel inclination, row 3 of TABLE VI, 218.2kWh/m².

TABLE VI
ANNUAL OUTPUT FOR DIFFERENT PANEL INCLINATIONS ON THE CONCRETE ROOF OF BUILDING 1, PV EFFICIENCY η =15.7%

PV area (m²)	Panel azimuth, Inclination	floor utilization rate	system annual output (MWh)	Unit area output (kWh/m²)
413.3	-25°, 0°	83.33%	82.4	199.4,
291.4	-25°, 22°	58.75%	63.6	218.2

The efficiency of thin film technology panel is about 57% of the polycrystalline one, it is unfavorable to the floor utilization even cheaper price is the advantage of thin film technology. The monocrystalline module has higher optical-electrical conversion efficiency, its performance is subject to the undesirable temperature effect and partial shading effect [5], moreover, it is expensive than the other two. Therefore, our calculations are focus on the polycrystalline PV panels.

The annual electricity output for the three buildings in the school campus based on the polycrystalline module of efficiency η = 15.7% is shown in TABLE VII.

TABLE VII
ANNUAL OUTPUT FOR THE THREE BUILDINGS

Standing seam roof						
Building	Available roof area (m²)	PV area (m²)	Panel azimuth, Inclination	Annual avg. solar hours (h/day)	System annual output (MWh)	# of 20kW inverters
1	337.63	198.4	-13°, 22°	5.42	43.5	1
3	444.04	274.3	-45°, 19°	5.30	58.9	2
Sum	781.67	472.7			102.4	3
Concrete roof						
1	495.94	291.4	-25°, 22°	5.39	63.6	2
2	1221.48	730.0	45°, 19°	5.30	156.6	4
Sum	1717.42	1021.3			220.2	6
Total		1494.0			322.6	9

The azimuth of the panel in the fourth column is positive for southwest oriented and negative vice verse. The sun light incident angle for southwest oriented panel is set to be 25.8° at 9:00, winter solstice, on the other hand, the sun light incident angle for southeast oriented panel is set to be 24.1° at 15:00, winter solstice, respectively. The roof utilization rate depends on the sun light incident angle and the panel inclination. The slope of standing seam roof of building one is 11.31°, panel arranged on the roof is 22° rather than its natural slope, two advantages are thus obtained, steeper inclination less dust accumulation and more annual insolation hours. The panel inclination on all the other roofs is mounted in its optimal inclination, too. In addition, the numbers of inverter is calculated under the assumption of 110% nominal power installed in the inverters [6].

Annual unit area energy output for those three buildings is depicted in Fig. 5, the best inclination improves the energy

harvest not much. The reason why for building one is the standing seam roof has already a significant slope of 20%, rather close to its best inclination, while the reason for the other two building is that they don't face to due South but a 45° azimuth to South. The best inclination is most helpful to a north-south oriented PV array.

Fig. 5 Unit area energy output for three buildings in the campus, the unit is $MWh/year/m^2$.

As a usual, the construction fee is estimated on the basis of installation capacity, the capacity can be derived from the total PV area and the optical-electricity efficiency. In our case, refer to TABLE VII, the perspective photovoltaic capacity is

$Capacity = 1494.0m^2 \times 1kW/m^2 \times 15.7\%(\eta) = 234.55kW$

The photovoltaic facility construction fee per kilowatt is assumed to be NT\$60,000, the total construction fee is

$Spend = 234.55kW \times NT\$60,000/kW = NT\$14,073,000$

The income of the facility comes from the electricity selling back to Taiwan Power Company under the price of "photovoltaic electricity purchase wholesale rates"[7]. The rate remains constant from the very beginning of the purchase till the coming up next twenty years. Therefore, the expected yearly income is

$Income = 322,600kW \times NT\$5.3627/kW = NT\$1,730,000$

The payback period is 8.13 years. While for the parallel to roof surface installation, the PV capacity is 326.967kW, the construction fee is NT\$19,618,000, the expected annual electricity selling income is NT\$2,295,270, and the payback period is 8.55 years. The initial investment for parallel to roof installation is forty percent higher than the best inclination scheme, the funding access is of course more difficult, still, the payback period is five percent longer.

REFERENCES

[1] Soherwardi Engineering, http://www.se-solarenergy.com /poly_crystalline_solar_panels_60cells.html.
[2] Endecon Engineering, *A Guide to Photovoltaic(PV) System Design and Installation*, California Energy Commission, Jun. 14, 2001, pp. 6-9.
[3] Roger A. Messenger and Jerry Ventre, *Photovoltaic Systems Engineering*, 2nd Ed., CRC Press LLC, Boca Raton, 2004, ch 3.
[4] Peter J. Lunde, *Solar Thermal Engineering, Space eating and Hot Qater Systems,*. New York: John Wiley & Sons, 1980, ch. 3.
[5] Bernhard Weller, Claudia Hemmerle, Sven Jakubetz, and Stefan Unnewehr, *Photovoltaics*.Detail Practice, Munich: Institut für internationale Architektur-Dokumentation Gmbh & Co, 2010, pp. 24-25.
[6] ABB Group, *TRIO-20.0-27.6-TL-OUTD-Product manual (20.0 to 27.6 kW) EN Rev E (M000001EG) of ABB solar inverters*, 2013, pp. 101..
[7] Photovoltaic electricity purchase wholesale rates, Taiwan Power Company, http://www.taipower.com.tw/content/new_info/new_info-b33.aspx?Link ID=8
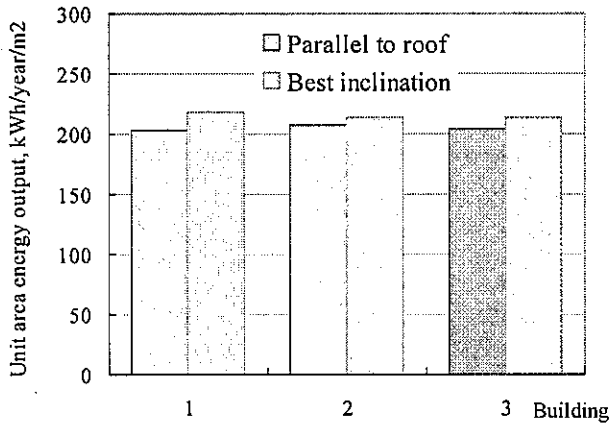
Microfabrication of Three-Dimensional SU-8 Structures Using Positives SPR Photoresist as a Sacrificial Layer for Integration of Microfluidic Components on Biosensors

Su Yin Chiam, Qing Xin Zhang, Jaehoon Chung

Abstract—Complementary metal-oxide-semiconductor (CMOS) integrated circuits (ICs) have obtained increased attention in the biosensor community because CMOS technology provides cost-effective and high-performance signal processing at a mass-production level. In order to supply biological samples and reagents effectively to the sensing elements, there are increasing demands for seamless integration of microfluidic components on the fabricated CMOS wafers by post-processing. Although the Polydimethylsiloxane (PDMS) microfluidic channels replicated from separately prepared silicon mold can be typically aligned and bonded onto the CMOS wafers, it remains challenging owing the inherently limited aligning accuracy (> ± 10 μm) between the two layers. Here we present a new post-processing method to create three-dimensional microfluidic components using two different polarities of photoresists, an epoxy-based negative SU-8 photoresist and positive SPR220-7 photoresist. The positive photoresist serves as a sacrificial layer and the negative photoresist was utilized as a structural material to generate three-dimensional structures. Because both photoresists are patterned using a standard photolithography technology, the dimensions of the structures can be effectively controlled as well as the alignment accuracy, moreover, is dramatically improved (<± 2 μm) and appropriately can be adopted as an alternative post-processing method. To validate the proposed processing method, we applied this technique to build cell-trapping structures. The SU8 photoresist was mainly used to generate structures and the SPR photoresist was used as a sacrificial layer to generate sub-channel in the SU8, allowing fluid to pass through. The sub-channel generated by removing the sacrificial layer works as a cell-capturing site. The well-controlled dimensions enabled single-cell capturing on each site and high-accuracy alignment made cells trapped exactly on the sensing units of CMOS biosensors.

Keywords—Micro-electro-mechanical Systems (MEMS), Microfluidic, Single cell capturing structure, SU-8 photoresist.

Su Yin Chiam, Qing Xin Zhang and Jaehoon Chung are with the Institute of Microelectronics, A*STAR (Agency for Science, Technology and Research), 11 Science Park Road Singapore 117685 (Corresponding author Tel: (65) 6770 5759; fax: (65) 6774 5747; e-mail: chiamsuy@ ime.a-star.edu.sg).

The Design, Development, and Optimization of a Capacitive Pressure Sensor Utilizing an Existing 9 DOF Platform

Andrew Randles, Ilker Ocak, Cheam Daw Don, Navab Singh, Alex Gu

Abstract—Nine Degrees of Freedom (9 DOF) systems are already in development in many areas. In this paper, an integrated pressure sensor is proposed that will make use of an already existing monolithic 9 DOF inertial MEMS platform. Capacitive pressure sensors can suffer from limited sensitivity for a given size of membrane. This novel pressure sensor design increases the sensitivity by over 5 times compared to a traditional array of square diaphragms while still fitting within a 2 mm x 2 mm chip and maintaining a fixed static capacitance. The improved design uses one large diaphragm supported by pillars with fixed electrodes placed above the areas of maximum deflection. The design optimization increases the sensitivity from 0.22 fF/kPa to 1.16 fF/kPa. Temperature sensitivity was also examined through simulation.

Keywords—Capacitive pressure sensor, 9 DOF, 10 DOF, sensor, capacitive, inertial measurement unit, IMU, inertial navigation system, INS.

I. INTRODUCTION

MANY areas of consumer, medical and industrial applications a 9 degrees of freedom (9 DOF), 3 axis accelerometer, 3 axis gyroscope and 3 axis magnetometer, systems are used. By adding a pressure sensor to a 9 DOF system it will improve navigation by adding the ability to detect barometric pressure, which would be an indication of the elevation of the sensor. These pressure sensors can also be used in other industrial applications such as pipeline inspection tools, or areas where an integrated inertial sensor system and pressure sensor could be put together such as medical tracking.

Pressure sensors can be based on four different sensing principals, piezoresistive, resonant, optical and capacitive detection [1]. All of these methods have different advantages and disadvantages. For piezorestive they are simple to fabricate, only diffused piezoresistors and a diaphragm are needed to fabricate the sensor. These devices have been commercialized by many companies today. They suffer from limited temperature range and temperature sensitivity. Resonant beam sensors can have a wide temperature range, however they can be complicated to fabricate and require specialized circuit for detection. Other examples of pressure sensors include sensors that make use of changes in resonant frequency or time delay of acoustic wave devices such as surface acoustic wave or LAMB wave devices [2]. The acoustic wave based sensors are not applicable here because a piezoelectric layer is not available in this platform. Optical sensors can be very sensitive by monitoring the displacement of the diaphragm. Integration of optical sensors into a 9DOF system would be problematic for a mass produced system.

In the design of capacitive pressure sensors there is a tradeoff between the size of the device, the sensitivity and the static capacitance. A sensor with a higher sensitivity for a given static capacitance will have a larger chip size compared to a device with a lower sensitivity but the same static capacitance. Some improvement of the sensitivity and the chip size can be achieved by optimizing the fixed electrode and moving electrode dimensions and shape. Capacitive sensors have low thermal drift but a small signal and parasitic capacitance in the packaging needs to be addressed.

In the Institute of Microelectronics (IME) a monolithic CMOS compatible 9DOF process has been developed [3]. Many of the needed process modules have been characterized and initial structures have been fabricated. With the structure it is also possible to add a monolithic capacitive pressure sensor to the platform. The entire sensor stack could be bonded to an application specific IC which would reduce the parasitic capacitance in the system. This paper examines the design of the capacitive pressure sensor by optimizing the design to achieve better sensitivity and also examines the temperature dependence of the structure.

II. FABRICATION OF THE PRESSURE SENSOR

The fabrication platform for the 9 DOF has been discussed in a previous paper [3]. It is included here for completeness.

A. Process

The process to realize the pressure sensors on the mentioned 9DOF inertial measurement platform is summarized below. Figs. 1 (a)-(c) show the MEMS wafer which starts with 20 μm deep cavity etching on the handle layer. It is followed with buried oxide (BOX) growth, fusion bonding and thinning the device layer of the cavity SOI wafer to 20 μm. Metal and via layers are formed using via last dual damascene process. The primary reason to fabricate these metal and via layers are to build magnetic coil structures for magnetometers.

Approximately 2 μm thick dielectric is containing the Cu lines is then patterned and used as a hard mask to etch the 20 μm thick device layer underneath. This final DRIE step

A. Randles, I. Ocak, Cheam D.D., N. Singh and A. Gu is with the Institute of Microelectronics, A*STAR (Agency for Science, Technology and Research), Singapore 116875 (Phone: +65-6770-5466; Fax: +65-6774-54747; e-mail: randlesab@ime.a-star.edu.sg).

suspends all the inertial sensors with the help of the cavity underneath them and completes the fabrication of the MEMS wafer. In the case of the pressure sensors the device layer is not etched and cavity is left sealed under high vacuum.

TSI wafer fabrication shown in Figs. 1 (d)-(g) starts with via etching, liner oxide growth on the inner walls, and filling with highly doped n++ epi-poly silicon. It is followed by grinding extra poly-silicon and then front side Al redistribution layer (RDL) fabrication. The wafer was then thinned down to 300 μm from backside to reveal TSVs and then followed by deposition of the spacers, RDL and getter on the backside of the wafer. The Process was completed by bonding MEMS to TSI wafer using Al\Ge bonding (5). Fig. 2 shows an image of the pressure sensor before TSI vacuum packaging, fabricated using the 9DOF inertial MEMS platform.
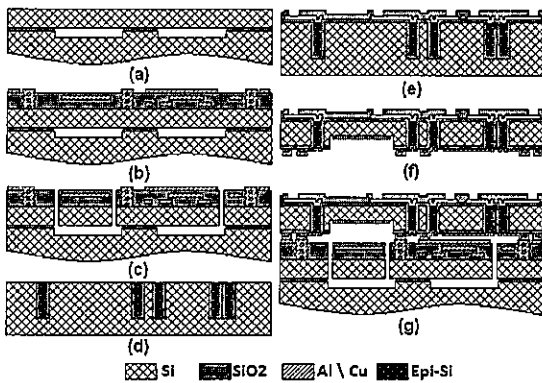
Fig. 1 MEMS wafer (a) cavity wafer (b) 3 metal and via layer deposition (c) structural etch (d) TSI etch and filling (e) Front side RDL and pad etch (f) grinding, stand-off, getter & back RDL (g) Bonded TSI & MEMS wafer bonding [3]

TABLE I
SILICON MATERIAL PROPERTIES FOR UNROTATED SI [4]

elastic constants, c_{ij} [GPa]	c_{11}	164
	c_{12}	64
	c_{44}	80
1st order TCE Tc_{ij} [10^{-6}/K]	Tc_{11}	-73.25
	Tc_{12}	-91.59
	Tc_{44}	-60.14
2nd order TCE $T2c_{ij}$ [10^{-9}/K^2]	$T2c_{11}$	-49.26
	$T2c_{12}$	-32.70
	$T2c_{44}$	-51.28

Fig. 2 Fabricated MEMS chip

III. SIMULATION SETUP

The basic layers of the simulation are shown in Fig. 3. The structure is made up of the silicon diaphragm which is also acting as the ground layer in the structure. An air cavity with a moving mesh is the next layer with a variable pressure. Finally the active electrodes are defined above the moving mesh layer. The opposite side of the diaphragm is at vacuum. So the pressure load is applied at the interface between the moving mesh and the Si diaphragm. The vacuum sealed cavity under the moving diaphragm is at 50 mBar. This is set by the fabrication process.

For the Si layer an anisotropic material model was used for the Si that included temperature dependent coefficients for the Si stiffness contestants, Table I. In the simulation software the stiffness matrix was rotated by 45 degrees to align with the XY axis in a (100) wafer. Simulations were done over a range of pressures and temperature to capture the change in sensitivity as a function of pressure.

Many capacitive pressure sensors are designed where the capacitive plates are on either side of the sealed cavity, for example [5]. The proposed design has one disadvantage compared to these other sensors because the atmosphere between the electrodes will change as the outside air changes. This can be accounted for by adding reference capacitors.

TABLE II
DIMENSIONS USED IN SIMULATIONS

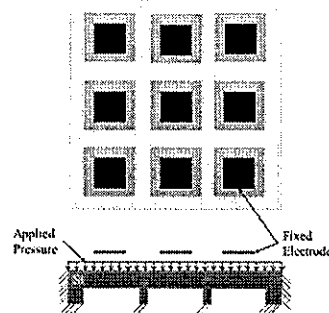| Chip Size	2mm x 2mm
Maximum distance for unsupported diaphragm	<0.4 mm
Si Thickness	20μm
Air Gap	2μm
Pillar Size	50 μm
Target Static Capacitance	1.67 pF

Fig. 3 Standard capacitive sensor setup with multiple diaphragms

IV. SENSITIVITY OPTIMIZATION

A. Square Diaphragms

In the fabrication platform that was used for this pressure sensor, the design constraints for the sensor were a 2 mm x 2 mm square with the largest unsupported diaphragm 0.4 mm x 0.4 mm. The designed static capacitance was set to 1.67 pF. Other details can be found in Table II. A series of simulations were run, where the top electrode size was varied and the number of diaphragms was increased to match the desired static capacitance. An example of the deflection pattern for a square diaphragm is shown in Fig. 4.

Next, a series of simulations were run where the static capacitance was held constant, and the coverage of the top electrode was varied. The sensitivity is plotted in Fig 5.
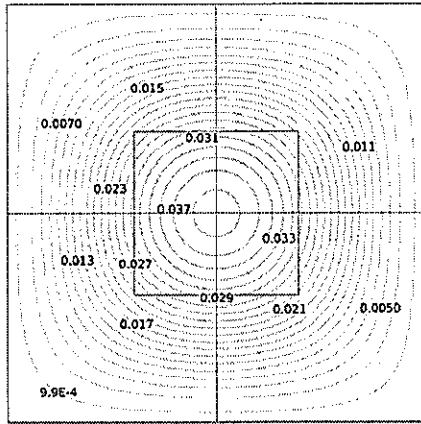
Fig. 4 Deflection of a single square diaphragm, 0.4 mm x 0.4 mm
Contour lines mark the deflection of the diaphragm in μm. The
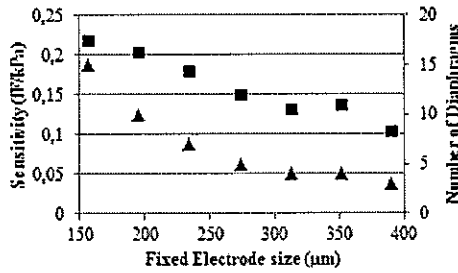central square marks where the top electrode would be located

Fig. 5 Sensitivity of the set of diaphragms for different amounts of
fixed electrode coverage, the sensitivity of the array of diaphragms is
calculated from the sensitivity of one diaphragm times the closest
integer of diaphragms

The maximum number of diaphragms was capped at 16 as
this is the maximum number that would fit within the 2 mm
square. The sensitivity was calculated from the sensitivity of a
single diaphragm multiplied by the number of diaphragms that
would be required to meet the static capacitance.

B. Optimized Diaphragm Design

To address the low sensitivity of the fully fixed membrane
an alternative design using multiple pillars to support the
membrane and the active electrode is designed to be placed
only over the areas of maximum deflection. The structure is
shown in Fig. 6.
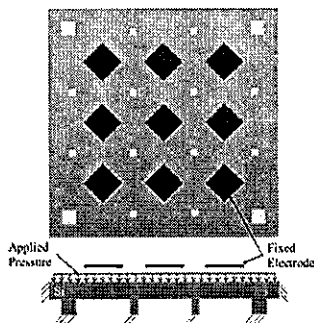
Fig. 6 Layout of an optimized sensor

The total size of the diaphragm was limited to 1.7 mm by

1.7 mm to leave space around the edge for bonding and dicing.
The electrodes were set to 200 μm on a side. Simulations of
the deflection and sensitivity were performed. The deflection
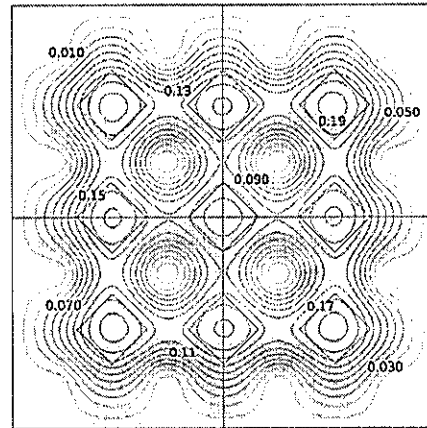pattern of the device is shown in Fig. 7.

Fig. 7 Deflection of the optimized membrane 1.7 mm x 1.7 mm,
contour lines marks the deflection of the diaphragm in μm. The
diamonds represent where the fixed electrode is located.

The sensitivity from the optimized structure is 1.16 fF/kPa,
more than 5 times increase over the best device shown in Fig.
5. As can be seen in Fig. 4 some further optimization could be
done on the electrode shape for them to better follow the
contour lines.

C. Temperature Sensitivity of the Optimized Design

The temperature sensitivity of the sensor is critical for
determining the error in the sensor and for accounting for the
temperature drift. One way to address some of the temperature
drift would be to add reference capacitors to the system.
Reference capacitors would account for changes in the
permittivity of air due to temperature and humidity changes.
These capacitors could be placed around the diaphragm edges
where there is very little deflection. This will only leave the
changes in the Si stiffness as a function of temperature as the
main environmental variable not accounted for.

The temperature sensitivity of the optimized diaphragm was
studied by using a stiffness matrix that included temperature
dependence for Si, Table I. In Fig. 8 is a plot of the sensitivity
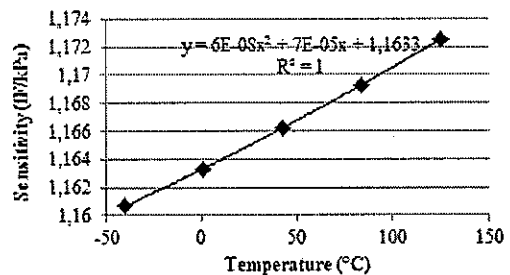as a function of temperature.

Fig. 8 Sensitivity as a function of temperature for the optimized
structure, the sensitivity is changed by 57 ppm/K for the first order
effect and 52 ppb/K^2 for the second order dependence

The temperature sensitivity could be reduced by making use of the oxide layer which already exists in the platform. This would likely reduce but not completely eliminate the temperature drift of the sensor. The remaining temperature drift would need to be accounted for in signal processing.

V. CONCLUSION

In this paper a simulation of an optimized capacitive pressure sensor was developed. The sensor showed a more than 5 times improvement of the sensitivity over a traditional array of Si diaphragms with a similar static capacitance and chip area. The temperature sensitivity of the structure was also simulated.

REFERENCES

[1] W. P. Eaton and J. H. Smith. "Micro machined pressure sensors: review and recent developments." In *Smart Structures and Materials' 97*, 1997, pp. 30-41.

[2] P. Kropelnicki, K. Muckensturm, X. J. Mu, A. B. Randles, H. Cai, W. C. Ang, J. M. Tsai and H. Vogt. "CMOS-compatible ruggedized high-temperature Lamb wave pressure sensor." *Journal of Micromechanics and Micro-engineering*, vol. 23, no. 8, 2013, pp. 085018.

[3] I. E. Ocak, D. D. Cheam, S. N. Fernando, A. T. Lin, P. Singh, J. Sharma, G. L. Chua, B. Chen, A.Y.D. Gu, N. Singh, and D. L. Kwong "A monolithic 9 degree of freedom (DOF) capacitive inertial MEMS platform." in *Electron Devices Meeting (IEDM), 2014 IEEE International*. San Francisco, 2014, pp. 22-6.

[4] M. Hopcroft, W. D. Nix, and T. W. Kenny. "What is the Young's Modulus of Silicon?" *Micro-electromechanical Systems, Journal of*, vol. 19, no. 2, 2010, pp. 229-238.

[5] M. Narducci, L. Yu-Chia, W. Fang, and J. Tsai. "CMOS MEMS capacitive absolute pressure sensor." *Journal of Micromechanics and Micro-engineering*, vol. 23, no. 5, 2013, pp. 055007.

Preparation of Porous Metal Membrane by Thermal Annealing for Thin Film Encapsulation

Jaibir Sharma, Lee JaeWung, Merugu Srinivas, Navab Singh

Abstract—This paper presents thermal annealing de-wetting technique for the preparation of porous metal membrane for Thin Film Encapsulation (TFE) application. Thermal annealing de-wetting experimental results reveal that pore size formation in porous metal membrane depend upon i.e. 1. The substrate at which metal is deposited, 2. Melting point of metal used for porous metal cap layer membrane formation, 3. Thickness of metal used for cap layer, 4. Temperature used for formation of porous metal membrane. In order to demonstrate this technique, Silver (Ag) was used as a metal for preparation of porous metal membrane on amorphous silicon (a-Si) and silicon oxide. The annealing of the silver thin film of various thicknesses was performed at different temperature. Pores in porous silver film were analyzed using Scanning Electron Microscope (SEM). In order to check the usefulness of porous metal film for TFE application, the porous silver film prepared on amorphous silicon (a-Si) and silicon oxide was released using XeF_2 and VHF, respectively. Finally, guide line and structures are suggested to use this porous membrane for robust TFE application.

Keywords—De-wetting, thermal annealing, metal, melting point, porous.

I. INTRODUCTION

MICROELECTROMECHANICAL SYSTEM (MEMS) devices have achieved a great attention in industry and research groups in recent past due to their cutting edge applications, including sensors, optics and RF devices [1], [2]. MEMS packaging with controlled ambient is in much demand in order to provide the proper operating condition and protect the MEMS devices from the harsh environment [3], [4]. The bonding is a known commercialized technique and many products are available in the market. However, bonding is expensive technique in terms of occupying wide area per dice due to wide seal rings, wide dicing area requirement for dicing the stack of wafers. This results in a less number of devices per wafer [5], [6].

Thin film encapsulation (TFE) is emerging as an alternative technique in recent past due to the possibility of overall thickness reduction and area saving in seal ring as well as low cost from elimination of a cap wafer. This technique uses surface micromachining process such as deposition, etching and release steps to realize the encapsulation of MEMS devices. However, TFE technique suffers with issues like long release time and mass loading on MEMS devices during the sealing process. To solve these issues, many different approaches have been tried by researchers and reported in the

Jaibir Sharma, Lee JaeWung, Merugu Srinivas, Navab Singh are with the MEMS Program, Institute of Microelectronics, Singapore (phone: +65-67705472; e-mail: sharmaj@ ime.a-star.edu.sg).

literature. These approaches are based on the location of etch channels or formation of pores (channel) in the cap layer to remove the sacrificial layer in TFE [7]-[11]. In one of the approach, the etch channels were distributed all over the cap layer as shown in Fig. 1 (a). The uniform distributions of many etch holes in the cap layer results in a short release time of TFE. However, it has a drawback of mass loading [7], [10] as sealing material may deposit on the MEMS device through etch holes as shown Fig. 1 (c). This mass loading may cause damage to the MEMS device or change the design parameter of the same. The mass loading is very critical for many devices like FBAR, SAW etc. as mass loading can change the operating frequency of these devices. In second approach, etch channels are fabricated at the sidewall of the cap layer (sidewall located channel scheme) as shown in Fig. 1 (b). The sidewall located channel scheme helps in preventing the mass loading on the MEMS device during sealing process. However, this scheme has a drawback of longer release time because sacrificial layer material should be removed through long etching path from sidewall to center of TFE as shown in Fig. 1 (b) [9]-[11]. On the other hand, porous cap layer with micro-or nano-etch holes may also be used to solve the above issues [12], [13]. In these approaches, the nano- or micron-sized pores play the role of etch channel which helps in fast removal of sacrificial layer and safe sealing of the TFE without mass loading on MEMS devices.
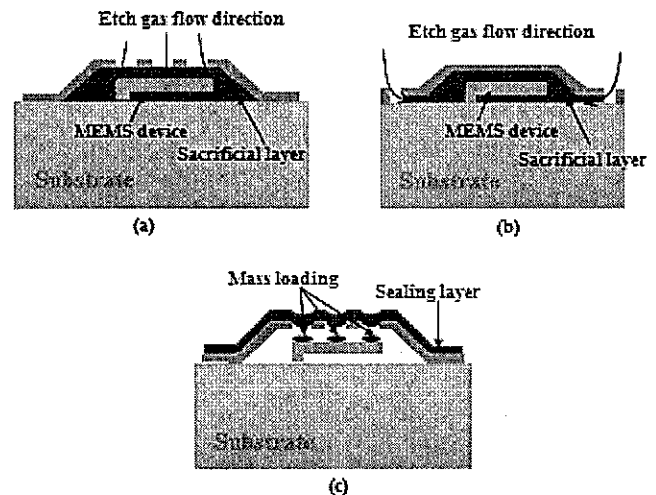

Fig. 1 Schematic diagrams of TFE for (a) uniformly distributed etch hole on the cap layer, (b) sidewall located etch channels and (c) mass loading on MEMS device during sealing for TFE realized using a approach as shown in (a)

There are many approaches in the literature for the

fabrication of nano- or micro-pores in thin film which has been used for TFE application. Lee et al. [14] used anodization technique to create pores in Chromium (Cr) thin film for releasing the structure under the porous membrane. However, these approaches are very costly and complicated by nature for the fabrication of pores. In this paper, a simple and cost effective technique has been discussed to fabricate the porous metal membrane. This technique simply used thermal annealing of thin metal film at particular temperature called de-wetting temperature of metal to create the porous metal films. The pore size in the metal film can be controlled by controlling temperature of the annealing. However, pore size also depends on type's substrate and, metal etc. factors.

II. POROUS MEMBRANE FORMATION

In this paper, we proposed a simple thermal annealing de-wetting technique for formation of porous metal film (membrane). The pore size in the metal film can be controlled by i.e. 1. Proper selection of sacrificial layer (substrate) on which metal is deposited, 2. Proper selection of metal (cap layer) used for porous formation (lower melting point is preferred). However, cap layer metal selection should also be done by considering its selectivity with respect sacrificial etchant, 3. Thickness of metal used for formation of porous cap layer, 4. Temperature used for formation of porous in metal cap layer. The number of temperature cycles used for annealing, also affect the size of pore formation.

In this paper, silver (Ag) was used as a cap layer material and amorphous silicon (a-Si) was used as a sacrificial material. Three different annealing temperatures (250°C, 300°C and 350°C) and four different thicknesses (20nm, 50 nm, 100 nm and 200 nm) were used for the fabrication of porous membrane. Table I summarizes thickness of film and temperature ranges used for formation of porous Ag film on a-Si.

III. RESULTS AND DISCUSSION

Fig. 2 shows the Scan Electron Microscope (SEM) image of pores in the membrane fabricated using 200 nm thick silver and annealed 350°C for 1 hour in nitrogen ambient. The pores size is more than 1 um in width and close 2 um in length was achieved. Grain formation of silver can be seen Fig. 2. Fig. 3 shows the SEM image of pores fabricated on a-Si and oxide substrate on same sample using 200 nm thick silver and annealed 350°C for 1 hour in nitrogen ambient. A-Si substrate was created on same sample by etching a window in oxide layer and filling the same with a-Si. Finally, CMP was performed for planarization. In Fig. 3, right side shows Ag on oxide and left side Ag on a-Si window. It can be observed from image that there are large number and big size of pores formation on oxide substrate. However, less number and small size pores are formed on a-Si substrate. This means that oxide surfaces are more favorable for fabrication silver porous membrane.

Table I shows different thickness and their behavior at three different temperatures. It can be observed that de-wetting

become serious for very thin silver (Ag) film. A 20 nm thin Ag film shows good pores formation at 250°C. However, same thickness gets severely de-wet at 300°C. The severity of de-wetting of metal film depends on annealing temperature. Thicker film may severely de-wet at higher temperature. For example, 50 nm Ag film form a good pores at 250°C and 300°C. However, it gets severely de-wet at 350°C as can be seen Table I. At the same time, very thick metal may not de-wet at all as can be seen from table that 200 nm silver films does get de-wet at 250°C and 300°C, respectively and pore formation only starts at 350°C. It means that formation of pores and their size depend on cap layer metal thickness, annealing temperature used for de-wetting. To de-wet thicker film, longer time and higher temperature is required.
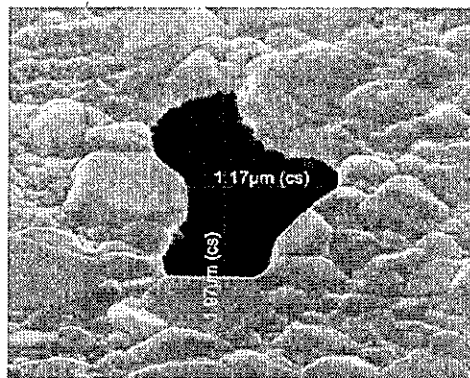

Fig. 2 SEM image of the pores fabricated by annealing 200 nm silver film at 350°C for 1 hour
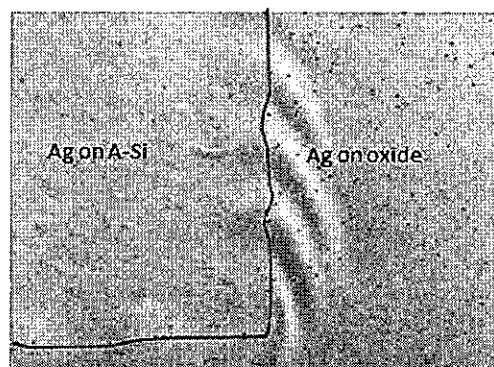

Fig. 3 SEM image of the pores fabricated on a-Si and oxide substrate

A. Porous Metal Membrane for Thin Film Encapsulation (TFE) Application

In order to check the feasibility of these porous metal membranes as a cap layer for TFE application, sacrificial a-Si and oxide were etched through small pores in the porous metal membrane.

Fig. 4 (a) shows FIB–SEM cross-section image of the sample where a-Si sacrificial was etched with the help of Xenon Fluoride (XeF$_2$). It can observed from the image that sacrificial a-Si was removed through pores and Ag thin membrane collapsed after a-Si sacrificial layer removal. Fig. 4 (b) shows the FIB–SEM cross-section image of the similar sample where oxide is considered as a sacrificial layer and

etched with the help of Vapour Hydrofluoric (VHF) through small pores. It can be observed from the image that oxide sacrificial was etched through pores. However, there was oxide residues left behind. These residues [15] are very common after VHF process for PECVD oxide which is usually deposited with recipe that includes NH_3 gas.

As observed in Fig. 4 (a) that thin porous Ag membrane is not strong enough to use as a structural cap layer for TFE application. On releasing the sacrificial layer, this porous Ag membrane collapses on to the substrate and hence not useful for TFE. In order to use this thin porous Ag film as a cap layer for TFE application, a second cap layer such as oxide or a-Si material (depending upon use of sacrificial material) can be prepared in the form of net on sacrificial layer and metal porous film can be formed above it as shown in Fig. 5. The second cap layer have small patterned etch hole in it. Pores formed on these etch holes makes sacrificial layer accessible to sacrificial etchant. Sacrificial layer is etched through these pores available on etch holes. TFE can be released through these small pores. After releasing TFE, it is sealed by depositing sealing layer. This should be noted here that mass loading on encapsulated device is reduced as sealing material does not fall on device due to very small pore size. In order to reduce mass loading (require small pore size) and fast releasing (require beg pore size) which are opposite requirement by nature, there is need to optimize metal thickness and temperature value for annealing. From Table I, it is clear that one can select proper thickness and temperature for the fabrication of porous cap layer membrane to achieve fast releasing and less mass loading.

TABLE I
SEM IMAGE FOR DIFFERENT THICKNESS OF POROUS SILVER FILM FABRICATED AT DIFFERENT TEMPERATURE

Annealing Temperature	Thickness of Ag film						
	20 nm		50 nm		100nm	200 nm	
250°C		~100nm		~1µm	No dewetting	No dewetting	
300°C		No connection		~100nm		~1µm	No dewetting
350°C	Serious dewetting			No connection		~100nm	~1µm
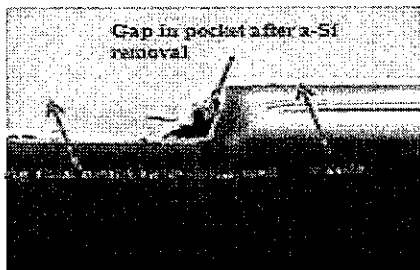
(a)
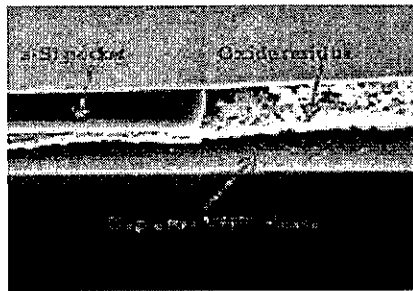
(b)

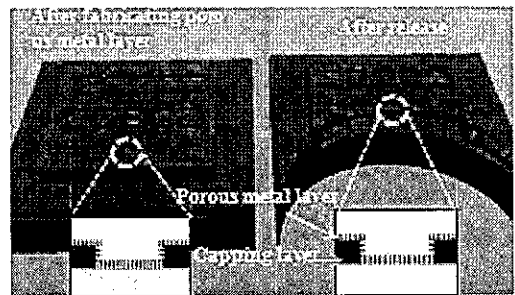Fig. 4 FIB-SEM image of the samples after: (a) XeF₂ (b) VHF, release

Fig. 5 Schematic diagrams of TFE by formation of strong net structure in second cap layer and porous metal on it

IV. CONCLUSION

This paper demonstrates the porous metal layer formation by using a simple thermal annealing technique. The size of pores can be controlled by substrate, thickness of metal, temperature and selection of metal. This work also successfully demonstrates the removal of a-Si and oxide sacrificial layer through pores generated using thermal annealing technique. This paper also outline how this porous

metal can be used as a robust cap layer for encapsulating
MEMS device without mass loading during sealing.

REFERENCES

[1] G. H. Mohamed, The MEMS Handbook, 2nd ed., New York, USA:
Taylor & Francis, 2002.

[2] M. Perlmutter and L. Robin High-Performance, "Low Cost Inertial
MEMS: A Market in Motion!" Position Location and Navigation
Symposium (PLANS), 2012, pp.225-229.

[3] R. R. Tummala and E. J. Rymaszewski "Microelectronics Packaging
Handbook", 2nd ed., Massachustts, USA: Kluwer Academic Publishers
1989.

[4] K. Najafi, "Micropackaging Technologies for Integrated Microsystems:
Applications to MEMS and MOEMS", Micromaching and
Microfabrication Process Technology VII, Proc. Of SPIE Vol. 4979,
2003, pp.1-19.

[5] Lutz M. Partridge, B. Kim, M. Hopcroft, R. N. Candler, T.W. Kenny,
"MEMS Resonators: Getting the Packaging Right", in: SEMICON-
Japan, 2005.

[6] H. Stark and K. Najafi, "A Low-Temperature Thin-Film Electroplated
Metal Vacuum Package", J. Microelectromech. Syst., vol. 13, 2004, pp.
147–157.

[7] V. Lindroos, M. Tilli, A. Lehto and T. Motooka, Handbook of Silicon
Based MEMS Materials and Technologies, 1st ed., Elsevier, chap 38,
2010, pp. 569-574.

[8] J. L. Pornin, C. Gillot, G. Parat, F. Jacquet, E. Lagoutte, N. Sillon, G.
Poupon, F. Dumont, "Wafer Level Thin Film Encapsulation for BAW
RF MEMS.", Electronic Components and Technology Conference,
2007, pp. 605-609.

[9] C. Gillot, J.L. Pornin, A. Amaud, E. Lagoutte, N.Sillon, J.C. Souriau,
"Wafer Level Thin Film Encapsulation for MEMS", Electronic
Components and Technology Conference , 2005, pp. 243-247.

[10] US patent 7,344,907 B2 Mar. 18, 2008

[11] C. O'Mahony, M. Hill, Z. Olszewski and A. Blake, "Wafer-Level Thin-
Film Encapsulation for MEMS", Microelectronic Engineering vol. 86,
2009, pp. 1311–1313.

[12] R.H. Rico, B. Du Bois, A. Witvrouw, C. Van Hoof, J.-P. Celis,
"Fabrication of Porous Membranes for MEMS Packaging by One-Step
Anodization in Sulfuric Acid", J. Electrochem. Soc. 154 (9) K74 – K78,
2007.

[13] J. Zekey, S. D Tezcan, J.-P. Celis, R. Puers, C. Van Hoof, and H.A.C.
Tilmans, "Wafer-Level Thin Film Vacuum Packages for MEMS using
Nanoporous Anodic Alumina Membrane", Transducers conference,
2011, pp. 975-977.

[14] B. K. Lee, D. H. Choi and J. B. Yoon "Use of nanoporous columnar thin
film in the wafer level packaging of MEMS devices" J. Micromech.
Microeng. 20 045002 (9pp), 2010.

[15] W. I. Jang, C. A. Choi, M. L. Lee, C. H. Jun and Y. T. Kim "Fabrication
of MEMS devices by using anhydrous HF gas-phase etching with
alcoholic vapor" J. Micromech. Microeng. 12, 297–306, 2002.

Investigation of Chord Protocol in Peer to Peer-Wireless Mesh Network with Mobility

P. Prasanna Murali Krishna, M. V. Subramanyam, K. Satya Prasad

Abstract—File sharing in networks is generally achieved using Peer-to-Peer (P2P) applications. Structured P2P approaches are widely used in adhoc networks due to its distributed and scalability features. Efficient mechanisms are required to handle the huge amount of data distributed to all peers. The intrinsic characteristics of P2P system makes for easier content distribution when compared to client-server architecture. All the nodes in a P2P network act as both client and server, thus, distributing data takes lesser time when compared to the client-server method. CHORD protocol is a resource routing based where nodes and data items are structured into a 1-dimensional ring. The structured lookup algorithm of Chord is advantageous for distributed P2P networking applications. However, structured approach improves lookup performance in a high bandwidth wired network it could contribute to unnecessary overhead in overlay networks leading to degradation of network performance. In this paper, the performance of existing CHORD protocol on Wireless Mesh Network (WMN) when nodes are static and dynamic is investigated.

Keywords—Wireless mesh network (WMN), structured P2P networks, peer to peer resource sharing, CHORD protocol, DHT.

I. INTRODUCTION

PEER-TO-PEER networks are typically formed by a large number of distributed, heterogeneous, self-configurable and dynamic peers. All the peers cooperate to provide a common service. Applications using peer-to-peer networks use sophisticated discovery mechanisms at each peer to find and communicate with other peers. If the resource discovery mechanism is centralized then it is not scalable, so decentralized discovery mechanisms are required. Peer-to-Peer (P2P) applications have been significantly used for content distribution and sharing in the networks and more than 70% of the traffic are created in the internet by P2P applications.

Major peer-to-peer applications are categorized into three classes. They are distributed file sharing, person-to-person messaging and distributed computing [1]. In Distributed file sharing, each peer shares the file content with other peers in the network based on the requirement of the application. Some examples are Freenet, Lime Wire and Morpheus. In Person-to-person messaging systems, each peer allows to exchange text messages. Some examples are Jabber, Groove, and Yahoo Messenger. Distributed computing systems make the peers to

compute some values needed for other peers. Some examples are SETI@home and Entropia.

Some of the advantages of P2P networks are: (1) improvement in scalability because resources are aggregated from peers and reducing the dependency on centralized servers, (2) Reduce the cost by utilizing available resources from other peers and eliminating the need for fixed infrastructure, and (3) load balancing by dividing all the computing at the end systems. In P2P layered architecture a software layer used to construct and maintain the peers in the network is called as P2P substrate. It may be structured or unstructured [2]. Since P2P networks do not have the distinction between client and server nodes as all peers are both clients and servers simultaneously, lesser time is needed to distribute data in comparison to the client-server method [3], [4]. Peer-to-peer networks were started in a wired domain, when being implemented initially for file sharing and distributed computing.

There are two types of overlay networks; Structured and unstructured method [5]. In Structured methods, the P2P overlay network topology is tightly controlled and contents are placed at specified locations to make subsequent data requests more efficient. One of the structured P2P systems use the Distributed Hash Table (DHT), in which data object location information is placed deterministically, at the peers with identifiers corresponding to the data object's unique key. Content Addressable Network (CAN), Tapestry, Chord, Pastry, Kademlia and Viceroy are some of the structured P2P overlay networks.

In unstructured P2P overlay networks, peers are organized in a flat or hierarchical manners and use flooding or expanding-ring and Time-To-Live (TTL) search, to query content stored in the overlay peers. Each peer is visited and evaluated whether content for a query is located locally and will support for complex queries. This is in efficient because queries for content that are not widely replicated must be sent to a large fraction of peers and there is no coupling between topology and content's location. Some of the unstructured P2P overlay networks are Freenet, Gnutella, FastTrack KaZaA and BitTorrent.

In the distributed P2P applications, a node is chosen which stores data. This is solved by the Chord protocol in a decentralized very effectively: provided with a key, it determine which node stores the key's value efficiently. When in steady state, every node maintains routing information only for $O(logN)$ other nodes (for N-node network), and resolves lookups via $O(logN)$ messages to other nodes. Chord's major advantages are simplicity, provable correctness and

P. Prasanna Murali Krishna is with the SGIT, Markapur, India (e-mail: pprasannamurali@gmail.com).
M. V. Subramanyam is with the Santhi Ram Engineering College, ECE Department, India (e-mail: mvsraj@yahoo.com).
Satya Prasad K. is with the JNTUK, ECE Department, India.

performance even while node join or leave network. It also scales well with increase in nodes, pull through from simultaneous node failures, joins and even when recovering answers most lookups appropriately. When a node has only partially correct information, the network performance degrades.

Wireless Mesh Networks (WMNs) are fast emerging wireless networks inspiring numerous applications such as community scale, Peer-to-Peer networking. WMNs include mesh clients and mesh routers, with the latter having minimal mobility forming the spine of the networks [6]. These networks are self-configuring and self-organizing with the nodes establishing an ad hoc network. Communications take place through multi-hop routing. Gateway and bridging processes in mesh routers integrate WMNs with other networks like Internet, IEEE 802.15, IEEE 802.16, cellular, IEEE 802.11, and sensor networks [7]. WMNs have advantages such as low cost, easy maintenance, reliable coverage, robustness when compared to other ad hoc networks. WMNs deliver wireless services for several applications in campus, metropolitan areas, local, and personal. Many research challenges remain in protocol layers even when there are advances in wireless mesh networking.

Mesh clients are either static or mobile, and they form a client mesh network amid themselves and with mesh routers. In WMN, all nodes serve as both host and router. The packets are advanced through multi-hop communication within the network. The characteristics of WMN are ad hoc networking, multi-hop communication with a wireless backbone provided by a mesh routers, mobility of nodes supported by the mesh routers and ability of mesh routers to integrate with heterogeneous networks necessitate new design principle for efficient performance of the network. Some of the factors, which influence the performance of WMN, are radio techniques, scalability, mesh connectivity, compatibility, and inter-operability.

The possibility for distributed P2P networking applications is vast using a structured lookup algorithm such as Chord. However, a structured approach improves lookup performance in a high bandwidth wired network is proved; the overlay networks create unnecessary overhead that negatively impacts performance in an unstable environment such as a WMN. This study investigates CHORD protocols on WMN when the nodes are static and dynamic.

II. CHORD PROTOCOL

Stoica et al. [8] presented a scalable peer-to-peer lookup protocol-chord: for internet applications. The Chord protocol used Distributed Hash table (DHT). All the nodes were organized in an identifier circle based on the node identifiers as shown in Fig. 1. Keys were assigned to their successor node in the identifier circle. Hash function was used for even distribution of nodes and the keys on the circle. In the ring, all the peers and the resources were assigned to a unique identifier. Each peer stored its identity in the format of (key, value).

For efficient routing each Chord node stored the details about O (log N) other nodes. If these stored details were out of date then the performance degradation occurred. It was difficult to maintain consistent details of O (log N) nodes because any node might join or leave at any time. So chord node should maintain the dynamic information about other nodes. Whenever a node left from the network, it was considered as node failure.

When requesting content or a resource, each node performed one operation: For the given a key, it mapped the key onto a node. Depending on the application using Chord, that node might be responsible for storing a value associated with the key. Chord used consistent hashing methods to assign keys to Chord nodes. Consistent hashing was used for load balancing, since each node had to store the some number of key, value pairs approximately, and required relatively little movement of keys whenever any node joined or left in the network.

CHORD protocol used Consistent hashing like SHA-1 to generate corresponding identifier. It also generates key, which is the basis for a node and data item location of nodes on a circular overlay. Node identifiers are generated by hashing an IP address, while hashing its unique name produced data item's key. Regular hashing mapped keys to nodes as follows: Nodes were ordered on to an identifier circle. Then key k was assigned to that node. Then this node follows it directly in the identifier space and was designated the successor node of k. Chord uses virtual nodes to maintain uniform key distribution in nodes. In such cases, multiple Ids are assigned to every physical node in the same Chord system ensuring uniform key distribution for nodes [9]. The peer ID could be obtained by hashing the IP address of a particular peer; and data value are hashed to obtain resource ID. Resource ID was kept in the first peer, whose ID >= Resource ID. Finger table are kept by each peer, which stores routing information records.
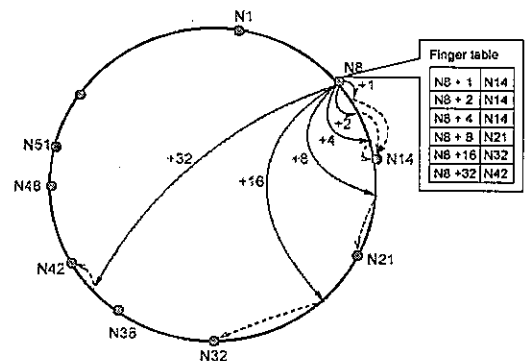

Fig. 1 The CHORD Protocol Ring

Each node had a finger table to record log N successors where N is the number of peers. Every peer checked its successors for the updating the Finger table. It contacted a peer predecessor, as it was useful when a peer leaves the ring and asks previous peer to bring the finger table up to date.

Chord routed the message by forwarding to a successor near to destination identifier. First peer checked in finger table

records; chose a successor near the destination, and then forwarded a request to it. The peer on receiving requests would also do some checking and forward a message to a successor. The entire cost was not more than log N hops and ½ log N in average where N is the number of overlay peers [10]. Chord defined advertisement function about joining/leaving procedure for peers.

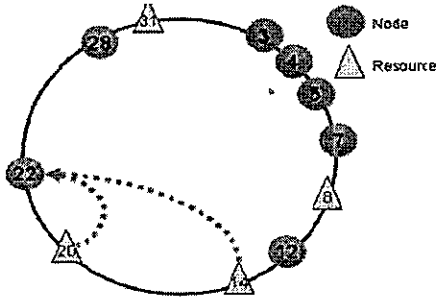Fig. 2 Chord Overlay with Peers and Resources

A. System Model

Chord streamlines peer-to-peer systems design by addressing some difficult issues.

- **Load balance:** Due to distributed hash function, the keys are spread evenly over nodes providing some natural load balance in Chord.
- **Decentralization:** Chord improves robustness as it is fully distributed. This makes Chord suitable for loose peer-to-peer applications.
- **Scalability:** As the cost of a Chord lookup is proportional to the log of number of nodes, it is feasible for large systems.
- **Availability:** Chord automatically updates internal tables to reveal every new node and node failures, so that the node responsible for a key is always found.

The Chord protocol is implemented either in an iterative or recursive style. In iterative method, lookups are initiated by communicating queries to a series of nodes for information from their finger tables, moving closer to a successor on the Chord ring. Whereas in recursive method, every intermediate node forwards a request to the next node until the successor is reached. The simulations conducted in this study implements the Chord protocol in an iterative style.

Node updates its successor during stabilization process, and one other entry in its successor list/finger table. Therefore, all the unique entries in the node's successor list/finger table is refreshed once during stabilization rounds.

Many modifications for Chord have been proposed in the literature. Karger and Ruhl [11] proposed a modified chord protocol where only a subset of nodes offers a service without forming their own chord ring. The creations of the subgroups carry out the functions and the routing functionality of the existing chord ring with less resource. The proposed diminished Chord requires only O (k) storage per k-sized subgroup compared of O (k log k) from creating a new Chord ring.

Zöls et al. [12] presented the Hybrid Chord Protocol (HCP) to solve the problem of frequent joins and leaves of nodes. The proposed HCP supports the grouping of shared objects in interest groups for efficient search. Information profiles of the shared objects help in automatically establishing context space for assigning and transferring. It also significantly reduces the traffic load.

Burresi et al. [13] adapted the Chord for WMN, by exploiting location awareness and 1-hop broadcast of WMN. The proposed MeshChord reduces message overhead and improves the information retrieval performance. Novak and Zezula [14] proposed M-Chord, a distributed data structure for metric-based similarity search, which also distributes the storage space and executes similarity queries in parallel. Thaalbi et al. [15] proposed a new distributed lookup protocol for mobile P2P networks with the aim to reduce the overhead traffic and the lookup delay. Simulation results demonstrate the efficiency of the proposed scheme when compared to Chord protocol and Backtracking Chord protocol.

III. METHODOLOGY

In Chord, every node has a finger table, which implements searches in the forward direction. Nodes based on the position of join are arranged to form a ring. The positions are determined using hello messages with neighbor nodes. In normal P2P network, one query message is sufficient to identify the correct node using the finger table. However, in the case of ad hoc networks, these queries are lost consistently due to the dynamic nature of the nodes and instability of the wireless medium. Similarly, the consistency of the ring for the nodes in the network is hard to maintain, due to node failure and mobility. Thus, when a node joins the network, the steps involved in the finger table updating/stabilization is given by

1) The node joining must first find a node already in the network.
2) The node already in the network uses the CHORD mechanism and its finger table to find a successor for the new node.
3) Since the system is dynamic, finger table updating operations are carried out periodically such that each node sees that its successor and predecessor have not changed.
4) When there is a change in the successor or predecessor, the node in the network assumes that a new node has joined the network, or its successor or predecessor has left the network.
5) If a newly joined node lies amid two nodes, they update their successor values to reflect change.

The Chord protocol maintains just one operation: it maps the given key details into a node. Depending on the application, the node might be accountable for storing a value connected with the key. In this work, the IP address generated dynamically are taken as keys. The pseudo code is shown in Fig. 3.

IV. EXPERIMENTAL SETUP

The performance of WMN using CHORD protocol when the nodes are static and dynamic is evaluated through simulations. A test bed network is constructed in the simulator, which consists of 17 nodes spread over an area of 4000m by 4000m. The wireless links communicate with a bandwidth of 2 Mbps. The simulations are run initially for static scenario and later for dynamic nodes where the node is moving with a speed of 60 kmph. The simulations are run for 240 sec. Table I gives the specifications used in the simulations.

TABLE I
SIMULATION SPECIFICATIONS

Number of Nodes	17
Bandwidth	2 Mbps
Area	4 km X 4 km
Routing Protocol	CHORD
Mobility Speed	60 kmph
Simulation Time	240 Sec

```
// ask node n to find the successor of id
n.find _ successor (id )
if (id ∈ (n, successor))
return successor;
else
// forward the query around the circle
n0 = closest _ preceding _ node(id );
return n0.find _ successor (id );
// search the local table for the highest
//Predecessor of id //
n.closest _ preceding _ node (id )
for i = m down to 1
if (finger [i] ∈ (n,id ))
return finger [i];
return n;
```

Fig. 3 Pseudocode

V. RESULTS

Figs. 4-6 show the simulation results for average query response time, number of hops to look up and data exchanged. Simulations were also conducted for varying number of nodes to evaluate average path length and average search time as shown in Figs. 7 and 8.
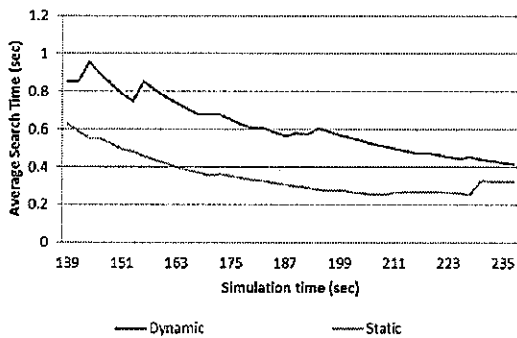

Fig. 4 Average Query response time

It is observed from Fig. 4 that the average query response time for the static nodes is considerably lower than the dynamic node scenario.
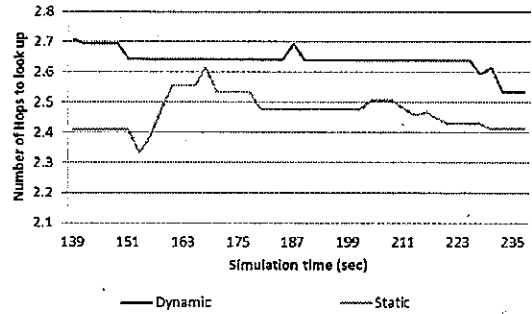

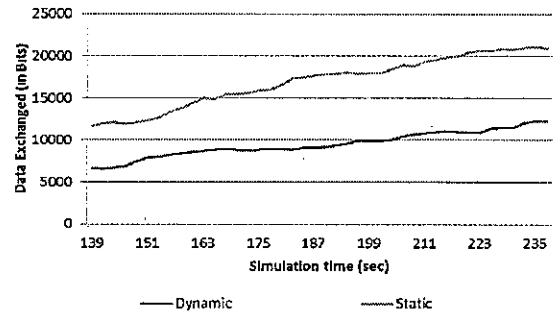Fig. 5 Number of hops to look up

Fig. 6 Data Exchanged in number of bits

From Fig. 5, it is observed that the lookup time increases owing to the dynamic nature of nodes. As seen from Fig. 6, the data exchanged increases considerably for static network when it is compared to the dynamic network.
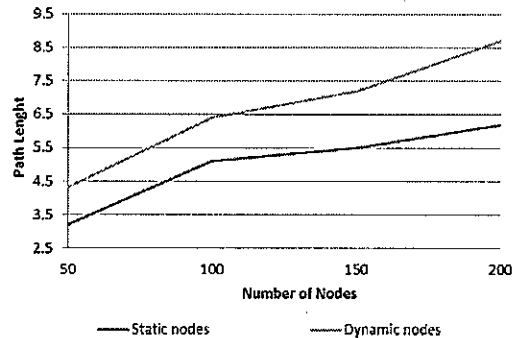

Fig. 7 Average Path Length

Simulation was conducted for varying number of nodes to evaluate average path length. From Fig. 7 it is observed that the Average path length for static node is significantly lower than the dynamic node by an average of 28.07%.

It is observed from Fig. 8 that the average search time increases for dynamic node when compared to static node scenario. On an average, the dynamic nature of nodes requires 33.36% more average search time than static nodes.
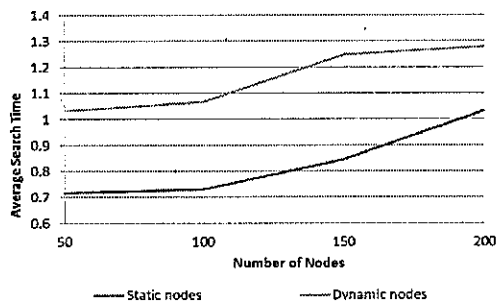
Fig. 8 Average Search Time

VI. CONCLUSION

Chord algorithm is an efficient lookup algorithm for the distributed P2P networking applications. A structured approach enhances the lookup performance in a high bandwidth wired network; though unnecessary overhead is generated in overlay networks that impact performance negatively in Wireless Mesh Network (WMN). It has been proved that a structured approach increases lookup performance for a high bandwidth wired network; also, overlay networks may create pointless overhead that could adversely impact performance in an unstable environment such as a WMN. This study investigates existing CHORD protocol on WMN when nodes are static and dynamic. The performance of CHORD protocol for metrics like average search time, response time, is evaluated for WMN. Simulation results demonstrate that the dynamic nodes affect the performance of the WMN negatively when compared to the static nodes.

REFERENCES

[1] M. Kelaskar, V. Matossian, P. Mehra, D. Paul, and M. Parashar, "A Study of Discovery Mechanisms for Peer-to-Peer Applications.

[2] Mohamed Hefeeda, "Peer-to-Peer Systems". School of Computing Science, Simon Fraser University, Canada.

[3] Stratis Ioannidis, Peter Marbach. "On the Design of Hybrid Peer-to-Peer Systems" (J). ACM SIGMETRICS Performance Evaluation Review, 2008, 36(1): 157-168.

[4] Bartosz Biskupski, Jim Dowling, "Jan Sacha. Properties and Mechanisms of Self-Organizing MANET and P2P Systems". ACM Transactions on Autonomous and Adaptive Systems (TAAS), 2007, 2(1): 1-34.

[5] Eng Keong Lua, Jon Crowcroft, Marcelo Pias, Ravi Sharma and Steven Lim, "A Survey and Comparison of Peer-to-Peer Overlay Network Schemes, IEEE Communications Survey and Tutorial", March 2004.

[6] Ian F. Akyildiz, Xudong Wang, Weilin Wang, "Wireless Mesh Networks: A Survey, Computer Networks" 47 (2005) 445–487.

[7] J. Jun, M.L. Sichitiu, "The Nominal Capacity of Wireless Mesh Networks, IEEE Wireless Communications" 10 (5) (2003) 8–14.

[8] Ion Stoica, Robert Morris, David Liben-Nowell, David R. Karger, M. Frans Kaashoek, Frank Dabek, Hari Balakrishnan, "Chord: A Scalable Peer-to-peer Lookup Protocol for Internet Applications University of California".

[9] Xianghan Zheng and Vladimir Oleshchuk, "Improvement of Chord Overlay for P2Psip-Based Communication Systems, International Journal of Computer Networks & Communications (IJCNC)", Vol. 1, No.3, October 2009.

[10] Jani, H. and C. Gonzalo, "Evaluation of DHTs from the Viewpoint of Interpersonal Communications, in Proceedings of the 6th International Conference on Mobile and Ubiquitous Multimedia." 2007, ACM: Oulu, Finland.

[11] Karger, D. R., & Ruhl, M. (2005) "Diminished Chord: A Protocol for Heterogeneous Subgroup Formation in Peer-to-Peer Networks. In Peer-to-Peer Systems III" (pp. 288-297). Springer Berlin Heidelberg.

[12] Zöls, S., Schollmeier, R., Kellerer, W., & Tarlano, A. (2005). "The Hybrid Chord Protocol: A Peer-to-Peer Lookup Service for Context-Aware Mobile Applications. In Networking-ICN" 2005 (pp. 781-792). Springer Berlin Heidelberg.

[13] Burresi, S., Canali, C., Renda, M. E., & Santi, P. (2008, March). "MeshChord: a Location-Aware, Cross-Layer Specialization of Chord for Wireless Mesh Networks (Concise Contribution). In Pervasive Computing and Communications", 2008. PerCom 2008. Sixth Annual IEEE International Conference on (pp. 206-212). IEEE.

[14] Novak, D. & Zezula, P. (2006, May). "M-Chord: A Scalable Distributed Similarity Search Structure. In Proceedings of the 1st International Conference on Scalable Information Systems" (p. 19). ACM.

[15] Thaalbi, M., Meddahi, A., Bejaoui, T. & Tabbane, N. (2011, October). "An Enhanced Chord-Based P2P Lookup Protocol for Mobile Ad Hoc Networks. In Wireless Days (WD)", 2011 IFIP (pp. 1-5). IEEE.

Mechanical Properties and Chloride Diffusion of Ceramic Waste Aggregate Mortar Containing Ground Granulated Blast–Furnace Slag

H. Higashiyama, M. Sappakittipakorn, M. Mizukoshi, O. Takahashi

Abstract—Ceramic Waste Aggregates (CWAs) were made from electric porcelain insulator wastes supplied from an electric power company, which were crushed and ground to fine aggregate sizes. In this study, to develop the CWA mortar as an eco–efficient, ground granulated blast–furnace slag (GGBS) as a Supplementary Cementitious Material (SCM) was incorporated. The water–to–binder ratio (W/B) of the CWA mortars was varied at 0.4, 0.5, and 0.6. The cement of the CWA mortar was replaced by GGBS at 20 and 40% by volume (at about 18 and 37% by weight). Mechanical properties of compressive and splitting tensile strengths, and elastic modulus were evaluated at the age of 7, 28, and 91 days. Moreover, the chloride ingress test was carried out on the CWA mortars in a 5.0% NaCl solution for 48 weeks. The chloride diffusion was assessed by using an electron probe microanalysis (EPMA). To consider the relation of the apparent chloride diffusion coefficient and the pore size, the pore size distribution test was also performed using a mercury intrusion porosimetry at the same time with the EPMA. The compressive strength of the CWA mortars with the GGBS was higher than that without the GGBS at the age of 28 and 91 days. The resistance to the chloride ingress of the CWA mortar was effective in proportion to the GGBS replacement level.

Keywords—Ceramic waste aggregate, Chloride diffusion, GGBS, Pore size distribution.

I. INTRODUCTION

CERAMIC wastes discarded worldwide from ceramic industries, demolition/construction sites, electric power companies, and railway companies are one of the materials possibly recyclable as aggregate and/or pozzolans. The utilization of the ceramic wastes has been investigated by many researchers. In the existing literature [1]–[4], however, there is a shortage on the utilization of ceramic waste aggregates (CWAs) provided from electric porcelain insulators. They have concluded that the CWAs in concrete/mortar showed no negative influence on mechanical and permeation properties. The authors [5]–[8] have also investigated on the compressive strength and the resistance to chloride ingress on the CWA

H. Higashiyama is an Associate Professor at the Department of Civil and Environmental Engineering, Kinki University, Higashiosaka, Osaka 577-8502 Japan (corresponding author to provide phone: +81-6-4307-3553; fax: +81-72-995-5192; e-mail: h-hirosi@civileng.kindai.ac.jp).

M. Sappakittipakorn is an Assistant Professor at the Department of Civil Engineering, King Mongkut's University of Technology North Bangkok, Bangkok, 10800 Thailand (e-mail: manote.s@eng.kmutnb.ac.th).

M. Mizukoshi is a Professor at the Department of Civil Engineering, Kagawa National College of Technology, Takamatsu, Kagawa 761-8058 Japan (e-mail: m-mizu@t.kagawa-nct.ac.jp).

O. Takahashi is a General Manager at The Kanden L&A Company, Ltd., Osaka 550-0013 Japan (e-mail: o_takahashi@kla.co.jp).

mortars. The replacement of entire fine aggregates with the CWA in mortar reduces the chloride ion penetration when compared with river sand (RS) mortar. On the other hand, it is well–known that a mineral admixture of Ground Granulated Blast–furnace Slag (GGBS) with a supplementary cementitious material (SCM) with partial cement replacement is advantage in the long-term strength gain and the resistance to weathering and aggressive chemical action. In [9], [10], the chloride ingress tests were performed on the CWA mortars partially replaced with GGBS at 15, 30, and 45% by weight. But, the water–to–binder ratio (W/B) of the CWA mortar was only 0.5. From the results [10], the GGBS significantly decreased the penetration depth of chloride ion into the CWA mortar. The changing of the apparent chloride diffusion coefficients of the CWA mortars with the GGBS was relatively small along the immersion time up to 96 weeks. Consequently, the chloride resistance of the CWA mortar was more effective with increasing the GGBS replacement level up to 45% tested.

In this study, the CWA mortars with further wide range of W/B, i.e., 0.4, 0.5, and 0.6 were investigated on the mechanical properties and the chloride ingress. The cement was partially replaced with the GGBS at 20 and 40% by volume. The mechanical tests on compressive and splitting tensile strengths were carried out at the age of 7, 28, and 91 days while the chloride ingress test was performed after 48 weeks immersion in a 5.0% NaCl solution. The chloride concentration profiles of the CWA mortars were obtained by using the electron probe microanalysis (EPMA). Furthermore, the pore size distribution in the CWA mortars was measured by using a mercury intrusion porosimetry to understand a relation with the apparent chloride diffusion coefficient.

II. MATERIALS AND TEST METHODS

A. Materials and Mixture Proportions

Electric porcelain insulators such as suspension porcelain insulators as shown in Fig. 1 were transferred to CWAs at a recycle plant of The Kanden L&A Company, Ltd. in Japan via the processes of crushing and grinding. After obtaining the blunt edge CWAs through these processes, the particle size ranging from 0.075 to 5.0 mm by sieving was used as fine aggregate in this study as shown in Fig. 2. The grain size distribution of the CWA with the grading requirements (dashed lines) of the standard distribution specified in JIS A 5005 [11] is presented in Fig. 3. The grain size distribution of the CWA after going through the above processes is within the standard

distribution except for one particle size of 2.5 mm. The specific gravity, water absorption, and the fineness modulus of the CWA were 2.40, 0.7% by weight, and 3.20.
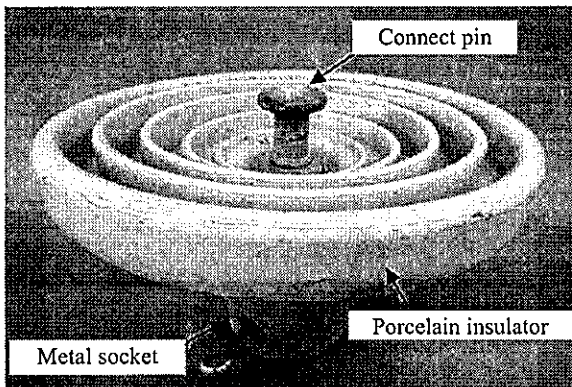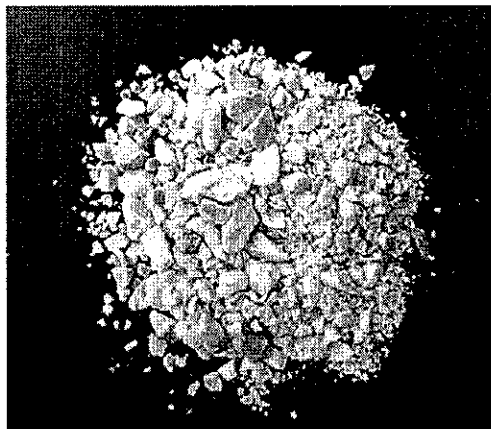

Fig. 1 Suspension porcelain insulator

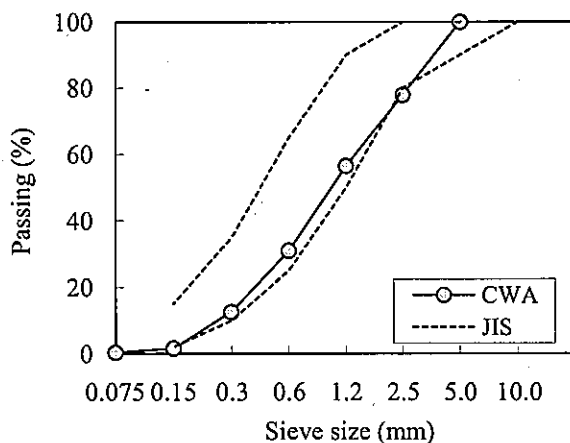Fig. 2 Ceramic waste fine aggregates

Fig. 3 Grain size distribution of CWA

The cement was ordinary Portland cement (OPC) with the specific gravity of 3.15 and the specific surface area by Blaine of 3360 cm^2/g. The GGBS supplied from a slag cement company was used as a SCM in this study. The GGBS was with the specific gravity of 2.91 and the specific surface area by Blaine of 6230 cm^2/g. The chemical and physical properties of

cement, GGBS, and CWA used in this study are given in Table I.

TABLE I
CHEMICAL AND PHYSICAL PROPERTIES

Properties	Cement	GGBS	CWA
Chemical compositions (wt.%)			
SiO_2	20.68	33.80	70.90
Al_2O_3	5.28	15.00	21.10
Fe_2O_3	2.91	0.27	0.81
CaO	64.25	43.10	0.76
MgO	1.40	5.63	0.24
SO_3	2.10	–	–
Na_2O	0.28	0.28	1.47
K_2O	0.40	0.31	3.57
TiO_2	0.28	0.52	0.33
P_2O_5	0.25	–	–
MnO	0.09	0.20	–
SrO	0.06	–	–
S	–	0.77	–
Cl	0.015	0.004	–
Loss on ignition	1.80	0.05	–
Specific gravity	3.15	2.91	2.40
Specific surface area (cm^2/g)	3360	6230	–

TABLE II
MIXTURE PROPORTION OF CWA MORTAR

Mixture	W/B (%)	Water (kg/m^3)	Cement (kg/m^3)	CWA (kg/m^3)	GGBS (kg/m^3)
CWA40-0	40.0	303	758	1095	0
CWA40-20	40.6	303	607	1095	140
CWA40-40	41.2	303	455	1095	280
CWA50-0	50.0	303	606	1211	0
CWA50-20	50.8	303	485	1211	112
CWA50-40	51.5	303	364	1211	224
CWA60-0	60.0	303	505	1288	0
CWA60-20	60.8	303	404	1288	94
CWA60-40	61.8	303	303	1288	187

In the mixture proportion of the previous study [9], [10], the CWA–to–binder ratio (S/B) of the CWA mortars with and without GGBS was simply kept constant at 2.0 by weight. In this study, however, the mixture proportion was designed by volume as presented in Table II. Accordingly, the cement in the CWA mortar was also replaced by the GGBS at 20 and 40% by volume. Therefore, the W/B was almost 0.4, 0.5, and 0.6.

B. Specimens

For all mixtures, the CWA mortars were prepared in a Hobart mixer of 5 L capacity. The mixing process started with the blending of the OPC, GGBS and CWA for 1 min and was followed with the addition of water and further mixing for 3 min. For each mixture, eighteen cylindrical specimens of 50 mm diameter and 100 mm height were cast; nine of which were used in compression tests and the other nine were used in splitting tensile tests at the age of 7, 28, and 91 days (three specimens at each time). Furthermore, two cylindrical specimens of 100 mm diameter and 200 mm height were prepared for chloride ingress tests at 48 and 96 weeks immersion (one specimen at each time) which were employed

in EPMA. In this paper, a result of the chloride ingress test at 48 weeks immersion was reported. The specimens for 96 weeks immersion are under continuing. After casting, all specimens were covered with a plastic waterproof sheet for 24 h. Subsequently, they were demoulded and cured in a water tank at 20±2 °C.

C. Test Methods

Compression and splitting tensile tests were carried out on the three specimens for each mixture at the age of 7, 28, and 91 days. In the compression test, two strain gauges were glued on a specimen to calculate the elastic modulus.

At the age of 7 days, the specimens for the chloride ingress test were cut down from 200 mm to 150 mm height with 50 mm top end discarded to eliminate the influence of segregation. After the specimens were allowed to dry in a laboratory condition at 20±2°C for 24 h, they were epoxy coated leaving only one sawn surface free of coating and were kept for additional 24 h to cure the epoxy resin. Then, they were fully immersed in a 5.0% NaCl solution in hermetic tanks at 20±2 °C for 48 weeks until the EPMA. The NaCl solution was changed at each three months interval.

After the immersion was completed, one specimen for each mixture was followed with the EPMA. The specimens were cut into 25 mm width and 60 mm length as shown in Fig. 4. By using the JEOL JXA-8200 instrument, the resized specimens were scanned to identify the amount of chloride ions at tiny single spot throughout its surface. The measurement conditions were an accelerating voltage of 15 kV, a beam current of 0.2 μA, a pixel size of 200 μm, a probe diameter of 150 μm, and the number of mapping points of 400 × 400 pixels. The chloride concentration profiles were plotted and were analyzed to find the apparent chloride diffusion coefficient.
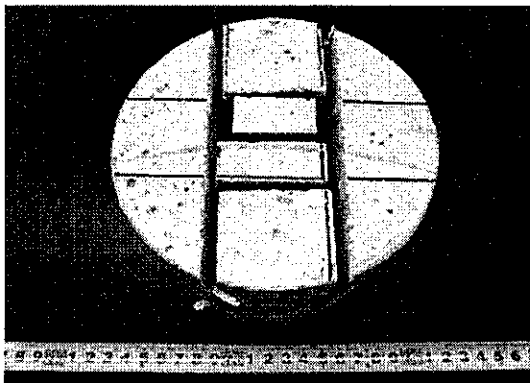

Fig. 4 Preparation of specimen for EPMA

By using the same CWA mortars of the EPMA, the test pieces with 2.5 to 5.0 mm size were obtained from the center of cylindrical specimen by crushing. The samples of 30 g were collected from them and were vacuum–dried for 24 h. The pore size distribution test was performed using a mercury intrusion porosimetry (PoreMaster 60GT, Quantachrime). For each mortar, the sample of the pore size distribution ranging from 0.007 to 200 μm of pore diameter was measured.

TABLE III
AVERAGED RESULTS OF MECHANICAL PROPERTIES

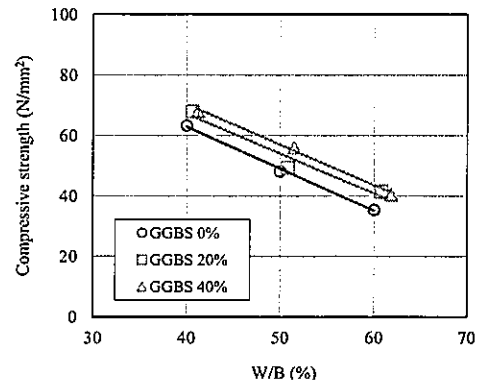| Mixture	Compressive strength (N/mm²)	Tensile strength (N/mm²)	Elastic modulus (kN/mm²)
CWA40-0	63.3	3.65	31.9
CWA40-20	68.0	4.20	32.1
CWA40-40	68.1	3.90	32.1
CWA50-0	48.2	3.33	28.5
CWA50-20	49.5	3.26	28.5
CWA50-40	56.1	4.13	29.8
CWA60-0	35.5	2.91	28.3
CWA60-20	41.5	3.51	29.2
CWA60-40	40.5	3.95	28.4

Fig. 5 Compressive strength and W/B

III. RESULTS AND DISCUSSION

A. Mechanical Properties

The averaged values of compressive and splitting tensile strengths and elastic modulus at the age of 28 days for all mixtures are listed in Table III. The compressive strength as a function of W/B is presented in Fig. 5. It is observed that the compressive strength was linearly increased with decreasing the W/B. From those regression lines, the compressive strength increased with the GGBS replacement level. The tensile strength and elastic modulus are presented with the compressive strength in Figs. 6 and 7, respectively. The tensile strength of the CWA mortar was increased with the compressive strength and was increased at a higher rate when the GGBS was incorporated. However, the influence of GGBS replacement level on such increase was small. The elastic modulus was also increased when the compressive strength was increased. But, there was no difference on the increasing rate between the CWA mortar with and without the GGBS.

B. Chloride Ion Penetration Depth

By using the EPMA method, the 25 × 60 mm cross sectional area of specimens was scanned to quantify the chloride concentration. The mapping result, for example, of specimens with W/B of 0.5 is shown in Fig. 8. In this figure, the upper side is the exposed surface. The chloride ion penetration depth was decreased with increasing the GGBS replacement level. The chloride concentration profiles, which were averaged along the same penetration depth at 0.2 mm intervals, are shown in Fig. 9. It can be seen that the GGBS has great inhibiting ability against

the chloride ingress. The effectiveness of GGBS as the SCM has been widely reported so far. Similarly, as reported in the previous study [9], [10], the chloride ion penetration depth becomes shorter when the W/B is lower and the GGBS replacement level is higher. This is attributed to the more refined pore structure of the hydrated cementitious material using the GGBS and the binding adsorption capacity which is chloride ion onto the hydrated slag wall [12].
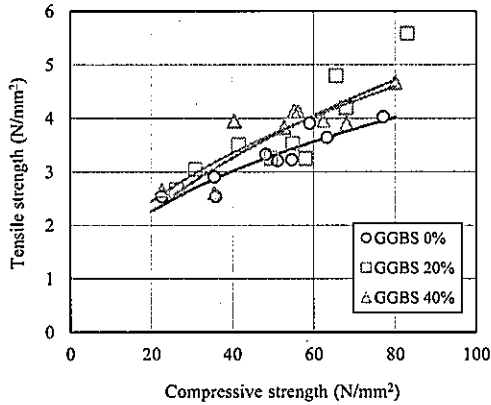

Fig. 6 Tensile strength and compressive strength
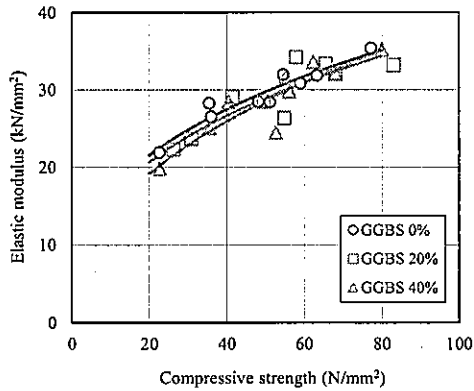
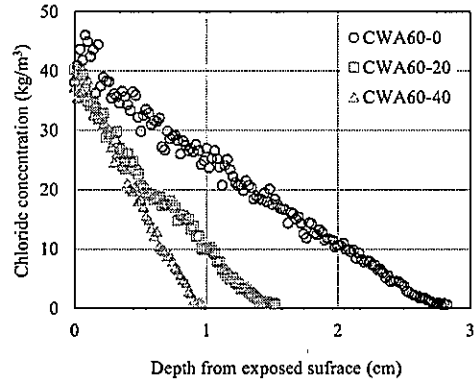Fig. 7 Elastic modulus and compressive strength
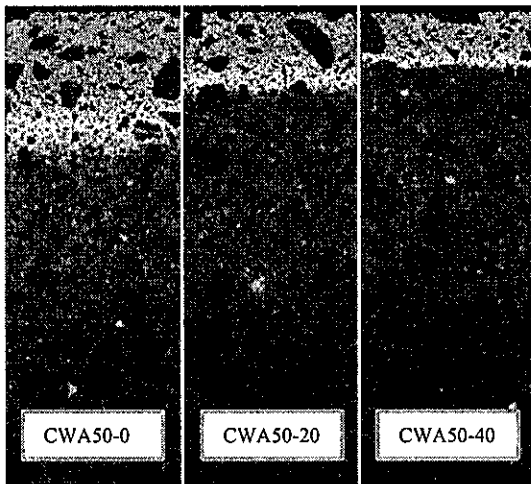
Fig. 8 Mapping results of chloride concentration
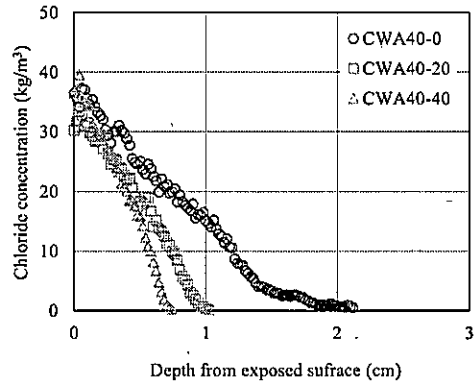
(a) W/B = 40%
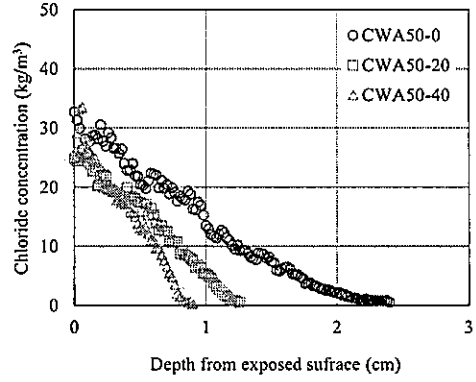
(b) W/B = 50%

(c) W/B = 60%

Fig. 9 Chloride concentration profiles

C. Apparent Chloride Diffusion Coefficient

The apparent chloride diffusion coefficient was determined by fitting the chloride concentration profile to the following Fick's second low.

$$C(x,t) = C_i + C_0 \left(1 - erf \frac{x}{2\sqrt{D_a \cdot t}} \right) \qquad (1)$$

where $C(x, t)$ is the chloride concentration (kg/m^3) at depth x (cm) and exposure time t (year), C_i is the initial chloride concentration (kg/m^3), C_0 is the surface chloride concentration (kg/m^3), D_a is the apparent chloride diffusion coefficient

(cm²/year), and *erf* is the error function.

In the analysis of the chloride concentration profile, for the surface chloride concentration, the maximum value obtained from the result of EPMA was used and the apparent chloride diffusion coefficient was obtained by the curve fitting. The apparent chloride diffusion coefficients after analyzed are given in Table IV. Furthermore, the relation of the apparent chloride diffusion coefficient and the GGBS replacement level is shown in Fig. 10. The apparent chloride diffusion coefficient decreased with increasing the GGBS replacement level. Especially, the apparent chloride diffusion coefficient of the CWA mortar with the W/B of 60% decreased sharply when the

TABLE IV
APPARENT CHLORIDE DIFFUSION COEFFICIENTS

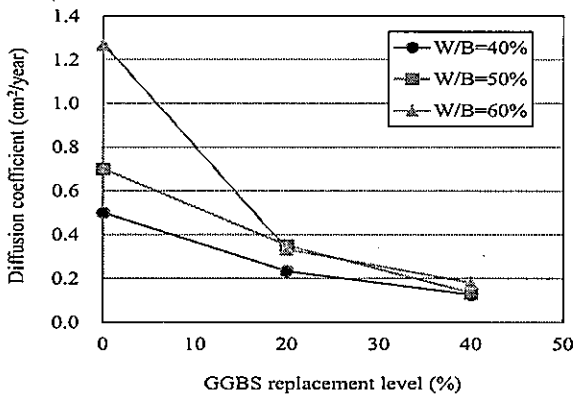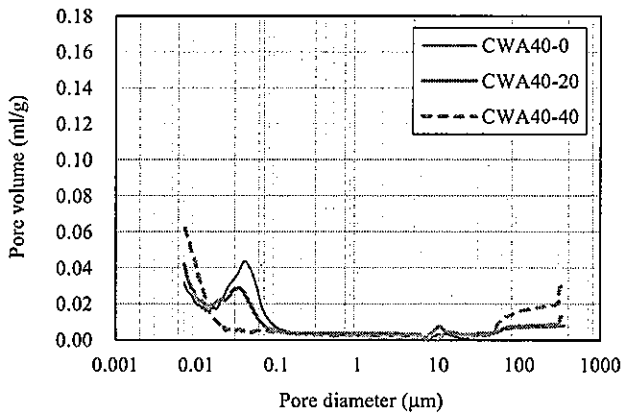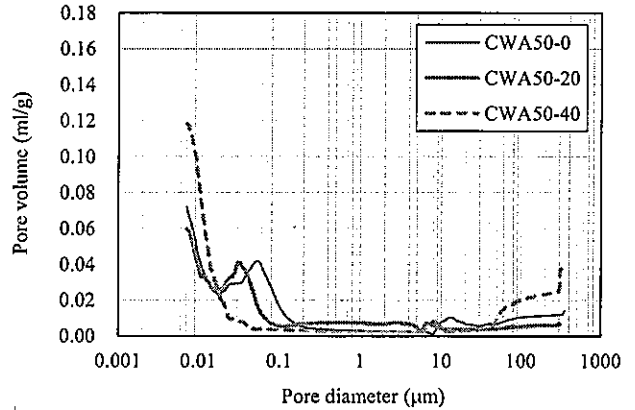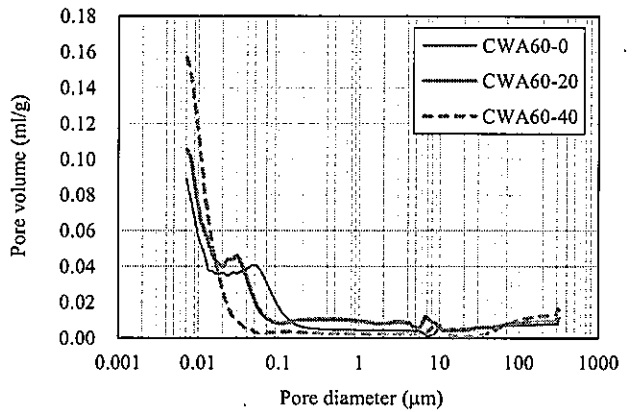| Mixture	W/B (%)	GGBS replacement (vol.%)	Apparent chloride diffusion coefficient (cm²/year)
CWA40-0	40.0	0	0.500
CWA40-20	40.6	20	0.233
CWA40-40	41.2	40	0.126
CWA50-0	50.0	0	0.700
CWA50-20	50.8	20	0.351
CWA50-40	51.5	40	0.134
CWA60-0	60.0	0	1.271
CWA60-20	60.8	20	0.333
CWA60-40	61.8	40	0.181

Fig. 10 Relation of apparent chloride diffusion coefficient and GGBS replacement level

(a) W/B = 40%

(b) W/B = 50%

(c) W/B = 60%

Fig. 11 Pore size distributions

GGBS was contained at 20% by volume. At the GGBS replacement level of 40%, the apparent chloride diffusion coefficient of each specimen was close.

D. Pore Size Distribution

The pore size distributions ranging from 0.007 to 200 μm pore diameter are shown in Fig. 11. The pore volume was clearly decreased in the region of the smaller pore size when the W/B was lower. Furthermore, the pore size distribution was shifted to the smaller pore diameter with increasing the GGBS replacement level. One peak value of the pore volume was observed around 0.04 μm in the CWA mortar without and with the GGBS of 20%. However, in the CWA mortar with the GGBS of 40%, no peak value exhibited and the smaller pore size less than 0.04 μm mostly occupied the pore volume.

From the results shown in Fig. 11, the pore size distribution significantly changed in the smaller pore size less than about 0.2 μm. In this study, the average pore volume ranging from 0.007 to 0.2 μm pore diameter was calculated for all the specimens. Then, an exponential relation of the apparent chloride diffusion coefficient and the average pore volume can be obtained as shown in Fig. 12. Both the apparent chloride diffusion coefficient and the pore size distribution depend on the hydration of cementitious material and the binding adsorption capacity depends on the hydrated slag wall.

However, those are changed with the time. Therefore, further investigation might be needed to understand its relation shown in Fig. 12.
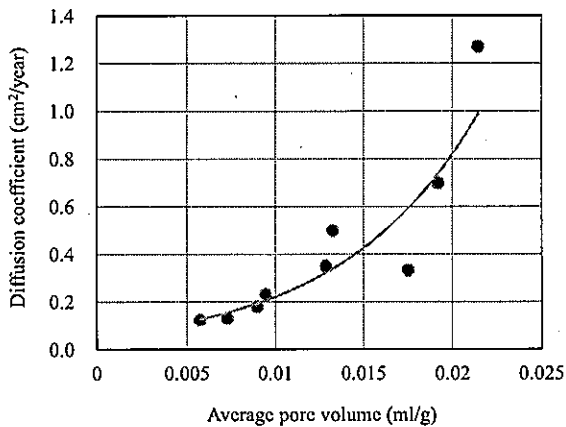

Fig. 12 Relation of apparent chloride diffusion coefficient and average pore volume

IV. CONCLUSIONS

In this study, the mechanical properties and chloride diffusion of the CWA mortars containing the GGBS with different W/B and replacement levels were investigated. The following conclusions can be drawn.

(1) The compressive strength of the CWA mortar increased with increasing the GGBS replacement level. The splitting tensile strength of the CWA mortar with the GGBS increased in the region of the higher compressive strength while the influence of containing the GGBS to the elastic modulus was small.

(2) The GGBS has great inhibiting ability against the chloride ingress. The apparent chloride diffusion coefficient decreased with increasing the GGBS replacement level. However, in the higher GGBS replacement of 40%, the difference of the apparent chloride diffusion coefficient was small within the W/B of 40 to 60% tested.

(3) The pore volume in the region of the smaller pore size was clearly decreased by the GGBS replacement. The pore size distribution significantly changed in the smaller pore size less than about 0.2 μm. The average pore volume ranging from 0.007 to 0.2 μm pore diameter might be related to the apparent chloride diffusion coefficient as an exponential function.

REFERENCES

[1] H. Hata, A. Nakashita, T. Ohmura, and H. Itou, "Strength development of concrete containing granulated abandonment insulator," *Proceedings of Japan Concrete Institute*, vol. 26, no. 1, 2004, pp. 1683–1688.

[2] R. M. Senthamari and P. D. Manoharan, "Concrete with ceramic waste aggregate," *Cement and Concrete Composites*, vol. 27, 2005, pp. 910–913.

[3] R. M. Senthamari, P. D. Manoharan, and D. Gobinath, "Concrete made from ceramic industry waste: durability properties," *Construction and Building Materials*, vol. 25, 2011, pp. 2413–2419.

[4] A. E. P. G. A. Jacintho, M. A. Campos, V. A. Paulon, G. Camarini, R. C. C. Lintz, and L. A. G. Barbosa, "The use of crushed porcelain electrical isolators as fine aggregate in mortars," Proceedings of Concrete under Sever Conditions, 2010, pp.1593–1600.

[5] H. Higashiyama, F. Yagishita, M. Sano, and O. Takahashi, "Compressive strength and resistance to chloride penetration of mortars using ceramic waste as fine aggregate," *Construction and Building Materials*, vol. 26, 2012, pp. 96–101.

[6] H. Higashiyama, M. Sappakittipakorn, M. Sano, and F. Yagishita, "Chloride ion penetration into mortar containing ceramic waste aggregate," *Construction and Building Materials*, vol. 33, 2012, pp. 48–54.

[7] H. Higashiyama, K. Yamauchi, M. Sappakittipakorn, M. Sano, and O. Takahashi, "A visual investigation on chloride ingress into ceramic waste aggregate mortars having different water to cement ratios," *Construction and Building Materials*, vol. 40, 2013, pp. 1021–1028.

[8] H. Higashiyama, M. Sappakittipakorn, M. Sano, O. Takahashi, and S. Tsukuma, "Charateristics of chloride ingress into mortars containing ceramic waste aggregate," *Journal of Material Cycles and Waste Management*, DOI: 10.1007/s10163-014-0264-8.

[9] H. Higashiyama, M. Sappakittipakorn, M. Mizukoshi, and O. Takahashi, "Efficiency of ground granulated blast–furnace slag replacement in ceramic waste aggregate mortar," *Cement and Concrete Composites*, vol. 49, 2014, pp. 43–49.

[10] H. Higashiyama, M. Sappakittipakorn, M. Mizukoshi, and O. Takahashi, "Time dependency on chloride diffusion of ceramic waste aggregate mortars containing ground granulated blast–furnace slag," *Journal of The Society of Materials Science, Japan*, to be published.

[11] JIS A 5005, "Crushed stone and manufactured sand for concrete," *Japanese Industrial Standards*, 2010, pp. 146–148.

[12] R. N. Swamy and A. Bouikni, "Some engineering properties of slab concrete as influenced by mix proportioning and curing," *ACI Materials Journal*, vol. 87, 1990, pp.210–220.

Human Walking Vertical Force and Vertical Vibration of Pedestrian Bridge Induced by Its Higher Components

M. Yoneda

Abstract— The purpose of this study is to identify human walking vertical force by using FFT power spectrum density from the experimental acceleration data of the human body. An experiment on human walking is carried out on a stationary floor especially paying attention to higher components of dynamic vertical walking force. Based on measured acceleration data of the human lumbar part, not only in-phase component with frequency of $2f_w$, $3f_w$, but also in-opposite-phase component with frequency of $0.5f_w$, $1.5f_w$, $2.5f_w$ where f_w is the walking rate is observed. The vertical vibration of pedestrian bridge induced by higher components of human walking vertical force is also discussed in this paper. A full scale measurement for the existing pedestrian bridge with center span length of 33 m is carried out focusing on the resonance phenomenon due to higher components of human walking vertical force. Dynamic response characteristics excited by these vertical higher components of human walking are revealed from the dynamic design viewpoint of pedestrian bridge.

Keywords—Simplified method, Human walking vertical force, Higher component, Pedestrian bridge vibration.

I. INTRODUCTION

NEEDLESS to say, human walking force is necessary when carrying out dynamic response analysis for the pedestrian bridges to check the discomfort for the users being on a pedestrian bridge. Generally speaking, the relationship between footstep and dynamic load factor or footstep and walking speed proposed by Kajikawa [1] has been selected in Japan for the dynamic response analysis of the pedestrian bridges although several researchers have investigated the vertical forces imparted by individual pedestrians on a stationary floor. In the overseas, not only the resonant component (=footstep component f_w of generally about 2 steps / s) but also higher component ($2f_w$, $3f_w$) are often considered when carrying out dynamic response analysis for the pedestrian bridges [2].

On the other hand, the synchronization problem in the lateral direction on a footbridge is pointed out by Fujino , et al. [3]. The phenomenon of synchronous lateral excitation caused by pedestrians walking on pedestrian bridges such as the London Millennium Bridge has increasingly attracted public attention [4]. The dynamic load factor (DLF) in lateral direction is short

M. Yoneda is a Professor at the Department of Civil and Environmental Engineering, Kinki University, Higashiosaka, Osaka 577-8502 Japan (corresponding author to provide phone: +81-6-4307-3546; fax: +81-6-6730-1320; e-mail: yoneda@civileng.kindai.ac.jp).

of measured data compared with that in vertical direction.

Special experimental apparatus such as force transducers must be provided in order to measure a human walking force exactly. Accordingly, it will be acceptable from the practical viewpoint if a relatively simple and accurate method to evaluate human walking force for many pedestrians is used. It can be easily imagined that there is a method to measure the acceleration data using accelerometers set up to the lumber part of a person. In fact, it is already pointed out by Kobori and Kajikawa [5] that the human walking force measured by special experimental apparatus is nearly equal to an inertia force at the lumbar part of a person being tested (=[Weight of a person]×[acceleration measured at the lumbar part]). However, it may be noticed that the acceleration data of the human body involves so many responses in a lot of frequencies and that the main response in a principal frequency should be picked out by means of digital band-pass filter.

The purpose of this study is to propose the simplified method in order to identify human walking force by using FFT power spectrum density from the experimental acceleration data of the human body. An experiment on human walking is carried out on a stationary floor especially paying attention to higher components of dynamic vertical walking force. The vertical vibration of pedestrian bridge induced by higher components of human walking vertical force is also discussed in this paper. A full scale measurement for the existing pedestrian bridge with center span length of 33 m is carried out focusing on the resonance phenomenon due to higher components of human walking vertical force. Dynamic response characteristics due to these vertical higher components of human walking are revealed from the dynamic design viewpoint of pedestrian bridge.

II. ACCURACY OF PRESENT METHOD FOR SINUSOIDAL WAVE

In this Chapter, the accuracy of the proposed method by using FFT power spectrum density is discussed for the results of sinusoidal wave. Sinusoidal wave can be written in the form:

$$y = a\sin \omega t = a\sin 2\pi f t \qquad (1)$$

where a is the amplitude, ω is the circular frequency or angular velocity of the motion, f is the frequency of the motion. Power spectrum density P_f based on FFT (Fast Fourier Transform) in the frequency of f for the sinusoidal wave shown in equation (1) is given by
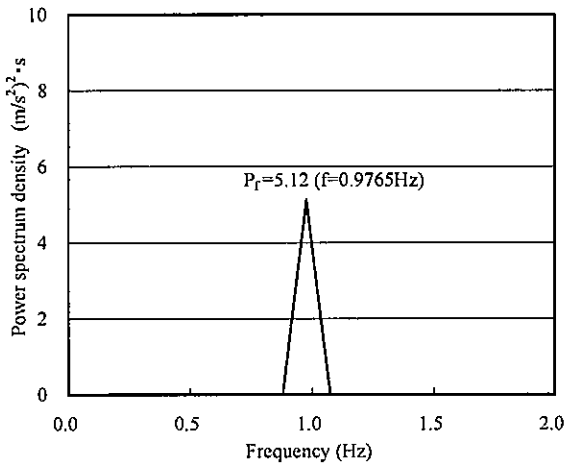
Fig. 1 Power spectrum density by FFT analysis (N=2,048, a=1.0m/sec², f=0.9765Hz)

Fig.2 Power spectrum density by FFT analysis (N=2,048, a=1.0m/sec², f=1.000Hz)

$$P_f = a^2 \times \frac{T}{2} \qquad (2)$$

where T is the duration of the wave without time corresponding to trailing zeros.

FFT analysis is carried out for the simulated acceleration wave with a =1.0m/s² and f =0.9765 Hz on condition that the sampling time Δt is 0.005 s and data number N is 2,048. Fig. 1 shows the power spectrum density obtained by FFT analysis. It can be seen from this Fig. 1 that the peak value of the power spectrum density is 5.12 (m/s²) · s. Substituting P_f =5.12 and T =2,048 × 0.005=10.24 s into equation [2] gives a =1.0m/s which is equal to the amplitude of the simulated original acceleration wave. However, attention needs to be paid to the fact that the power spectrum density based on FFT is given by every 1/(N Δt). For the example wave with a =1.0m/s² and f =0.9765 Hz (Δt=0.005 s), the power spectrum density in the frequency of 0.9765 Hz is correctly evaluated as the power spectrum density is given by every 1/(N Δt)=1/(2,048 × 0.005) ≒0.09765Hz.

On the other hand, FFT analysis is also carried out for the simulated acceleration wave with a =1.0m/s² and f =1.000 Hz on condition that the sampling time Δt is 0.005 s and data number N is 2,048. Fig.2 shows the power spectrum density
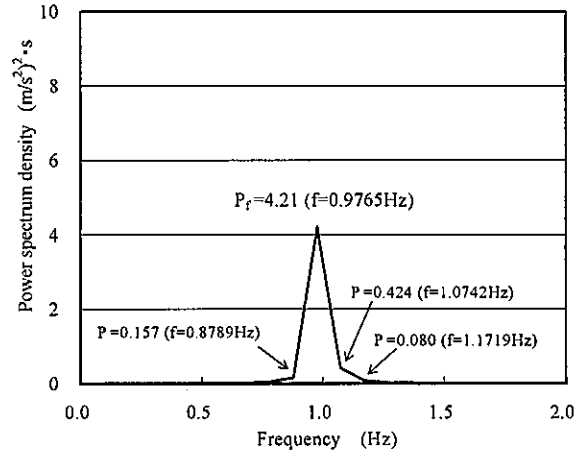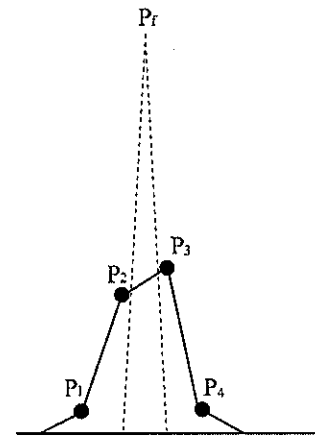

Fig. 3 Trapezoidal power spectrum density

obtained by FFT analysis. It can be seen from this Fig. 2 that the peak value of the power spectrum density is reduced to be 4.21 (m/s²) · s and scattered on both frequencies. This is the reason why the output frequency around 1 Hz by FFT analysis is 0.9765 Hz, 1.0742 Hz and 1.000Hz is not to be the output frequency. Accordingly, in this research, it is assumed that the power spectrum density on the top 4 (P_1, P_2, P_3, P_4) is summed

TABLE I

DIFFERENCE FOR THE SIMULATED ACCELERATION WAVE

Frequency (Hz)	Amplitude (m/s²)	Data Number	Δt (sec)	$P_1+P_2+P_3+P_4$ (m/sec)² · s	Calculated amplitude (m/s²)	Difference (%)
0.9765	1.0000	2,048	0.005	5.12	1.0000	0.00
1.0000	1.0000	2,048	0.005	4.87	0.9753	-2.47
0.9765	1.0000	2,049	0.005	4.64	0.9517	-4.83
1.0000	1.0000	2,049	0.005	4.87	0.9750	-2.50
0.9765	1.0000	3,072	0.005	7.09	0.9608	-3.92
1.0000	1.0000	3,072	0.005	7.26	0.9723	-2.77

up as shown in equation (3) with reference to Fig. 3.

$$P_f \doteqdot P_1 + P_2 + P_3 + P_4 \tag{3}$$

Generally speaking, FFT analysis requires data number which is equal to the raised 2 to the nth power. Therefore, in case of N=2,049, FFT analysis is carried out for data number of N=4,096 which is added to the trailing zero of 2,047. It follows that the differences may be varied because the dominant frequency is not equal to the output frequency owing to the change of resolution. Accordingly, the accuracy of the present method is checked by changing data number of the simulated acceleration wave. These analytical results are shown in Table 1. It can be seen from this Table 1 that the difference in estimated value for the simulated sinusoidal wave is within the range of −5%.

III. EXPERIMENTS ON HUMAN WALKING

A. Measuring Method

Experiments on human walking are carried out to investigate human walking characteristics according to the following procedure.

· Accelerometers in the vertical direction are set up to the lumbar part of a person being tested as shown Photo.1.

· The person being tested walks straight for 20 m on a stationary floor.

· The person being tested measures walking time with the stopwatch.

In principle, experiments on human walking were performed three times for every person being tested to obtain acceleration response which was filtered by 10 Hz analog low pass and sampled by Δt=0.005 s. All persons being tested were senior healthy students belonging to my research laboratory with the height and weight of 168-175cm and 530-686N for male students, 145-163cm and 392-510N for female students.

B. Measured acceleration

For instance, Fig. 4 shows the measured vertical acceleration at the right lumber part of male student Ya (height=169cm, weight=686N) when walking to match the sound of 2Hz from an electronic metronome. It is appended that the first transient wave up to 1.5 seconds has been removed in this Fig.4. Fig. 5 shows the power spectrum density obtained by FFT analysis for the measured vertical acceleration shown in Fig.4. In this Fig. 5, f_w =2.0508 Hz represents the footfall frequency in the vertical direction. It can be also seen from Fig.5 that not only the component with frequency of $2f_w$, $3f_w$, but also the component with frequency of $0.5f_w$, $1.5f_w$, $2.5f_w$ where f_w is the walking rate is observed. So, FFT analysis was also conducted for the measured vertical acceleration at the right and left lumber part of male student Na (height=173cm, weight=676N). Figs. 6 and 7 show the power spectrum density at the right and left lumber part respectively obtained by FFT analysis. It is found from these Figures that higher walking components (not only the component with frequency of $2f_w$, $3f_w$, but also the component with frequency of $0.5f_w$, $1.5f_w$, $2.5f_w$) are observed for male student Na. Therefore, FFT analysis has been carried out for the averaging data observed by the right and left lumbar part data as
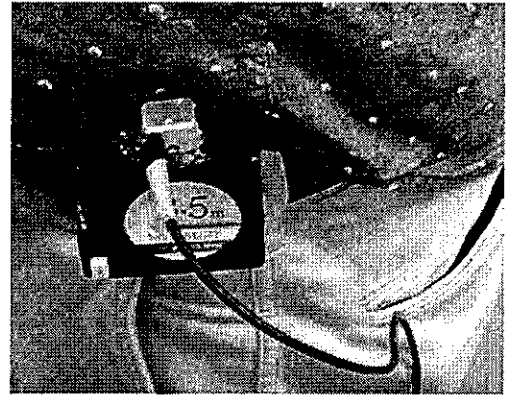

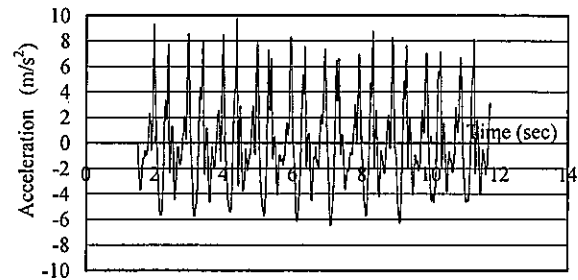Photo 1. Set up of accelerometer on a person being tested

Fig.4 Measured vertical acceleration at the right lumber part of male student Ya (height=169cm, weight=686N)
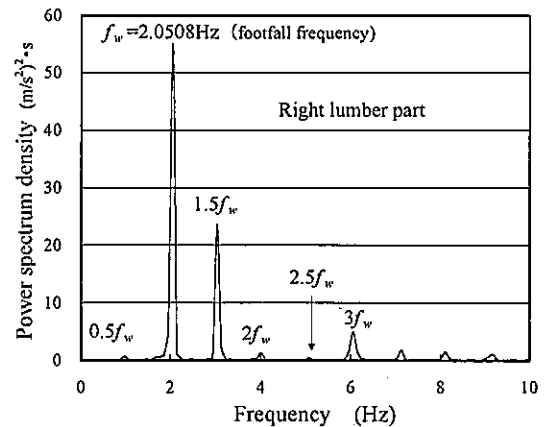

Fig.5 Power spectrum density obtained by FFT analysis for the measured vertical acceleration shown in Fig.4

shown in Fig.8. It can be seen from this Fig.8 that the component with frequency of $0.5f_w$, $1.5f_w$, $2.5f_w$ hardly exists and that it is the component with frequency of $2f_w$, $3f_w$ only be present. These results clearly demonstrate that the component with frequency of $2f_w$, $3f_w$ is in-phase and that the component with frequency of $0.5f_w$, $1.5f_w$, $2.5f_w$ is in-opposite-phase in right and left lumber part.
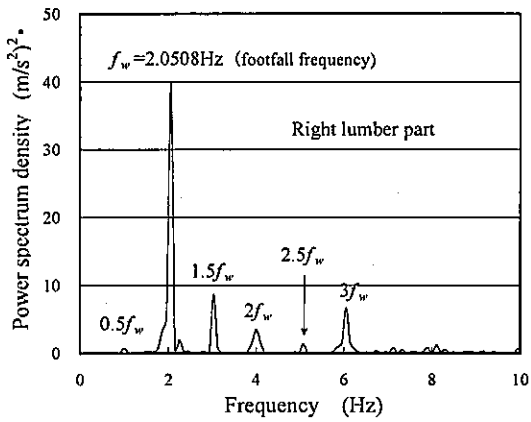
Fig. 6 Power spectrum density at the right lumber part of male student Na (height=173cm, weight=676N)
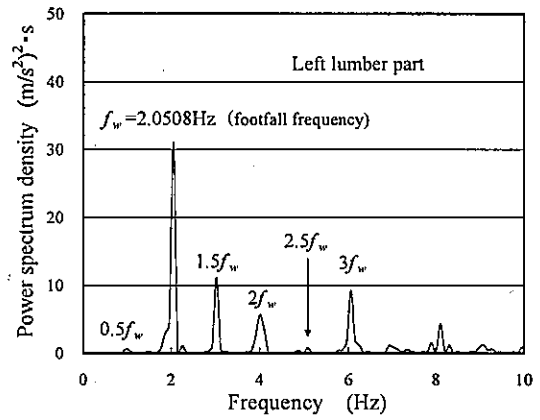

Fig.7 Power spectrum density at the left lumber part of male student Na (height=173cm, weight=676N)

IV. HUMAN WALKING FORCES (DYNAMIC LOAD FACTOR)

A.In-phase Component

FFT analysis is performed for the time history data (Δt=0.005s) of all the subjects which is derived from measured acceleration after 1.5 second. Fig. 9 shows the relationship between the dominant frequency and the in-phase vertical dynamic load factor (DLF). It is appended that the measured footfall component (f_w) is also plotted in this Figure. It can be seen from this Fig. 9 that the DLF of footfall component (f_w) estimated by the proposed method is fairly in good agreement with that measured based on force transducers by Kajikawa [1] although there is a slight difference from person to person in both values. Whereas, it can be also seen from Fig.9 that 2 and 3 times components ($2f_w$ and $3f_w$) do not increase even the dominant frequency is increased and that both average DLFs are almost around 0.1although measured values varied somewhat widely. These measured DLFs are fairly in good agreement with the reported values [6].

The walking vertical force can be estimated using the measured vertical acceleration on the lumbar part, from which a steady vertical acceleration a is calculated according to the method as shown in Chapter 2.

The walking vertical force due to a pedestrian can be evaluated in the following equation:

$$Walking \ force = \frac{W}{g} \times a = W \times \frac{a}{g} = W \times DLF \qquad (4)$$

where W is the weight of a person being tested, g is the gravity acceleration, DLF is the dynamic load factor ($DLF = a/g$).

B.In-opposite-phase Component

Fig. 10 shows the relationship between the dominant frequency and the in-opposite-phase vertical dynamic load factor (DLF). It can be seen from this Fig.10 that 0.5 and 1.5 times components ($0.5f_w$ and $1.5f_w$) show the tendency to increase according to the increase of dominant frequency. Although 1.5 times component ($1.5f_w$) is greatly distributed over around 0.05-0.3, this is the reason why 1.5 times
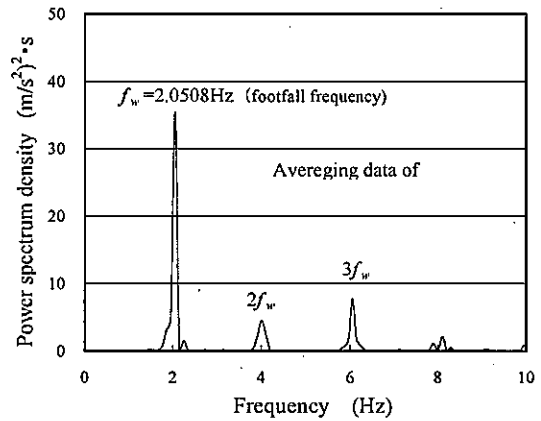

Fig.8 Power spectrum density for the averaging data observed by the right and left lumbar part of male student Na (height=173cm, weight=676N)
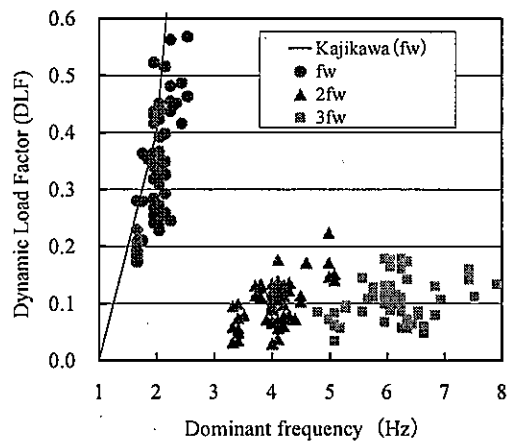

Fig. 9 Relationship between the dominant frequency and the in-phase vertical dynamic load factor (DLF)

component depends on the walking characteristics such as in-opposite-phase movement of the lumber part. On the other hand, 2.5 times component ($2.5f_w$) does not show the tendency to increase according to the increase of dominant frequency and the average value of this component is about 0.05.

By the way, assuming that the in-opposite-phase component is the rotary motion as shown in Fig.11, the walking vertical force of this component can be evaluated in the following equation:

$$Walking\ force = 2 \times \frac{W/2}{g} \times \frac{a}{2} = \frac{W}{2} \times \frac{a}{g} = \frac{W}{2} \times DLF \qquad (5)$$

Therefore, it can be said that the walking force due to the in-opposite-phase component becomes half values compared with that of the in-phase component if DLF value of both is the same.

V. FULL SCALE MEASUREMENT FOR THE PEDESTRIAN BRIDGE

In Japan, the vibration of the pedestrian bridge induced by the in-phase component with frequency of $2f_w$, $3f_w$ where f_w is the footfall frequency have not been almost investigated. Furthermore, the in-opposite-phase component with frequency of $0.5f_w$, $1.5f_w$ and $2.5f_w$ is not known in other countries. Therefore, in this Chapter, the vibration excited by 2 times and 1.5 times component of the walking force is investigated for the existing pedestrian bridge.

A. Pedestrian Bridge being Tested

Photo.2 shows the pedestrian bridge being tested. This pedestrian bridge with the span length of about 33m and the effective width of 1.5m is located in Osaka prefecture. It is appended that this pedestrian bridge is simply supported bridge because it has a hinge connection at middle bridge pier as shown in Photo.3.

One accelerometer is installed in the vertical direction of the bridge center point in order to measure the damped free vibration excited by bending and stretching movement of one person in condition that stationary 10 occupants are at the center point of the bridge. FFT analysis is carried out for the measured acceleration wave (sampling time Δt is $\Delta t = 0.005s$, 10Hz analog low-pass filter). Fig.11 shows the power spectrum density obtained by FFT analysis. It can be seen from this Fig.11 that fundamental frequency of this bridge is about 2.8 Hz in condition that stationary 10 occupants are at the center point of the bridge.

B. Overview of Walking Experiment for the Bridge

Male students Ma (height 167cm, weight 530N) walked on the bridge from end to end (about 33m) as the same pace as the tone of the electronic metronome.

Because the tone of electronic metronome was set from 1.25 times/s (walking step=1.25 steps/s) to 2.2 times/sec (walking step=2.2 steps/s), it seems that walking experiment in these tone range does not cause resonance with the fundamental frequency of the bridge (about 2.8Hz) in case that only the footstep component is taken into account. However, 2 times walking component of walking steps (1.25×2=2.5~1.65× 2=3.3 steps/s) might cause resonance with the fundamental
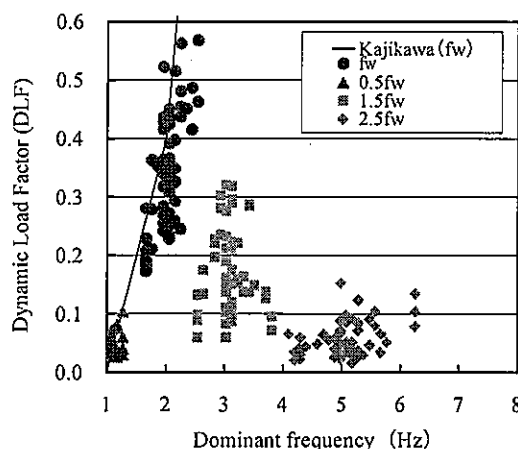

Fig.10 Relationship between the dominant frequency and the in-opposite-phase vertical dynamic load factor (DLF)
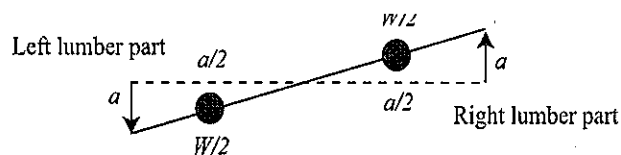
Fig.11 In-opposite-phase component (rotary motion)
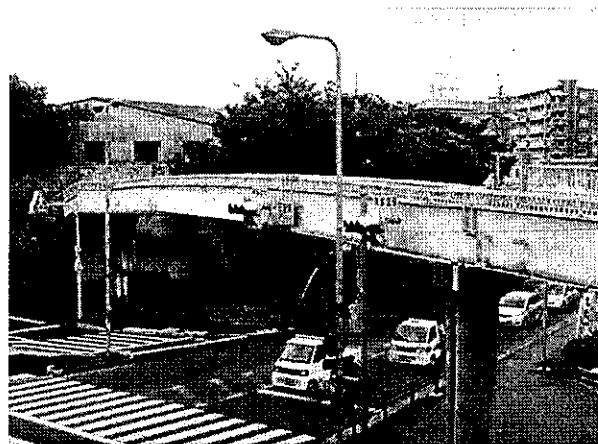
Photo.2 Pedestrian bridge being tested

frequency of the bridge (about 2.8Hz). Moreover, 1.5 times walking component of walking steps (1.7×1.5=2.55~2.2× 1.5=3.3 steps/s) also might cause resonance with the fundamental frequency of the bridge (about 2.8Hz).

C. Experimental Results and Discussion

Walking experiment for the pedestrian bridge mentioned above was performed three times. As almost the same results were obtained, second experimental results will be discussed in this Chapter. It is appended that 3 people of the standing position dealt with measurement work at the center point of the bridge in a stationary state.

Photo.3 Hinge connection at middle bridge pier

Fig.11 Power spectrum density obtained by FFT analysis for pedestrian bridge being tested (10Hz analog low-pass filter)

Fig.12 Relationship between footfall frequency and evaluated maximum acceleration at the center

Fig.13 Relationship between the 2 times footfall frequency and evaluated maximum acceleration at the center

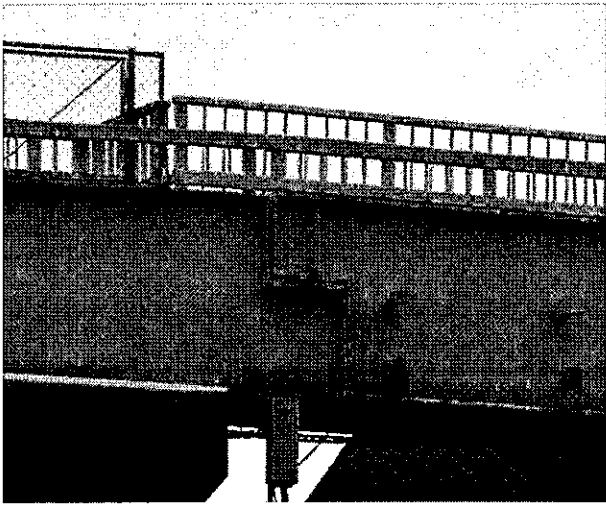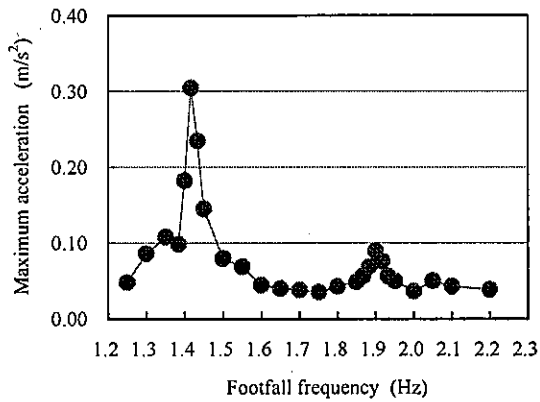The maximum acceleration is estimated from the band-pass filtered wave of 2.3Hz-3.5Hz. Fig.12 shows the relationship between the footfall frequency and evaluated maximum acceleration at the center. It can be seen from Fig.12 that two acceleration peaks are observed in both around 1.42Hz and 1.90Hz which differs significantly from the 2.7832Hz (fundamental frequency of the pedestrian bridge).

Fig.13 shows the relationship between the 2 times footfall frequency ($2 \times$ footfall frequency$=2f_w$) and evaluated maximum acceleration at the center in order to pay attention to the 2 times component. Fig.14 shows that the power spectrum density for the acceleration measured at the left lumber part of subject Ma in case of 1.417 step/s. Therefore, it can be seen from these Figures that the peak of the response at the frequency of around 2.83 Hz is the vibration excited by the 2 times component ($2f_w$) of walking vertical force.

Fig.15 shows the relationship between the 1.5 times footfall frequency (1.5$\times$footfall frequency$=1.5f_w$) and evaluated
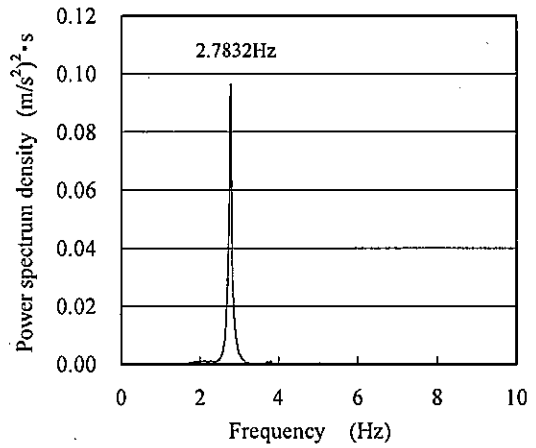

Fig.14 Power spectrum density for the acceleration measured at the left lumber part of subject Ma in case of 1.417 step/s
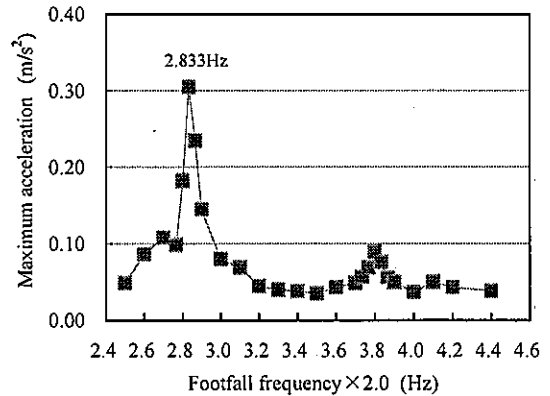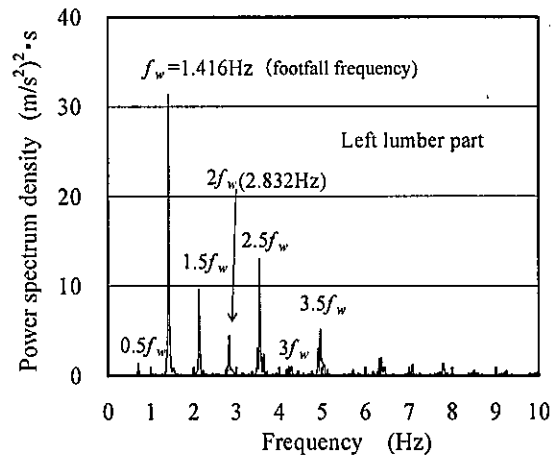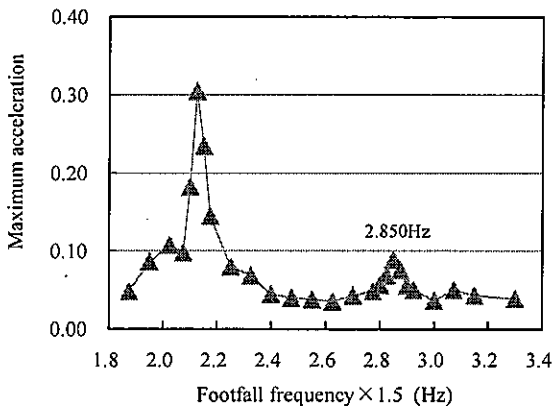
Fig.15 Relationship between the 1.5 times footfall frequency and evaluated maximum acceleration at the center
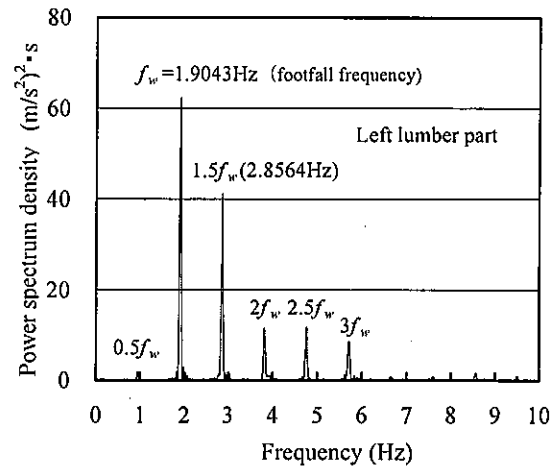

Fig.16 Power spectrum density for the acceleration measured at the left lumber part in case of 1.90 step/s

maximum acceleration at the center in order to pay attention to the 1.5 times component. Fig.16 shows that the power spectrum density for the acceleration measured at the left lumber part in case of 1.90 step/s. Therefore, it can be seen from these Figures that the peak of the response at the frequency of around 2.85 Hz is the vibration excited by the 1.5 times component ($1.5 f_w$) of walking vertical force.

Based on the results of walking experiment for the pedestrian bridge, it can be said that it might be important to take into account the higher components in order to check the vibration serviceability of slender and lighter pedestrian bridge.

VI. CONCLUSIONS

This paper deals with the simplified method to identify human walking force by using FFT power spectrum density from the experimental acceleration data of the human body. The vertical vibration of pedestrian bridge induced by higher components of human walking vertical force is also discussed. The results are summarized below:

(1) A simplified method to identify human walking force by using FFT power spectrum density from the experimental acceleration data of the human body is proposed.

(2) The difference in estimated value for the simulated sinusoidal wave is within the range of -5%.

(3) It was found that the dynamic load factor (DLF) for walking step component in vertical direction estimated by the proposed method is in fairly good agreement with those measured by force transducers although there is a slight difference due to the body type.

(4) In addition to walking step component with the footfall frequency of f_w, it is found that higher walking components (not only the component with frequency of $2 f_w$, $3 f_w$, but also the component with frequency of $0.5 f_w$, $1.5 f_w$, $2.5 f_w$) are also observed.

(5) It was verified that the component with frequency of $2 f_w$, $3 f_w$ is in-phase and that the component with frequency of $0.5 f_w$, $1.5 f_w$, $2.5 f_w$ is in-opposite-phase in right and left lumber part.

(6) The pedestrian bridge vibration excited by 2 times and 1.5 times component ($2 f_w$ and $1.5 f_w$) is observed through a walking test for the existing bridge with a center span of about 33m.

Needless to say, a lot of further study might be necessary to identify human walking force by using FFT power spectrum from the experimental acceleration data of the human body. It is hoped that this study will provide useful information for bridge engineers in investigating dynamic behavior of pedestrian bridges.

REFERENCES

[1] Y.Kajikawa, " Ergonomical serviceability analysis to highway bridge vibrations", *Journal of Structural Mechanics and Earthquake Engineering*, JSCE, no.325, 1980, pp.47–58 (in Japanese).

[2] S. Kim, K. Cho, M.Choi and J. Lim, "Development of human body model for the dynamic analysis of footbridges under pedestrian induced excitation, *Steel Structures 8*, 2008, pp.333–345.

[3] Y. Fujino, M.B., Pacheco, S.Nakamura and W. Pennung, " Synchronization of human walking observed during lateral vibration of a congested pedestrian bridge", *Earthquake Engineering and Structural Dynamics*, vol.22, 1993, pp741–758.

[4] P. Dallard, A.J. Fitzpatrick, A. Flint, S.LE. Bourva, R.M. Ridsdill Smith and M. Willford, "The London Millennium Footbridge", The structural Engineer, vol.79, no.22, 2001, pp.17–33.

[5] T. Kobori, Y. Kajikawa, and T. Kido, "Design of footbridges considering psychological effects", *Bridge and Foundation*, 1974, pp.23–29 (in Japanese).

[6] V.racic, A. Pavic and J.M.W.Brownjohn, "Experimental identification and analytical modeling of human walking (Literature review)", *Journal of Sound and Vibration*, vol.326, 2009, pp.1–49.

Attenuative Effect of Vitamin E on Experimental Cataract in Rats

Seyedeh Zeinab Peighambarzadeh, Mehdi Tavana

Abstract—Cataract is the most common cause of blindness worldwide and its incidence will increase as the World's population ages. Even in modern ophthalmology, there is no effective medical treatment for cataract except surgery. Development of a drug which could prevent or delay the onset of cataract will lessen this burden andreduce the number of blind patients waiting for cataract surgery. This study was undertaken to evaluate the protective effect of vitamin E on Selenite-induced Cataract in Sprague-dawely rats. Cataracts were induced in rats by administration of sodium selenite. On postpartum day ten, in group I, saline was injected subcutaneously. Group II rat pups received subcutaneous injection of vitamin E (60mg/kg B.W.) at day 8 postpartum and every other day thereafter. Group III and IV rat pups received a subcutaneous injection of sodium selenite (13mg/kg B.W.) at day 10 postpartum. Group IV also received subcutaneous injection of vitamin E (60mg/kg B.W.) at day 8 postpartum and every other day thereafter. The development of cataract in rats was assessed clinically by slit-lamp biomicroscope from day 14 up to postpartum day 28. After sacrifie, extricated pup lenses were analyzed for total and soluble protein concentrations and eletrophoretic pattern (SDS-PAGE). There was no opacification of lens in Group I and II. There was mature catarct in 95% of Group III. In group IV, 55% of rats developed sub capsular or cortical cataract. Cataractous and biochemical changes of the crystalline lens proteins due to selenite can be retard or prevented by vitamin E.

Keywords—Attenuative effect, selenite-induced cataract, vitamin E, rat.

Seyedeh Zeinab Peighambarzadehis with the Department of Veterinary Medicine, Faculty of Agriculture, Shoushtar Branch, Islamic Azad University, Shoushtar, Iran, PO Box:6451741117 (e-mail: peighambarzade@yahoo.com).
Mehdi Tavana is with theDepartment of Veterinary Medicine, Faculty of Agriculture, Shoushtar Branch, Islamic Azad University, Shoushtar, Iran, PO Box:6451741117 (e-mail: tavana7@yahoo.com).

Pyelography by Intraosseous Injection of Iodixanol in Persian Squirrel

Mehdi Tavana, Seyedeh Zeinab Peighambarzadeh

Abstract—Pyelography is used for morphologic and especially functional studies of the urinary tracts.There are many indications for excretory Pyelography in humans and animals. Intravenous Pyelography is the most practical method; other Pyelography techniques were manipulated because of difficulties for finding veins in small size of the patients. At the best of times, the combination of small veins and abundant subcutaneous tissue makes vascular access difficult or impossible, therefore, another methods of administration of contrast media is desired. This study was performed to evaluate the feasibility of intraosseous injection of iodixanol in providing a safe and diagnostic urogram in Persian squirrel. Fourteen hundred mg iodine per kilogram body weight of iodixanol was injected subcutaneously over tibial tuberosity on ten clinically healthy adult Persian squirrels with no signs of urinary system disorder. Lateral and ventrodorsal radiographs were taken every 2 minutes until the pyelogram was finished. Intraosseous injection of iodixanol was successful to show nephrogram, pyelogram, uretrogram and cystogram clearly. There were no abnormal clinical signs after one week of experiments. Biochemical and hematological profiles were in normal ranges. It is concluded that intraosseous Pyelography is an effective and reliable method for Pyelography studies in squirrel. Microscopic examinations of the kidneys and the site of injection after one week were normal.

Keywords— Pyelography, Intraosseous injection, iodixanol, Persian squirrel.

Mehdi Tavana is with the Department of Veterinary Medicine, Faculty of Agriculture, Shoushtar Branch, Islamic Azad University, Shoushtar, Iran, PO Box:6451741117 (e-mail: tavana7@yahoo.com).
Seyedeh Zeinab Peighambarzadeh is with the Department of Veterinary Medicine, Faculty of Agriculture, Shoushtar Branch, Islamic Azad University, Shoushtar, Iran, PO Box:6451741117(e-mail: peighambarzade@yahoo.com).

A Conceptual Framework of Scheduled Waste Management in Highway Industry

Nurul Nadhirah Anuar, Muhammad Fauzi Abdul Ghani

Abstract—Scheduled waste management is very important in environmental and health aspects. In delivering services, highway industry has been indirectly involved in producing scheduled wastes. This paper aims to define the scheduled waste, to provide a conceptual framework of the scheduled waste management in highway industry, to highlight the effect of improper management of scheduled waste and to encourage future researchers to identify and share the present practice of scheduled waste management in their country. The understanding on effective management of scheduled waste will help the operators of highway industry, the academicians, future researchers, and encourage a friendly environment around the world. The study on scheduled waste management in highway industry is very crucial as highway transverse and run along kilometers crossing the various type of environment, residential and schools. Using Environmental Quality (Scheduled Waste) Regulations 2005 as a guide, this conceptual paper highlight several scheduled wastes produced by highway industry in Malaysia and provide a conceptual framework of scheduled waste management that focused on the highway industry. Understanding on scheduled waste management is vital in order to preserve the environment. Besides that, the waste substances are hazardous to human being. Many diseases have been associated with the improper management of schedule waste such as cancer, throat irritation and respiration problem.

Keywords—Asia Region, Environment, Highway Industry, Scheduled Waste.

I. INTRODUCTION

WASTE management is one of the priority issues concerning protection of the environment and conservation of natural resources [1]. Poor management of waste led to contamination of water, soil and atmosphere as well as a major impact on public health [2]. Increasing population levels, demand for better living standard and rapid urbanization have increase the waste generation in a country. Scheduled waste management (SWM) is very important in environmental and health aspect. Scheduled waste is a small percentage of hazardous waste that has been regarded for a

Nurul Nadhirah Anuar is an undergraduate student from the Faculty of Administrative Science and Policy Studies at Universiti Teknologi MARA, Shah Alam, Selangor, Malaysia (phone: 017-885-7895; e-mail: nurull_nano@ yahoo.com).

Muhammad Fauzi Abdul Ghani is a PhD candidate from the Faculty of Business Management at Universiti Teknologi MARA, Shah Alam, Selangor, Malaysia (e-mail: fauzighani64@yahoo.com).

long time as intractable, or difficult to safely dispose of, without special technologies and facilities [3]. Scheduled waste is similar with the hazardous waste terminology using in world wide. In Malaysia, the government use terminology of scheduled waste instead of hazardous waste, referring to the only wastes listed in the First Schedule of Environmental Quality (Scheduled Waste) Regulations 2005. Under this schedule, 77 types of scheduled wastes are listed and the wastes are groups into five which are metal and metal-bearing wastes; wastes containing principally inorganic constituents which may contain metals and organic materials; wastes containing principally organic constituents which may contain metals and inorganic materials; wastes which may contain either inorganic or organic constituents; and other waste which is any residues from treatment or recovery of scheduled wastes [4]. Any import and export related to these wastes are subject to the same law and references to the international requirement of Basel Convention.

Despite SWM is very important, the understanding of scheduled waste management especially in highway industry is still lacking. This is very crucial as highway industry in the Asian Region is growing rapidly. To ensure sufficient protection of human health and environment in Malaysia, the government of Malaysia has developed Environmental Quality (Scheduled Waste) Regulations 2005, under the Environmental Quality Act 1974. This regulation is expected to be adhered by all industry in Malaysia including the highway industry. It should be noted that there are many unnoticeable wastes in highway industry that should be manage properly and fall under the categories of scheduled waste. The wastes produce by highway industry are waste of lead acid batteries in whole or crushed form; waste from electrical and electronic assemblies (containing components such as accumulators, mercury-switches, glass from cathode-ray tubes and other activated glass or polychlorinated biphenyl-capacitors, or contaminated with cadmium, mercury, lead, nickel, chromium, copper, lithium, silver, manganese or polychlorinated biphenyl); spent hydraulic oil; and spent mineral oil-water emulsion.

This paper provides a literature review of the SWM in the context of highway industry, conceptual framework on the SWM in highway industry and future research studies.

II. LITERATURE REVIEW

Human activities have always generated waste. This was not a major issue when the human population was relatively

small and nomadic, but became a serious problem with urbanization and the growth of large urban area [2]. Increasing population and urbanization caused billion of tons of waste are produced every year. The government holds the responsibility to develop the best practicable and environmentally sustainable waste management strategies. In Malaysia, scheduled wastes are listed under First Schedule of Environmental Quality (Scheduled Waste) Regulations, 2005. The wastes in the schedule are groups into five which are metal and metal-bearing wastes; wastes containing principally inorganic constituents which may contain metals and organic materials; wastes containing principally organic constituents which may contain metals and inorganic materials; wastes which may contain either inorganic or organic constituents; and other wastes which includes any residues from treatment or recovery of scheduled wastes [4].

A waste management hierarchy based on the most environmentally sound criteria favors waste prevention/ minimization, waste re-use, recycling, and composting. In many countries, a large percentage of waste cannot presently be re-used, re-cycled or composted and the main disposal methods are landfilling and incineration [2]. Scheduled waste management will also go through these procedures for storage, packaging and labeling. Highway industry produces wastes such as waste of lead acid batteries in whole or crushed form (SW 102); waste from electrical and electronic assemblies (SW110); spent hydraulic oil (SW 306); and spent mineral oil-water emulsion (SW307). The waste under SW110 contain components such as accumulators, mercury-switches, glass from cathode-ray tubes and other activated glass or polychlorinated biphenyl-capacitors, or contaminated with cadmium, mercury, lead, nickel, chromium, copper, lithium, silver, manganese or polychlorinated biphenyl [5].

In production of lead acid battery, huge amount of sulphuric acid (H_2SO_4) is used. It will lower the pH value of water when mixed up with water which raises the acidic property of water. In addition, in lead acid battery production, huge amount of lead is needed and a portion of that lead is wasted and mixed with the fume [6]. So it causes air pollution and presence of lead in air is very harmful especially for children [6].If lead acid batteries are disposed of in a solid waste landfill or illegally dumped, the lead and sulphuric acid can seep into the soil and sulfuric acid contaminated ground water, potentially affecting the quality of our drinking water supply. If the batteries are disposed of near rivers, streams, lakes or coastal waters, the lead and sulphuric acid can also threaten aquatic life [7]. Besides that, lead causes symptoms ranging from the loss of neurological function to death depending upon the extent and duration of exposure both children and adults can suffer from an illness including effects on central nerve system, kidneys, gastrointestinal tract and blood forming system [6]

Electronic waste or E-waste is relatively a novel addition to the ever-growing hazardous waste stream. It includes discarded electronic and electrical equipment [8]. E-Waste is defined as waste from the assembly of electrical or electronic appliances that consist of components such as accumulators, mercury switches, glass from cathode-ray tube sand other activated glass or polychlorinated biphenyl capacitors, or contaminated with cadmium, mercury, lead, nickel, chromium, copper, lithium, silver, manganese or polychlorinated biphenyl [9]. E-waste also represent component of waste from the appliances that can no longer be used such as air-condition, computer, printer, Photostat machine, video camera recording and fluorescent lamp.

Developing countries like India, today, is burdened with the serious problem of E-waste which is either locally generated or internationally imported, causing serious threat to human health and environment [8]. Often, hazards arise due to the improper recycling and disposal processes. Such offensive practices can have serious aftermath for those staying in proximity to the places where E-waste is recycled or burnt [8]. Electronic wastes that are landfilled produces contaminated leachates which eventually pollute the groundwater. Acids and sludge obtained from melting computer chips, if disposed on the ground causes acidification of soil. For example, in Guiyu, Hong Kong, a flourishing area of illegal E-waste recycling is facing acute water shortages due to the contamination of water resources. This is due to disposal of recycling wastes such as acids, sludge in rivers [8].

Hydraulic oil is not likely to present an inhalation hazard at normal temperatures and pressures. However, when aerosolizing, misting, or heating this product, high concentrations of generated vapor or mist may irritate the respiratory tract (nose, throat, and lungs). It can also cause throat irritation, nausea, vomiting, and diarrhea [10]. Breathing product into the lungs during ingestion or vomiting may cause lung injury and possible death. Individuals with pre-existing respiratory tract (nose, throat, and lungs), eye, and/or skin disorders may have increased susceptibility to the effects of exposure. Hydraulic oil also must keep away from sparks or flame. Where flammable mixtures may be present, equipment safe for such locations should be used. Use clean tools. When transferring large volumes of product, metal containers, including trucks and tank cars, should be grounded and bonded. Keep containers away from flame, sparks, static electricity, or other sources of ignition [10].

Mineral oil-in-water emulsions (OWEs) are used to ensure the corrosion protection of both processed metal parts and operating tools, and to provide assistance in taking away metal scraps and chips from the metal-processing area. During utilization, an OWE undergoes changes under the influence of mechanical, thermal, chemical and biological factors is no longer safe to be used because of reduced operating functions and emerging health hazards and it must be replaced. Generally, spent OWEs (SOWEs) contain residual mineral oil, tramp oils, greases, biocides, emulsifiers, metal ions, other components of original OWEs and the products of their

degradation. When irresponsibly and non-professionally handled, SOWEs appear as environmentally hazardous waste waters [11]. Mineral oil remains the main source of energy and other hydrocarbon based products. Pollution resulting from increasing use of mineral based oil could not be overemphasized. Large quantity of mineral based oil finds their way to the ground. Several millions of tons of oil cause pollution worldwide yearly [12]

Human exposure to substances released at waste management facilities can be acute in case of a serious accident causing short-term exposure to high levels of potentially hazardous substances, ionizing radiation, bioaerosols, and dusts. The situation can be chronic, when it involves long-term exposure to low concentrations of these substances or radiation [2]. Scheduled wastes shall be disposed of at prescribed premises only. Every waste generator shall ensure that scheduled wastes generated by him are properly stored, treated on-site, recovered on-site for material or product from such scheduled wastes or delivered to and received at prescribed premises for treatment, disposal or recovery of material or product from scheduled wastes. Every waste generator shall ensure that scheduled wastes that are subjected to movement or transfer is packaged, labeled and transported in accordance with the guidelines prescribed by the director general [4].

Waste management should be understood as a system composed of physical things, human activities, and links between and within physical things and human activities [13]. The regulatory bodies must encourage the prevention or reduction of waste and its harmfulness by encouraging the development of clean technologies, technical product improvements, and disposal techniques [14]. They must prohibit the abandonment, dumping or uncontrolled discharge of waste [14]. The issue of spillages, leakages, corroding container and improper marked labels of scheduled waste must be addressed. To facilitate the proper handling of scheduled wastes, information about the hazards associated with the wastes must be communicated through proper labels and should be used by wastes handlers [15]. To ensure that the wastes are safely handled, suitable containers are also needed to be used by the waste generators. It is the responsibility of the waste generators to ensure that scheduled wastes are packed based on the composition in a manner suitable for handling, storage and transportation [15]. A number of serious and highly publicized pollution incidents associated with incorrect waste management practices, led to public concern about lack of controls, inadequate legislation, environmental and human health impact [2].

Due to its quantity, concentration, physical, chemical or infectious characteristics, scheduled waste may cause to an increase in mortality, or an increase in irreversible or incapacitating illness. Nevertheless, scheduled waste may pose a substantial present or potential hazard to human health or the environment when improperly treated, stored or disposed of,

or otherwise mismanaged [16]. Malaysia is targeting to achieve 30% of total solid and scheduled waste recycling in 2020 besides 5% currently [16].

Urbanization has exploded with great speed and scale in recent decades with "more than half the world's population now living in urban centers", as countries and even individual cities struggle to be competitive in the global marketplace [17]. Good governance requires the participation and collaboration of all relevant parties, including government, non-governmental organizations (NGOs), community groups and the private sector. According to the Asian Development Bank, the four principle elements of good governance are accountability, participation, predictability, and transparency. Good governance allows low-income groups to influence policy and resource allocation, and therefore it is essential for equitable, effective, and efficient SWM [17].

III. CONCEPTUAL FRAMEWORK

Based on the literature review, it is hardly to find a SWM framework especially in the context of highway industry. A conceptual framework that addresses important aspects such as the list of scheduled waste produced by highway industry, the procedure to manage scheduled waste, the hazardous characteristics of scheduled waste, descriptions of the wastes and the effect of improper management of scheduled waste produced by highway industry is proposed in Fig. 1. Fig. 1 is the new conceptual framework of scheduled waste management in highway industry.
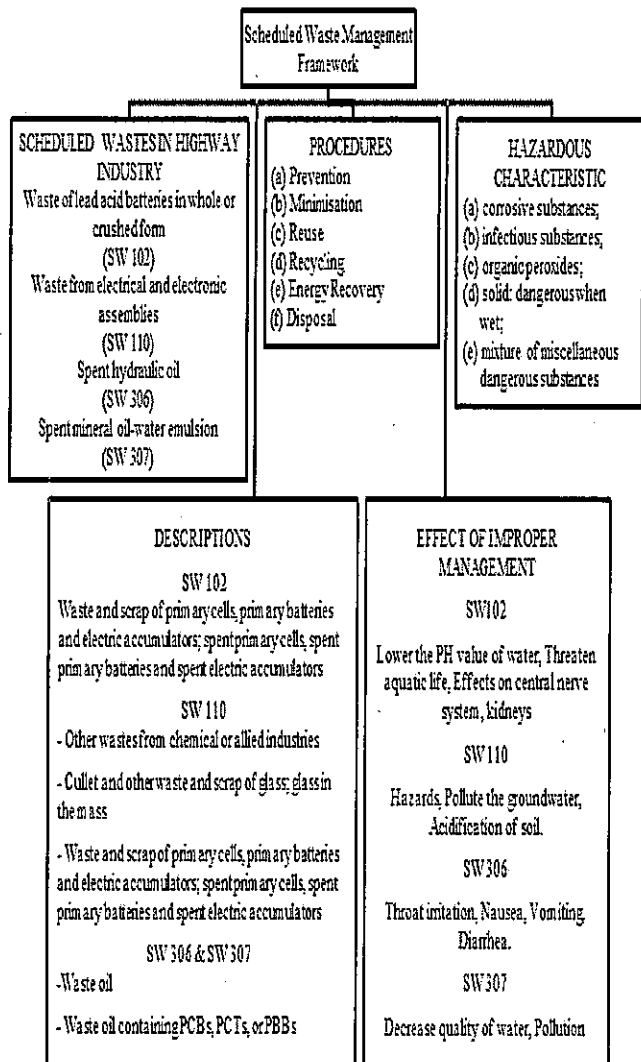
Fig. 1 Scheduled waste management framework for highway industry

This conceptual framework on scheduled waste management focuses on the scheduled wastes from highway industry in Malaysia. There are four categories of scheduled waste produced by the highway industry such as waste of lead acid batteries in whole or crushed form (SW 102); waste from electrical and electronic assemblies (SW110); spent hydraulic oil (SW 306); and spent mineral oil-water emulsion (SW307). The waste under SW110 contain components such as accumulators, mercury-switches, glass from cathode-ray tubes and other activated glass or polychlorinated biphenyl-capacitors, or contaminated with cadmium, mercury, lead, nickel, chromium, copper, lithium, silver, manganese or polychlorinated biphenyl [5]. The wastes will undergo six procedures which are prevention, minimization, reuse, recycling, energy and lastly, disposal. Scheduled waste has the hazardous characteristics such as corrosive substances, infectious substances, organic peroxides, solid: dangerous

when wet, and mixture of miscellaneous dangerous substances.

SW 102 includes waste and scrap of primary cells, primary batteries and electric accumulators; spent primary cells, spent primary batteries and spent electric accumulators. Besides that, SW 110 comprises of wastes from chemical or allied industries; cullet and other waste and scrap of glass; glass in the mass; waste and scrap of primary cells, primary batteries and electric accumulators; spent primary cells, spent primary batteries and spent electric accumulators. SW 306 and SW 307 consist of waste oil containing polychlorinated biphenyls (PCBs), polychlorinated terphenyls (PCTs) or polybrominated biphenyls (PBBs). All the hazardous substances must be handle and labeled correctly as they can lower the pH value of water, threaten aquatic life, decrease the quality of water, effects on central nerve system, pollute the groundwater, cause acidification of soil, throat irritation, nausea, vomiting and diarrhea.

IV. FUTURE RESEARCH STUDIES

The scheduled waste identified in this conceptual paper is based in the context of scheduled waste management in Malaysia. Future researchers should explore on the scheduled waste produced in other country. Despite many research studies on waste management have been published, there is still lack of information regarding SWM especially in the context of highway industry. More research article on SWM should be published to the public.

The conceptual framework will help and guide the future researchers and academician who are interested to study SWM in the future. They can develop more frameworks of SWM for other industry that are also involved in producing scheduled wastes such airlines, retails, furniture and agriculture industry. This will enrich schedule waste knowledge and practice. In addition, this conceptual paper will help the highway industry in other countries to identify new potential scheduled wasted for their highway industry.

Future studies to also look into the techniques that could address the issues relating to SWM in highway industry such as new green technology. Based on the hazardous characteristic of scheduled waste highlighted in this conceptual paper, every organization should identify the scheduled waste generated from their business and take the necessary steps to reduce the hazardous emission of scheduled waste and pollution to the environment and the people.

Besides that, future researchers should create an awareness regarding the SWM and the negative impact of the improper management of scheduled wastes. The study on scheduled waste management in highway industry is very crucial as compared to factories in which the factories are located on specified areas whereas, highway transverse and run along kilometers crossing the various type of environment, residential, forest and schools.

REFERENCES

[1] Costi, P., Riccardo Minciardi, Michela Robba, Mauro Rovatti, & Roberto Sacile. (2004). An environmentally sustainable decision model for urban solid. *Waste Management*, 277-295

[2] Giusti, L. (2009). A review of waste management practices and their impact on human health. *Waste Management*, 2227-2239.

[3] Australia, C. o. (n.d.). *Scheduled waste management*. Retrieved March 4, 2015, from Australian Government: http://www.environment.gov.au/protection/chemicals/scheduled-waste

[4] Boar, L. R. (2014). *Environmental Quality Act 1974(Act127)*. Malaysia: International Law Book Services.

[5] Environment, D. o. (2006). *Guidelines for the Classification of Used*. Putrajaya: Department of Environment.

[6] Uddin, M. J., Mondal, P. K., Rahman, M. A., & Rahman, M. H. (2013). An Approach to Reduce Waste in Lead Acid Battery Industries. *Global Journal of Researches in Engineering*, 16-22.

[7] *Requirements - Hazards and Disposal of Batteries*. (2006, September 6). Retrieved March 4, 2015, from Camden Electronic Ltd: http://www.farnell.com/datasheets/1504234.pdf

[8] Borthakur, A., & Singh, P. (2012). Electronic waste in India: Problems and policies . *International Journal of Environmental Sciences* , 354-362

[9] (2007). *E-Waste Volume I*. United Nations Environment Programme.

[10] Coordinator, P. M. (2008). *J. M. Reynolds Xtreme AW HYDRAULIC OIL ISO 32 & 46*. USA.

[11] Lazarević, V. B., Krstić, I. M., Lazić, M. L., Savić, D. S., Skala, D. U., & Veljković, V. B. (2013). Scaling up the chemical treatment of spent oil-in-water emulsions from. *Hem. ind.*, 59-68.

[12] Lawal, O. Y. (2007). *Transformation of an environmental friendly hydraulic oil in soil using gas chromatography*. The Tema Institute.

[13] Pohjola, V. J., & Pongra´cz, E. (2002). An approach to the formal theory of waste. *Resources, Conservation and Recycling*, 17-29.

[14] *Overview of EU environmental legislation*. (2015, February 16). Retrieved March 4, 2015, from Guide to the Approximation of European Union Environmental Legislation: http://ec.europa.eu/environment/archives/guide/part2c.htm

[15] Environment, D. o. (n.d.). *Guidelines for Packaging, Labelling and Storage of Scheduled Wastes In Malaysia*. Malaysia: Department of Environment.

[16] Hassan, N. (2012, July 19). *Recovery and recycling processes of scheduled waste in Malaysia*. Retrieved March 4, 2015, from Universiti Teknologi Malaysia Institutional Repository: http://eprints.utm.my/12308/

[17] Marshall, R. E., & Farahbakhsh, K. (2013). Systems approaches to integrated solid waste management in developing countries. *Waste Management*, 988-1003.

Potential of γ-Polyglutamic Acid for Cadmium Toxicity Alleviation in Rice

N. Kotabin, Y. Tahara, K. Issakul, O. Chunhachart

Abstract— Cadmium (II) (Cd) is one of the major toxic elemental pollutants which is hazardous for humans, animals and plants. γ-Polyglutamic acid (γ-PGA) is an extracellular biopolymer produced by several species of *Bacillus* which has been reported to be an effective biosorbent for metal ions. The effect of γ-PGA on growth of rice grown under laboratory conditions was investigated. Rice seeds were germinated and then grown at 30±1°C on filter paper soaked with Cd solution and γ-PGA for 7 days. The result showed that Cd significantly inhibited the growth of roots and shoots by reducing root and shoot lengths. Fresh and dry weights also decreased compared with control; however, the addition of 500 mg·L^{-1} γ-PGA alleviated rice seedlings from the adverse effects of Cd. The analysis of physiological traits revealed that Cd caused a decrease in the total chlorophyll and soluble protein contents and amylase activities in all treatments. The Cd content in seedling tissues increased for the Cd 250 μM treatment ($P<0.05$) but the addition of 500 mg·L^{-1} γ-PGA resulted in a noticeable decrease in Cd ($P<0.05$).

*Keywords—***Polyglutamic acid, cadmium, rice, *Bacillus subtilis***

I. INTRODUCTION

CADMIUM (II) (Cd) is one of the highly toxic, heavy metals and causes a serious threat to plant growth and human health due to its accumulation in edible plant tissues [1], [2]. Thus, Cd can be transferred to animals and humans via the food chain. Agricultural soils of many countries have been contaminated by Cd because of human activities, such as industrial wastes, zinc mining, sewage sludge and phosphate fertilizers [3], [4]. In Mae Sot district, Tak province, Thailand, the contamination of paddy fields and creeks by Cd released from zinc mining has been occurring for more than 20 years. Samples collected from sediments of the creeks, paddy soils, rice grains and soybeans cultivated in the contaminated areas had Cd concentrations exceed the maximum range of permissible levels [4]. Over 80% of rice grain samples collected contain Cd at a concentration exceeding the Codex Committee on Food Additives and Contaminants (CCFAC) Maximum Permissible Level for rice grain of 0.2 mg Cd kg^{-1} and the estimated weekly intake (WI) values ranged from 20 to 82 μg Cd kg^{-1} body weight [5]. Therefore, the people who live in the contaminated area and consume rice grown locally are always exposed to the risk of chronic Cd toxicity. Although the Thai government policies are designed to promote sugarcane cultivation in terms of renewable energy, local farmers are still interested in growing rice in this area because the government rice mortgage program has produced a high market price for rice.

Gamma-polyglutamic acid (γ-PGA) is a naturally occurring anionic polymer, biodegradable, edible, and nontoxic to humans and environments. γ-PGA consists of D- and L-isomers of glutamic acid linked by amide bonds between α-amino group and carboxyl group [6]. In the past few years, it has been interested in various applications such as thickeners, humectants, drug carriers, biological adhesives, foods, cosmetics, medicines, water absorbents, bioflocculants and wastewater treatment [7]. Moreover, it has been reported to be an effective biosorbent for several metal ions; Ni (II), Cu(II), Mn(II), Al(III) and Cr(III) [8], and Cd (II) [9] in water treatment. Thus, it is of interest to consider whether γ-PGA can be used as a Cd biosorbent with plants and to reduce Cd toxicity in rice. This study investigated the effect of Cd and γ-PGA on rice seedlings grown in the laboratory.

II. MATERIAL AND METHOD

A. γ-PGA production

γ-PGA was prepared by *Bacillus subtilis* NBRC16449 according to the method described previously [10].

B. Effect of γ-PGA and Cd on growth of rice seedling

The healthy rice seeds were surface sterilized in 10% sodium hypochlorite for 10 min, then rinsed 4 times with deionized water. Rice seeds were soaked in deionized water for 24 h. A filter paper was placed on a Petri dish (9 cm in diameter) and moistened with 5 mL of Cd (supplied as CdCl$_2$·2.5H$_2$O solution) and γ-PGA mixer solution in different series concentrations (Cd; 0, 50, 100, 250, 500 μM and γ-PGA; 0, 50, 100, 500, 1,000 mg·L^{-1}). Ten rice seeds were put on a Petri dish and incubated in the growth chamber with 12 h light and 12 h darkness at 28°C±1°C for 7 days. Three replications were

O. Chunhachart is with the Department of Science, Faculty of Liberal Arts and Science. Kasetsart University Kamphaeng Saen Campus, Nakhon Pathom 73140 Thailand (Phone: +66-34-281105-6 ext 7668, e-mail: faasowc@ku.ac.th).

Center for Advanced Studies in Tropical Natural Resources, National Research University-Kasetsart University, Kasetsart University, Bangkok 10900 Thailand

N. Kotabin Department of Science, Faculty of Liberal Arts and Science Kasetsart University Kamphaeng Saen Campus, Nakhon Pathom 73140 Thailand

Y. Tahara Department of Applied Biological Chemistry, Faculty of Agriculture, Shizuoka University, Shizuoka 422-8529 Japan

K. Issakul School of Energy and Environment, Department of Environmental Science, University of Phayao, Phayao 56000 Thailand

conducted in each treatment. Physical parameters of rice seedling were determined.

C. Chlorophyll analysis

Chlorophyll content in seedlings was determined by the method described previously [11].

D. Amylase activity

Amylase activities were determined by the method described previously [12].

E. Determination of cadmium content

Rice seedlings were soaked in 20 mM EDTA for 15 min to remove metal ions on surface [13]; then washed with deionized water three times. The seedlings were dried at 80°C until constant weight and ground to fine powder. Seedling powder was digested with $HNO_3:HClO_4$ mixture (4:1, v/v) at 120°C for 12 h. The Cd concentration in seedlings was determined using an atomic absorption spectrometer (Unicam M-Series Solaar, USA)

III. RESULT

A. Effect of γ-PGA and Cd on the Growth of rice Seedlings

Cd produced a significant decrease in shoot length compared with the control. Shoot length was gradually reduced by 15 %, 24%, 27% and 50% in the Cd treatments of 50, 100, 250 and 500 μM, respectively. The root length was decreased by 24%, 48% and 83 % and 96% in the Cd treatments of 50, 100, 250 and 500 μM, respectively. Interestingly, the addition of γ-PGA led to an increase in both root and shoot lengths. The addition of 1,000 mg·L^{-1} of γ-PGA significantly increased the shoot length in the Cd treatments with 250 and 500 μM compared with the same Cd treatments with no γ-PGA added. Furthermore, the root length slowly increased when γ-PGA was added. The fresh and dry weights were also found to decrease with increased Cd concentrations. The addition of γ-PGA significantly increased both fresh and dry weights under Cd stress (Table I). chlorophyll a slowly decreased with an increase in the Cd concentration. In the 250 μM Cd treatment without added γ-PGA, the amounts of chlorophyll a, b and total chlorophyll were significantly reduced compared with the control. Nevertheless, the addition of γ-PGA alleviated the chlorophyll a, b and total chlorophyll contents in the rice tissues, especially at 1,000 mg·L^{-1} γ-PGA which maintained the chlorophyll content at the same level as in the control (Fig. 1).

B. Chlorophyll content

The rice seedlings treated with Cd were clearly bleached and subsequent analysis indicated that the chlorophyll content gradually reduced at high concentrations of Cd. The amount of

C. Amylase activity

Total amylase activity in the rice seedlings treated with Cd gradually decreased with an increase in the Cd concentration compared with the control. Cd concentrations of 250 and 500

μM significantly reduced the total amylase and α-amylase activities. However, the β-amylase activity was not significantly different among all treatments. The addition of γ-PGA increased the total amylase, α-amylase and β-amylase contents compared with the Cd treatments without γ-PGA (Fig. 1).

D. Cd concentration

An increased Cd concentration in the solution resulted in an increased amount of Cd in the rice tissue samples (Table II). The Cd treatments of 250 and 500 μM without γ-PGA exhibited significantly increased amounts of Cd. After the γ-PGA was added, the Cd content in the rice tissues decreased compared with the treatment with only Cd. In particular, when the Cd solution concentration was 250 μM, the Cd tissue concentration was significantly reduced with the addition of either 500 or 1,000 mg/L γ-PGA. However, at the highest added Cd concentration (500 μM), γ-PGA at a concentration of 1,000 mg/L was unable to reduce the Cd content in the rice tissues which suggested that this very high concentration of Cd may exceed the adsorption ability of γ-PGA

E. The Correlation between γ-PGA Concentration and Cd Content in rice Tissue

Result of the correlation analyses between γ-PGA concentration used in the experiment (50, 100, 500 and 1,000 mg·L^{-1}) and Cd content in rice tissue is shown in Table 3. Cd 100 and 250 μM were significantly correlated ($P<0.05$) with negatively correlation coefficient of -.882 and -.893, respectively. It can be generally concluded that the cadmium content in rice tissue tend to be significantly decreased with the increasing of γ-PGA concentration (Table III).

IV. DISCUSSION

The present study indicated that γ-PGA has the potential to reduce Cd toxicities and decrease the Cd content in rice seedling tissues (Table II) based on the fact that the addition of γ-PGA to Cd-treated seedlings resulted in increased growth (Fig. 1), chlorophyll contents and amylase activities (Fig. 1). Cadmium at high concentrations inhibited the germination of rice consistent with the results from [3], [12]. The inhibition of growth is the first phenotypic evidence in Cd-treated plants, a reduced rates of elongation in the roots and shoots was apparent at low concentrations of Cd. Cd (1 μM) decreased the mitotic index of root tips and they observed noticeable inhibition when the Cd concentration was increased in rice seedling [12]. The effect of Cd was more apparent on roots than shoots because roots are the first point of contact with Cd and the distribution of metals was different in roots and shoots showing that roots had higher quantities of Cd and retained most of the heavy metal in the apoplastic environment outside the cell [14].

TABLE I
EFFECT OF PGA ON GROWTH OF RICE SEEDLING

Cd (µM):PGA(mg·L⁻¹)	Mean ±SD			
	Shoot length (cm)	Root length (cm)	Fresh weight (g)	Dry weight (g)
Control	5.35 ±0.61 ab	4.17 ±1.65 ab	0.0356 ±0.0088 ab	0.0072 ±0.0009 ab
Cd 0 : PGA 50	5.37 ±0.70 ab	4.20 ±1.87 ab	0.0331 ±0.0123 abc	0.0068 ±0.0012 abc
Cd 0 : PGA 100	5.22 ±0.69 abc	4.46 ±1.55 a	0.0352 ±0.0075 ab	0.0068 ±0.0009 abcd
Cd 0 : PGA 500	5.48 ±0.76 a	3.85 ±2.05 ab	0.0366 ±0.0132 a	0.0072 ±0.0012 ab
Cd 0 : PGA 1,000	5.61 ±0.79 a	4.22 ±1.83 a	0.0380 ±0.0176 a	0.0074 ±0.0012 ab
Cd 50 : PGA 0	4.52 ±0.50 def	3.16 ±0.83 bc	0.0303 ±0.0069 abcde	0.0061 ±0.0007 cdef
Cd 50 : PGA 50	4.49 ±0.62 defg	2.49 ±1.09 cdef	0.0284 ±0.0085 bcdef	0.0058 ±0.0008 efg
Cd 50 : PGA 100	4.43 ±0.52 efgh	2.66 ±1.23 cd	0.0314 ±0.0072 abcd	0.0059 ±0.0006 defg
Cd 50 : PGA 500	4.79 ±0.55 bcde	2.49 ±0.76 cdef	0.0366 ±0.0060 a	0.0064 ±0.0009 bcde
Cd 50 : PGA 1,000	5.06 ±0.39 abcd	3.14 ±1.33 bc	0.0358 ±0.0088 ab	0.0058 ±0.0011 efg
Cd 100 : PGA 0	4.06 ±0.64 fgh	2.15 ±0.80 cdef	0.0263 ±0.0062 cdefg	0.0054 ±0.0009 fgh
Cd 100 : PGA 50	4.52 ±0.56 def	1.96 ±0.82 def	0.0237 ±0.0068 defghij	0.0055 ±0.0007 fgh
Cd 100 : PGA 100	4.38 ±0.54 efgh	2.40 ±0.95 cdef	0.0245 ±0.0075 defghi	0.0053 ±0.0007 fgh
Cd 100 : PGA 500	4.53 ±0.46 def	2.77 ±1.14 cd	0.0283 ±0.0066 bcdef	0.0053 ±0.0008 fgh
Cd 100 : PGA 1,000	4.63 ±0.62 cdef	2.61 ±1.16 cde	0.0341 ±0.0059 ab	0.0059 ±0.0011 defg
Cd 250 : PGA 0	3.88 ±0.27 h	0.68 ±0.46 gh	0.0183 ±0.0044 hijk	0.0038 ±0.0005 kl
Cd 250 : PGA 50	3.91 ±0.36 gh	0.71 ±0.30 gh	0.0199 ±0.0041 ghijk	0.0047 ±0.0008 hij
Cd 250 : PGA 100	3.88 ±0.59 h	0.75 ±0.41 gh	0.0202 ±0.0060 ghijk	0.0043 ±0.0007 ijk
Cd 250 : PGA 500	4.39 ±0.49 efgh	1.53 ±0.79 fg	0.0235 ±0.0051 efghij	0.0051 ±0.0008 ghi
Cd 250 : PGA 1,000	4.73 ±0.47 cde	1.60 ±0.86 ef	0.0256 ±0.0055 cdefgh	0.0051 ±0.0008 ghi
Cd 500 : PGA 0	2.67 ±1.31 i	0.16 ±0.09 h	0.0142 ±0.0055 k	0.0027 ±0.0010 m
Cd 500 : PGA 50	3.07 ±0.88 i	0.24 ±0.17 h	0.0170 ±0.0042 ijk	0.0031 ±0.0008 lm
Cd 500 : PGA 100	3.21 ±0.83 i	0.33 ±0.26 h	0.0161 ±0.0068 jk	0.0029 ±0.0009 m
Cd 500 : PGA 500	3.90 ±0.28 gh	0.74 ±0.54 gh	0.0212 ±0.0028 fghijk	0.0041 ±0.0008 jk
Cd 500 : PGA 1,000	4.36 ±0.42 efgh	1.55 ±0.58 fg	0.0253 ±0.0048 defgh	0.0047 ±0.0007 hij

*Values in a column with different letters are significantly different at (P<0.05).

TABLE II
CADMIUM CONTENT IN RICE SEEDLING TISSUES

PGA concentration (mg·L⁻¹)	Cd content (mg·kg⁻¹ DW) ±SD			
	Cd 0 µM	Cd 50 µM	Cd 100 µM	Cd 250 µM
PGA 0	0.012 ±0.004 c	30.387 ±0.618 b	52.875 ±2.453 bc	998.849 ±35.324 b
PGA 50	0.049 ±0.008 a	35.225 ±0.157 a	61.791 ±1.251 a	985.767 ±30.652 b
PGA 100	0.022 ±0.004 bc	36.012 ±0.918 a	59.472 ±2.736 ab	1141.471 ±0.066 a
PGA 500	0.033 ±0.001 ab	36.389 ±1.040 a	51.987 ±0.702 c	74.891 ±2.571 c
PGA 1,000	0.026 ±0.001 bc	25.390 ±0.011 c	40.946 ±0.138 d	69.521 ±2.987 c

*Values in a column with different letters are significantly different at (P<0.05).
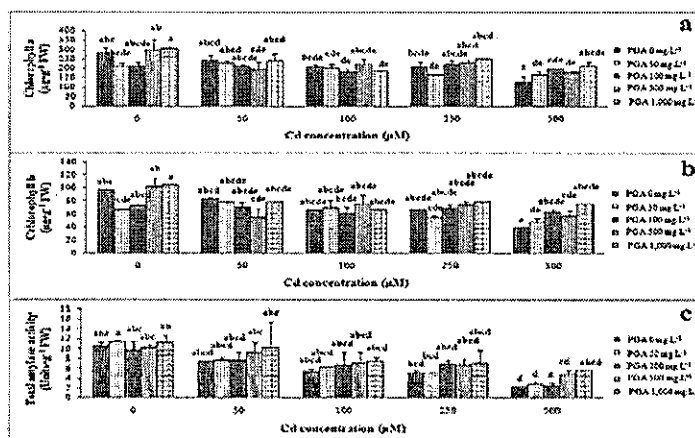

Fig. 1 Effect of PGA and Cd on chlorophyll a and b contents (a and b) and amylase activity (c)
(Error lines show standard deviation and bars with different letters are significantly different at (P<0.05))

TABLE III
THE CORRELATION BETWEEN PGA CONCENTRATION AND CD CONTENT
IN RICE TISSUE

	Treatments			
	Cd 0 μM	Cd 50 μM	Cd 100 μM	Cd 250 μM
Pearson Correlation	.025	-.620	-.882*	-.893*
Sig. (2-tailed)	.969	.264	.048	.042

*Correlation is significant different at the 0.05 level (2-tailed).

In addition, 55-62% of Cd in *Oryza sativa* L. cv Zhonghua 11 was bound onto the root cell wall [3]. A reduction in the chlorophyll content of rice seedlings under Cd stress may be due to an inhibition of the activity of protochlorophyllide reductase which is an important enzyme for chlorophyll synthesis [15]. Moreover, inhibition at the sulhydryl site of reductase protein can cause a decrease in the density and size of the chloroplast [15]. In addition, Cd induced the production of chlorophyllase, the enzyme that activates the degradation of the chlorophyll [16]. The inhibition of amylase activity resulted in a low rate of starch hydrolysis and insufficient energy supply during seed germination and seedling growth [12], [17]. Amylase activities in germinating seed are inhibited by Cd because Cd displaced calcium, which is a cofactor of amylase. The results of displacement are disporting of calcium from α-amylase and β-amylase or changing the steric configurations of α-amylase and β-amylase. The current study showed that the Cd content in rice seedlings sharply increased with an increase in the supplied Cd concentration (Table II) which was in agreement with the previous reports [2]. The addition of γ-PGA reduced the Cd toxicity resulting in a slow increase in the growth rate, amylase activities and the chlorophyll and Cd contents in seedling tissues. Moreover, the correlation between γ-PGA concentration used in the experiment and Cd content in rice tissue was negative correlation. Therefore, increasing of γ-PGA concentration decreased cadmium content in rice tissue. Because γ-PGA is an anionic polymer of glutamic acid; it has been used as a chelating material as it is capable of binding metal ions via its carboxylic and amide groups [18]. Heavy metal ions bind with γ-PGA in a similar chelation mechanism followed by a conformational change of γ-PGA into an enveloped aggregate precipitate [19]. Plants transport free metal ions by diffusion along the concentration gradient [20] as their results suggested that γ-PGA was bound to Cd outside the cell wall and formed a Cd-PGA complex which had difficulty in penetrating the cell wall. They also noted that the concentration of soluble Cd became low as a result of the formation of the Cd-PGA complexes which affected the Cd in flux or its transport rate by plantlet roots.

V. CONCLUSION

From the results of the current study, the application of γ-PGA was found to be an alternative way for alleviating Cd toxicity. Further study is to investigate effect of PGA on reduction of Cd in rice cultivated in a Cd-contaminated environment.

REFERENCES

[1] Y. F. Yan, D. H. Choi, D. S. Kim, and B. W. Lee, "Absorption, Translocation, and remobilization of cadmium supplied at different growth stages of rice," *J. Crop Sci. Biotech.*, vol.13, pp. 113-119, 2010.

[2] N. Rascio, F. D. Vecchai, N. L. Rocca, R. Barbato, C. Pagliano, M. Raviolo, C. Gonnelli, and R. Gabrielli, "Metal accumulation and damage in rice (cv. Vialone nano) seedlings exposed to cadmium," *Environ. Exp. Bot.*, vol. 62, pp. 267-278, 2008.

[3] J. Y. He, Y. F. Ren, C. Zhu, and D. A. Jiang, "Effects of cadmium stress on seed germination, seedling growth and seed amylase activities in rice (*Oryza sativa*)," *Rice Sci.*, vol. 15(4), pp. 319-325, 2008.

[4] W. Swaddiwudhipong, P. Limpatanachote, P. Mahasakpan, S. Krintratun, and C. Paduangtod, "Cadmium-exposed population in Mae Sot district, Tak province: 1. prevalence of high urinary cadmium levels in the adults," *Med. Assoc. Thai*, vol. 90, pp. 143-8, 2007.

[5] R. W. Simmons, P. Pongsakul, D. Saiyasitpanich, and S. Klinphoklap, "Elevated levels of cadmium and zinc in paddy soils and elevated levels of cadmium in rice grain downstream of a zinc mineralized area in Thailand: implications for public health," *Environ. Geochem. Health*, vol. 27, pp. 501-511, 2005.

[6] J. H. Jeong, J. N. Kim, Y. J. Wee, and H. W. Ryu, "The statistically optimized production of poly(γ-glutamic acid) by batch fermentation of a newly isolated *Bacillus subtilis* RKY3," *Bioresour. Technol.*, vol. 101, pp. 4533-4539, 2010.

[7] I. Shih and Y. Van, "The production of poly-(γ-glutamic acid) from microorganisms and its various applications," *Bioresour. Technol.*, vol. 79, pp. 207-225, 2001.

[8] R. C. McLean, D. C. Wolf, F. G. Ferris, and T. J. Beveridge, "Metal binding characteristics of the gamma-glutamyl capsular polymer of *Bacillus licheniformis* ATCC 9945," *Appl. Environ. Microbiol.*, vol. 56, pp. 3671-3677, 1990.

[9] S. S. Mark, T. C. Crusberg, C. M. Dacunha, and D. Iorio, "A heavy metal biotrap for wastewater remediation using poly-gamma-glutamic acid," *Biotechnol. Prog.*, vol. 22, pp. 523-531, 2006.

[10] Y. Ogawa, F. Yamaguchi, K. Yuasa, and Y. Tahara, "Efficient production of γ-polyglutamic acid by *Bacillus subtilis* (natto) in jar fermenters. *Biosci. Biotechnol. Biochem.*, vol. 61, pp. 1684-1687, 1997.

[11] S. Dere, T. Günes, and R. Sivaci, "Spectrophotometric determination of chlorophyll - A, B and total carotenoid contents of some algae species using different solvents," *Tr. J. Bot.*, vol. 22, pp. 13-17, 1998.

[12] J. He, Y. Ren, X. Pan, Y. Yan, C. Zhu, and D. Jiang, "Salicylic acid alleviates the toxicity effect of cadmium on germination, seedling growth, and amylase activity of rice," *J. Plant Nutr. Soil Sci.*, vol. 173, pp. 300-305, 2010.

[13] X. E. Yang, V. C. Baligar, D. C. Martens, and R. B. Clark, "Cadmium effects on influx and transport of mineral nutrients in plant species," *J. Plant Nutr.*, vol. 19, pp. 643-656, 1996.

[14] W. H. O. Ernst, J. A. C. Verkleij, and H. Schatm, "Metal tolerance in plants," *Acta Botanica Neerlandica*, vol. 41, pp. 229-248, 1992.

[15] C. S. Seth, P. K. Chaturvedi, and V. Misra, "The role of phytochelatins and antioxidants in tolerance to Cd accumulation in *Brassica juncea* L.," *Ecotoxicol. Environ. Saf.*, vol. 71, pp. 76-85, 2008.

[16] S. Hayat, B. Ali, A. Hansan, and A. Ahmad, "Brassinosteroid enhanced the level of antioxidant under cadmium stress in *Brassica juncea.*," *Environ. Exp. Bot.*, vol. 60, pp. 33-41, 2007.

[17] C. L. Ge, X. Y. Yang, J. H. Sun, and Z. G. Wang, "Effect of heavy metal stress on the amylase activity in germination rice seeds," *J. Northwest Sci. Tech. Univ.*, vol. 30(3), pp. 47-52, 2002.

[18] F. Y. Siao, J. F. Lu, J. S. Wang, B. S. Inbaraj, and B. H. Chen, "*In vitro* binding of heavy metals by an edible biopolymer poly (γ-glutamic acid) ," *J. Agric. Food Chem.*, vol. 57, pp. 777-784, 2009.

[19] G. H. Ho, T. I. Ho, K. H. Hsieh, Y.C. Su, P.Y. Lin, and J. Yang, "γ-Polyglutamic acid produced by *Bacillus subtilis* (natto): structural characteristics, chemical properties and biological functionalities," *J. Chinese Chem. Society*, vol. 53, pp. 1363-1384, 2006.

[20] B. P. Shaw, S. K. Sahu, and R. K. Mishra, "Heavy metal induced oxidative damage in terrestrial plants. In *Heavy metal stress in plants from biomolecules to ecosystems*, edited by Prasad, M.N.V. New Delhi: Narosa publishing house. pp. 84-126, 2004.

Diversity and Structure of Trichoptera Communities and Water Quality Variables in Streams, Northern Thailand

T. Prommi, P. Thamsenanupap

Abstract—The influence of physicochemical water quality parameters on the abundance and diversity of caddisfly larvae was studied in seven sampling stations in Mae Tao and Mae Ku watersheds, Mae Sot District, Tak Province, northern Thailand. The streams: MK2 and MK8 as reference site, and impacted streams (MT1-MT5) were sampled bi-monthly during July 2011 to May 2012. A total of 4,584 individual of caddisfly larvae belonging to 10 family and 17 genera were found. The larvae of family *Hydropsychidae* were the most abundance, followed by *Philopotamidae*, *Odontoceridae*, and *Leptoceridae*, respectively. The genus *Cheumatopsyche*, *Hydropsyche*, and *Chimarra* were the most abundance genera in this study. Results of CCA ordination showed the total dissolved solids, sulfate, water temperature, dissolved oxygen and pH were the most important physicochemical factors to affect distribution of caddisflies communities. Changes in the caddisfly fauna may indicate changes in physicochemical factors owing to agricultural pollution, urbanization, or other human activities. Results revealed that the order Trichoptera, identified to species or genus, can be potentially used to assess environmental water quality status in freshwater ecosystems.

Keywords—Caddisfly larvae, environmental variables, diversity, streams.

I. INTRODUCTION

FRESHWATER benthic macroinvertebrates inhabit river and stream beds, lakes and reservoirs and are associated with various types of substrates such as mineral sediments, detritus, macrophytes and filamentous algae [1]. They are essential elements in lentic and lotic trophic webs, participating in the energy flow and nutrient cycling [2]. They are also important food resources for fish [3] and some insectivorous birds [4]. The distribution of aquatic organisms is the result of interactions among their ecological role, the physical conditions that characterize the habitat, and food availability [5]. Thus, the community structure of benthic macroinvertebrates depends on a number of factors, such as water quality, type of substrate, particle size of sediment, water flow, sediment organic matter availability, oxygen concentration as well as environmental conditions surrounding the watercourse [4], [6]. Because they reflect environmental

T. Prommi is with the Faculty of Liberal Arts and Science, Kasetsart University, Kamphaeng Saen Campus, Nakhon Pathom Province, 73140 Thailand (phone: +66 34 281105-6; fax: +66 34 281057; e-mail: faastop@ku.ac.th).

P. Thamsenanupap was with Department of Environmental Education, Faculty of Environmental and Resources Studies, Mahasarakham University, Maha Sarakham, Thailand (e-mail: penkhae.t@msu.ac.th).

changes, benthic macroinvertebrates are often used as indicators of the effects of human activity on water system and they provide information on habitat and water quality [7]. The organic enrichment of water caused by both domestic and industrial effluents is a common anthropogenic impact on urban watercourses. This kind of pollution changes physical and chemical characteristics of lotic systems, thus affecting the assemblage of benthic macroinvertebrates [4], [8].

Amongst the benthic macroinvertebrates, order Trichoptera (or caddisflies) are probably the most widely distributed and larvae are common in running water (8-13% of total abundance) [9] and they represent one of the relatively well studied orders of aquatic insects in South East Asia [10], [11]. The larvae of many species coexist in running waters and they are known to have specific habitat and environmental requirements [12]. Caddisflies have been described as the most ecologically diverse group of aquatic insects, with 13,574 described species [11]. As a numerically dominant group in rivers and streams, caddisflies are important to the functioning of freshwater ecosystems because of their ability to partition habitats and trophic resources [13]. Their response to perturbation and reliance on plant matter for food are reasons why caddisflies are widely used in several aspects of water quality monitoring [14]. Furthermore, their well-described biology and taxonomy facilitate interpretation of water quality assessments. The use of species level identification to monitors water quality pollution is much more precise than using family or generic level [15]. The aim of this study was to investigate the diversity and structure of caddisflies communities in relation to water quality variables in order to explore the bioindication potential of caddisflies larvae for assessing water quality deterioration in northern Thailand.

II. MATERIAL AND METHODS

A. Description of the Study Area

Mae Tao and Mae Ku watersheds are located in the lower part of Mae Sot district, Tak Province, northern Thailand. The main agricultural products in this area are rice, soybean, sugar cane and garlic. The main industries are zinc mines and textiles. The seven sampling sites were selected in this study (Fig. 1). Study sites in Mae Tao watershed included MT1, MT2, MT3, MT4 and MT5, which runs through the mine. Agricultural activities were found along the length of this stream. MK2 and MK8, which both are parallel flow with

that stream, were located in Mae Ku watershed. The stream from Mae Tao and Mae Ku watersheds flows to the Moei River. This river is the borderline between Myanmar and Thailand. It is 327 km long, flowing towards the north unlike a river in general. Also, the stream from watershed in Phop Phra district, Tak Province flows to Mae Hong Son via Mae Sot, Mae Ramat, and Tha Song Yang, to merge into the Salween River in Myanmar before flowing into the Gulf of Martaban.
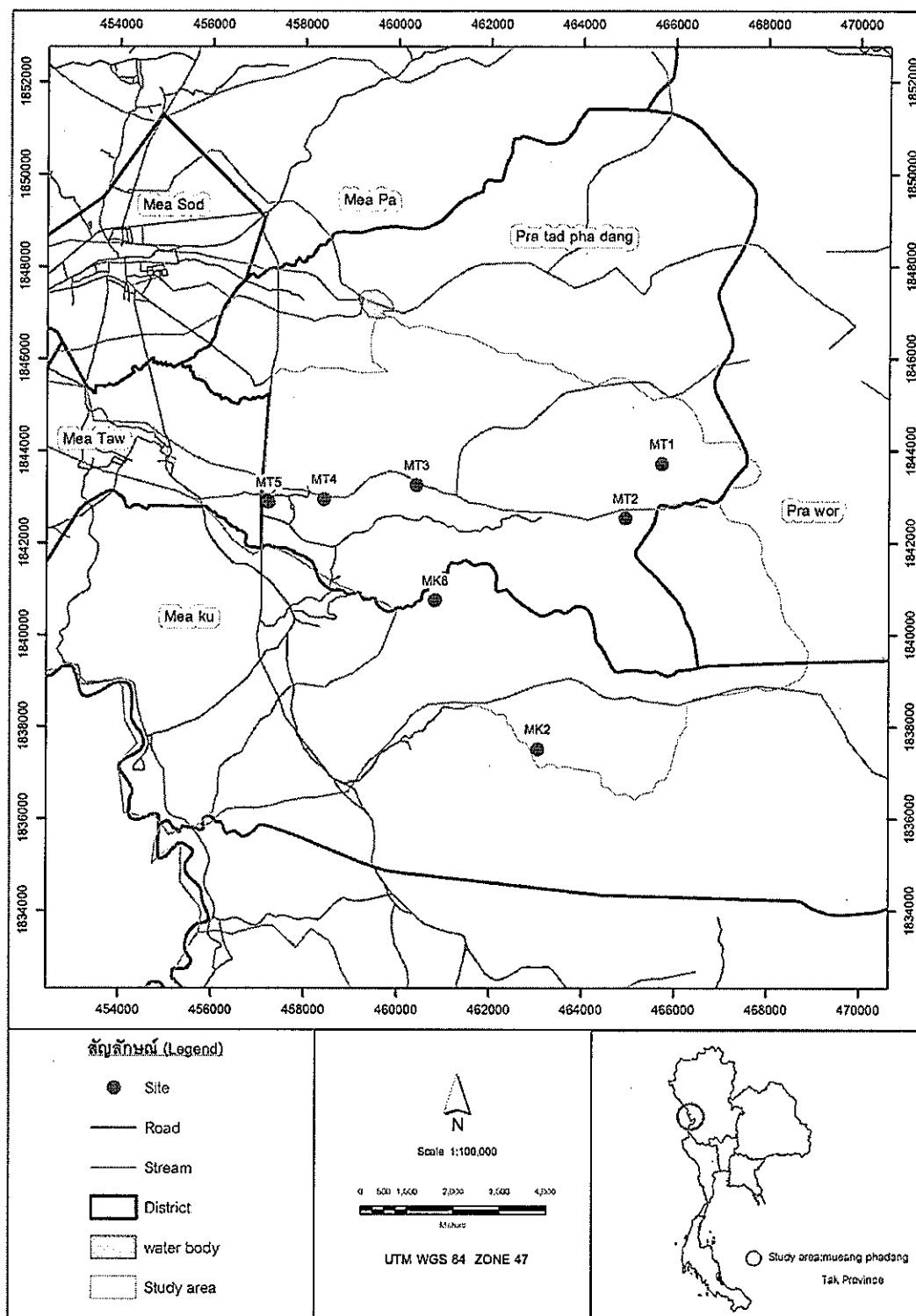

Fig. 1 The sampling sites in Mae Tao (MT1-MT5) and Mae Ku (MK2, MK8) watersheds, Mae Sot District, Tak Province, Northern Thailand

B. Sample Collection

At each site, the sample was collected bi-monthly during July 2011 to May 2012. The physicochemical water quality parameters were measured at all sampling stations between 09 a.m and 5 p.m prior to aquatic insect sampling. Three replicates of the physicochemical water quality parameters were recorded directly at each sampling site and included pH, measured by a pH-meter Waterproof Model Testr30, water temperature (WT) was measured by a hand-held thermometer, and dissolved oxygen (DO), which was measured by a HACH® Model sensION 6 DO meter cyberScan Model DO110, total dissolved solid (TDS) was measured by a EURECH CyberScan CON110 conductivity/TDS meter. Water samples from each collecting period were stored in polyethylene bottles (500 mL). The sulfate (SO_4^{2-}) and nitrate-nitrogen (NO_3-N) were determined in accordance with the standard method procedures [16].

At each sampling period, semi-quantitative samples of caddisflies larvae from the different microhabitats (riffles, depositional zones, different types of vegetation), were collected. A D-frame [5] aquatic hand net (mesh sieve 250 μm) was used. Lotic habitats with stony substrates were sampled during about 15 minutes along an approximately 100 m reach by hand-picking. Other habitats (fine sediments, roots, submerged and aquatic vegetation) were sampled at least in three different zones along the same reach. The contents of the aquatic hand net were poured into white trays. Living caddisflies were sorted and transferred into properly labelled plastic containers, preserved in 80% ethanol and taken back to the laboratory for analysis. In the laboratory, caddisflies larvae were sorted on a petri dish and identified to the genus and species level using taxonomic keys by several authors [13], [17]-[19]. All the sorted samples were kept in properly labelled vials containing 80% ethanol.

C. Data Analysis

The one-way ANOVA ($P < 0.05$) was used to test the difference in means of caddisfly larval abundance among various sampling occasions and among the sampling sites. Pearson's correlation was used to assess the influence of physicochemical variables on the abundance of the caddisfly larvae using the SPSS (Statistical Package for Social Science), Version 13.0. Canonical correspondence analysis (CCA) of PC-ORD Version 4.0 [20] investigate the contribution of the environmental stressors on the distribution and abundance of transformed caddisflies species data (log(x+1)). The Monte-Carlo test was applied to test the significance of the produced canonical axes with 998 permutations at $P < 0.05$. The biplot ordination diagram was produced using CanoDraw for Windows 10. In the CCA, taxa constituting more than 0.1% of the total abundance were selected, and in totals, 14 taxa were used in the analyses.

III. RESULTS

A. Physicochemical Water Quality Parameters

Table I summarized the means, standard deviations of measured physicochemical water quality parameters at the sampling sites taken during the six sampling periods. Dissolved oxygen was not varied significantly during the time of measured ($P>0.05$), whereas water temperature, pH, total dissolved solids, sulfate and nitrate-nitrogen were varied significantly during the time of measured ($P<0.05$). Temperature varied from 24.11 (MK2) to 27.22C° (MK8). The lowest mean value of dissolved oxygen (4.32 mg l^{-1}) was found in the downstream station (MT4 and MT5), and the highest values were observed in upper stream station (≥4.35 mg l^{-1}). Regarding the pH, the water of Mae Tao and Mae Ku watersheds were slightly alkaline with low variation of pH ((8.06 (MT 1) -8.78 (MK2)). The highest mean value of total dissolved solids (294.04 mg l^{-1}) was observed at MK8 and lowest was observed at MT1 (158.12 mg l^{-1}). The mean nitrate-nitrogen concentrations varied from 1.91 (MT1 and MT2) to 3.05 mg l^{-1} (MK8). The mean sulfate value concentration varied from 16.14 (MT1) to 36.85 mg l^{-1} (MT5).

TABLE I

MEAN ± SD SELECTED PHYSICOCHEMICAL WATER QUALITY PARAMETER MEASURED BI-MONTHLY IN MAE TAO AND MAE KU WATERSHEDS DURING JULY 2011 TO MAY 2012

Site/ parameter	WT (°C)	DO (mg l^{-1})	pH	TDS (mg l^{-1})	NO_3-N (mgl^{-1})	SO_4^{2-} (mg l^{-1})
MT1	26.24±2.04[ab]	4.35±1.00[a]	8.06±0.19[a]	158.12±31.96[a]	1.91±0.63[a]	16.14±2.85[a]
MT2	25.35±1.68[ab]	5.30±1.12[a]	8.58±0.11[bc]	231.04±21.24[bc]	1.91±0.49[a]	23.85±5.46[ab]
MT3	25.54±1.98[ab]	5.26±0.78[a]	8.66±0.13[cd]	228.71±52.61[bc]	2.07±0.49[a]	33.28±5.46[c]
MT4	25.02±2.31[ab]	4.32±1.07[a]	8.62±0.19[bcd]	211.28±50.20[ab]	2.55±1.19[ab]	34.42±5.79[c]
MT5	25.50±2.29[ab]	4.32±1.81[a]	8.43±0.27[b]	245.86±48.68[bc]	2.18±0.71[a]	36.85±7.01[c]
MK2	24.11±1.85[a]	5.38±1.03[a]	8.78±0.09[d]	244.33±62.18[bc]	3.01±0.62[b]	20.66±5.31[ab]
MK8	27.22±2.45[b]	5.04±0.85[a]	8.50±0.08[bc]	294.04±107.75[c]	3.06±0.33[b]	25.42±12.08[b]

Values with different letters indicate significant mean difference following Turkey post hoc tests ($P<0.05$)

B. Caddisfly Larvae Abundance and Distribution

The relative abundance and distribution of caddisflies larvae recorded at each of sampling sites during each of sampling periods are presented in Table II. Eighteen genera in ten families, with a total of 4 584 larvae, were collected (Table II). At MT1 and MT3, 599 and 213 specimens in 12 genera were identified, and *Marilia sumatrana* and *Cheumatopsyche lucida* were the most abundant. MT2 and MT5 had the largest abundance larvae, 883 and 1 887 specimens in 10 genera, of which *Cheunatopsyche lucida* were the most frequent. MT4 had the highest genera, 454 specimens in 14 genera were

collected, with *Cheunatopsyche lucida* were the most frequent. MK2 and MK8 had the lowest abundance, 178 and 370 specimens in 7 and 8 genera, respectively.

As shown in Table III, the abundance of caddisflies taxa (*Agapetus halong*, *Cheumatopsyche lucida* and *Lepidostoma doligung*) recorded from Mae Tao and Mae Ku watersheds shows significant difference among sampling dates (ANOVA, $F = 1.578$, 2.158, and 2.400, respectively). *Agapetus halong*, *Chimarra* spp., *Helicopsyche* spp., *Cheumatopsyche* spp., *Diplectrona* spp., *Ceraclea* spp., *Setodes* spp., *Marilia sumatrana*, *Anisocentropus erichthonios*, *Ganonema* spp., *Goera* spp. abundance differed significantly ($P<0.05$) among the investigated sites (ANOVA, F = 1.926, 1.648, 2.500, 3.939, 2.363, 2.250, 2.500, 2.339, 2.500, 3.235, and 2.500, respectively).

Table IV shows the correlation coefficients (Spearman's correlation test at $P<0.05$) between the physicochemical parameters and caddisflies taxa abundance. *Hydropsyche* spp. and *Macrostemum fenestratum* abundance were negatively correlated with water temperature ($P<0.05$). *Chimarra* spp. ($P<0.05$), *Cheumatopsyche* spp. ($P<0.01$) and *Diplectrona* spp. ($P<0.01$) showed negative correlation with dissolved oxygen. The abundance of *Agapetus halong* ($P<0.05$), *Diplectrona* spp. ($P<0.01$), *Anisocentropus erichthonios* ($P<0.01$), and *Ganonema* spp. ($P<0.01$) were negatively correlated with pH, indicating their preference for acidity habitat. The abundance of *Chimarra* spp. were negatively correlated with nitrate-nitrogen ($P<0.01$). The abundance of *Cheumatopsyche* spp., *Oecetis* spp., and *Lepidostoma doligung* were positively correlated with sulfate ($P<0.05$).

TABLE II

LIST OF CADDISFLIES LARVAE AND % RELATIVE ABUNDANCE (RA) IN MAE TAO AND MAE KU WATERSHEDS, TAK PROVINCE, NORTHERN THAILAND DURING JULY 2011 TO MAY 2012

Taxa	Abbr.	MT1	MT2	MT3	MT4	MT5	MK2	MK8	%RA
Hydroptilidae									
Orthrotrichia spp.	Orthro			1				1	0.04
Glososomatidae									
Agapetus halong	Agahal	99	33	8	2	24	1		3.64
Philopotamidae									
Chimarra spp.	Chimar	21	187	35	63	134	42	1	10.50
Helicopsychidae									
Helicopsyche spp.	Helico			2					0.04
Hydropsychidae									
Cheumatopsyche lucida	Cheluc	112	392	82	173	848	38	277	41.9
Cheumatopsyche spp.	Che pp.	45	52	34	98	680	1	59	21.1
Diplectrona spp.	Diplec	84	45	2	4	122	13		5.89
Hydropsyche spp.	Hydrop	36	161	1	24	35	80	3	7.42
Macrostemum fenestratum	Macfen		3		2				0.11
Potamyia spp.	Potamy		3		2	32			0.81
Leptoceridae									
Ceraclea spp.	Ceracl	36		3	1			2	0.92
Oecetis spp.	Oeceti	17	4	7	24	1		1	1.19
Setodes spp.	Setode				1				0.02
Odontoceridae									
Marilia sumatrana	Marsum	117	3	37	56	7	3	26	5.43
Lepidostomatidae									
Lepidostoma doligung	Lepdol	6		1		4			0.24
Calamoceratidae									
Anisocentropus erichthonios	Anieri	20							0.44
Ganonema spp.	Ganone	6			2				0.17
Goeridae									
Goera spp.	Goera				2				0.04
Total number of individual		599	883	213	454	1 887	178	370	
Total number of genera		12	10	12	14	10	7	8	

CCA was utilized to investigate the effect of the environmental parameters on the distribution of caddisflies larvae. The CCA biplot is shown in Fig. 2. The first axis explained 46.6% and the second axis 34.3% of the variances and the Monte Carlo permutation test (998 permutations) was significant at $P < 0.05$ (Table IV). Total dissolved solids and sulfate showed the highest positive correlation with axis 1. Axis 1 was interpreted as an environmental gradient of

increasing total dissolved solids and sulfate (Table V, Fig. 2). Taxa with high positive scores on the first CCA axis included *Cheumatopsyche lucida* and *Potamyia* spp. Taxa with high negative scores on axis 1 included *Agapetus halong*, *Diplectrona* spp. *Ceraclea* spp., *Marilia sumatrana*, *Oecetis* spp., *Lepidostoma doligung*, *Aniscocentropus erichthonios*, and *Ganoneema* spp. (Fig. 2). Axis 2 explained 34.3% of the variance in taxa–environment relations (Table IV). Water

temperature positively correlated while dissolved oxygen and pH negatively correlated with axis 2, so this axis was interpreted as a gradient of increasing values of water temperature and decreasing dissolved oxygen and pH

parameter. Taxa with high negative scores on axis 2 included *Chimarra* spp., *Hydropsyche* spp., *Macrostemum fenestratum*. Few taxa (*Cheumatopsyche* spp.) had high positive scores with axis 2 (Fig. 2).

TABLE III

RESULTS OF THE ONE-WAY ANOVA ON BI-MONTHLY VARIATION OF THE CADDISFLIES LARVAE ABUNDANCE FROM JULY 2011 TO MAY 2012

Taxa	ANOVA (factor month, df = 5)		ANOVA (factor site, df = 6)	
	F	Significance	F	Significance
Orthrotrichia spp.	0.800	0.557	0.833	0.522
Agapetus halong	1.578*	0.191	1.926*	0.104
Chimarra spp.	1.756	0.148	1.648*	0.163
Helicopsyche spp.	0.800	0.557	2.500*	0.410
Cheumatopsyche lucida	2.158*	0.081	1.292	0.286
Cheumatopsyche spp	1.170	0.343	3.939*	0.004
Diplectrona spp.	1.400	0.247	2.363*	0.051
Hydropsyche spp.	1.455	0.229	1.790	0.130
Macrostemum fenestratum	1.272	0.297	1.341	0.265
Potamyia spp.	1.395	0.250	0.947	0.475
Cereclea spp.	1.422	0.240	2.250*	0.061
Oecetis spp.	0.667	0.651	1.190	0.334
Setosdes spp.	0.800	0.557	2.500*	0.041
Marilia sumatrana	2.194	0.076	3.339*	0.053
Lepidostoma doligung	2.400*	0.560	0.833	0.552
Anisocentropus erichthonios	0.800	0.557	2.500*	0.041
Ganonema spp.	1.338	0.270	3.235*	0.120
Goera spp.	0.800	0.557	2.500*	0.041

TABLE IV

NON-PARAMETRIC CORRELATION (CORRELATION COEFFICIENT VALUES) BETWEEN CADDISFLIES SPECIES LARVAE AND WATER PARAMETERS

Taxa/parameters	Water temperature	Dissolved oxygen	pH	Total dissolved solids	Nitrate-nitrogen	Sulfate
Orthrotrichia spp.	-0.114	0.048	0.107	0.064	0.088	0.288
Agapetus halong	-0.173	-0.142	-0.335*	-0.297	-0.297	-0.229
Chimarra spp.	0.014	-0.378*	-0.173	0.031	-0.439*	0.200
Helicopsyche spp.	0.186	-0.046	0.137	0.182	-0.132	0.254
Cheumatopsyche lucida	-0.116	-0.062	-0.014	0.288	-0.169	0.186
Cheumatopsyche spp.	-0.042	-0.421*	-0.207	0.162	-0.289	0.319
Diplectrona spp.	0.247	-0.556*	-0.461**	0.057	-0.283	0.093
Hydropsyche spp.	-0.373*	0.218	0.243	-0.158	-0.057	-0.280
Macrostemum fenestratum	-0.334*	0.017	0.137	-0.076	-0.232	0.008
Potamyia spp.	-0.148	-0.170	-0.027	0.007	-0.191	0.144
Cereclea spp.	0.208	-0.101	0.121	0.195	-0.156	0.319*
Oecetis spp.	-0.035	-0.095	0.065	0.027	-0.169	0.078
Setosdes spp.	0.087	-0.175	-0.035	0.062	-0.090	0.231
Marilia sumatrana	0.100	-0.235	-0.021	0.169	-0.210	0.356*
Lepidostoma doligung	-0.136	0.010	-0.121	-0.157	-0.200	-0.120
Anisocentropus erichthonios	0.226	-0.293	-0.570**	-0.148	-0.132	-0.301
Ganonema spp.	0.112	-0.301	-0.395**	-0.039	-0.149	0.049
Goera spp.	0.087	-0.175	-0.035	0.062	-0.090	0.231

* $P<0.05$, ** $P<0.01$

IV. DISCUSSION

A. Physicochemical Water Quality Parameters

Components of the mean physicochemical status obtained in this study are associated with variety of contaminating practices, such as agricultural activities and mining activities, and they are simple summaries for the pollution status of each sampling station. However, caution must be exercised when interpreting these results, since the impacts of pollution on benthic assemblage structure are potentially confounded by an assemblage's dependence on other environmental characteristics, such as riparian forest, periphyton assemblage and sediment characteristics or channel morphology [21]. In this study, dissolved oxygen was not varied significantly among sampling sites of measured ($P>0.05$). The lowest mean value of dissolved oxygen (4.32 mg l^{-1}) was found in the

downstream station (MT4 and MT5), and the highest values were observed in upper stream station (≥4.35 mg l⁻¹). The low values of dissolved oxygen concentration recorded in downstream stations, is an indication of deterioration of the water quality as a result of various anthropogenic activities in these sites as observed. The plausible reason for high dissolved oxygen in upper station could be attributed to the high current velocity. Dissolved oxygen is considered one of the most important limnological variables, both for the characterization of aquatic ecosystems and for the maintenance of aquatic life. Many organisms, specially the indicators of good environmental quality require high concentrations of dissolved oxygen for their survival [22]. This situation was observed in this study, with a negative relationship between *Chimarra* spp., *Cheumatopsyche* spp., and *Diplectrona* spp. and oxygen concentration. The oxygen concentration of the water and the upper sediment of layer is of considerable important to benthic communities [23], [24]. Fluctuating oxygen levels are often observed in inland waters, as a result of complex diurnal and annual variations depending on both (a)biotic variables such as light intensity, current

velocity or disintegration processes, as well as human activities like hydrological and geomorphological modifications or additional input of organic matter [25], [26]. Minimal content of oxygen is an important factor limiting the distribution of benthic organisms and the ecological recovery of aquatic ecosystems. For example, Becker [27] demonstrated that re-colonization of the caddisfly *Hydropsyche contubernalis* in the River Rhine coincided with increasing oxygen levels.

TABLE V
SUMMARY OF CCA RESULTS FOR THE ABUNDANCE OF CADDISFLIES LARVAE AND WATER QUALITY VARIABLES AXES 1 AND 2 WERE SIGNIFICANT FOLLOWING MONTE-CARLO PERMUTATION PROCEDURES ($P < 0.05$)

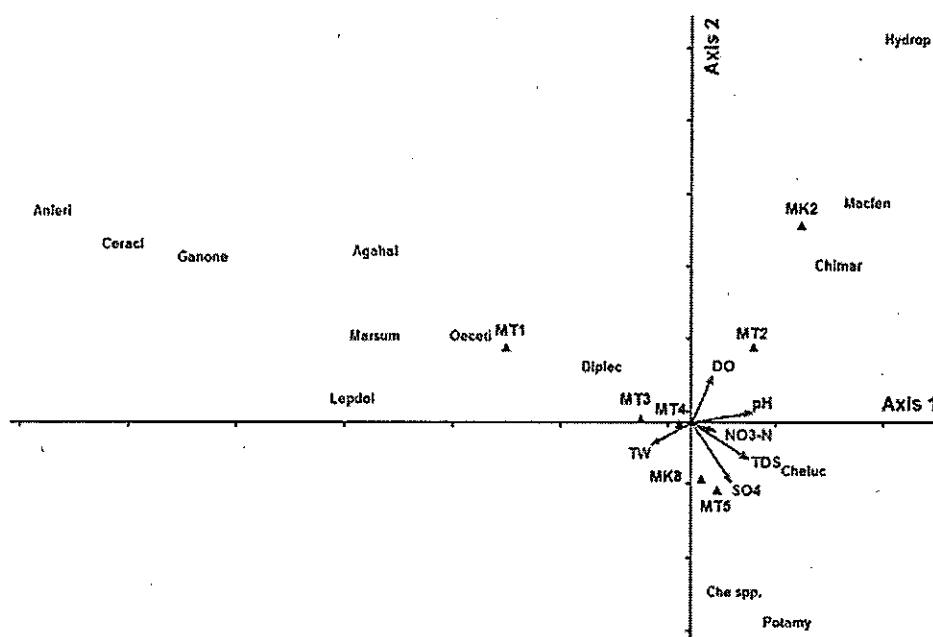|	Axis 1	Axis 2	Axis 3	Total variance
				0.6240
Eigenvalue	0.291	0.214	0.067	
% of variance explained in taxa data	46.6	34.3	10.7	
Cumulative % variance explained	46.6	80.9	91.7	
Pearson Correlation, Spp-Envt*	1.000	1.000	1.000	

Fig. 2 Correlation between aquatic insect taxa and physicochemical variables, Abbreviations of taxonomic are shown in Table II

Temperature is an important water quality parameter and is relatively easy to measure water bodies will naturally show changes in temperature seasonally. Temperature values recorded during the sampling period ranged from 24.11 to 27.22°C. This value falls within the optimal range for tropical freshwaters. The variation in temperature observed was because of low solar heat radiation across the stations. Inundation by run-off water into the stream also causes a reduction in temperature. This temperature reading indicates a great impact on the abundance and distribution of aquatic insects as more species were collected at relatively high temperature than when there was a drop in temperature.

Analysis between caddisflies taxa abundance and water temperature showed *Hydropsyche* spp. and *Macrostemum fenestratum* correlated negatively with water temperature. Possibly, because some caddisflies species are temperature dependent, this favours their rate of feeding, metabolism and reproduction [28].

Nitrate-nitrogen correlated negatively with caddisflies larvae. It is likely that input of nutrients in the stream enhanced secondary production. At MK8 recorded higher values in nutrients nitrate-nitrogen indicating significant input of organic discharges in this area. Zabbey and Hart [29] recorded similar trend in Woji creek in the Niger Delta where

organic wastes are discharged constantly into the stream. Arimoro et al. [30] also recorded similar result in Ethiope River in Niger delta. Nitrate-nitrogen is also an important factor in the distribution and abundance of *Chimarra* spp. The uses of agricultural fertilizers are believed to increase the ammonia, nitrate and phosphate concentrations because the absence of freshwater plants might affect the increase in Nitrogen ion concentrations in the stream.

In natural waters, the pH scale runs from 0 to 14. A pH value of 7 is neutral; a pH less than 7 is acidic and greater than 7 represents base saturation or alkalinity. Generally, tropical waters tend to have low pH. Lower values in pH are indicative at high acidity, which can be caused by the deposition of acid forming substances in precipitation. A high organic content will tend to decrease the pH because of the carbonate chemistry. As microorganisms break down organic material, the by-product will be CO_2 that will dissolve and equilibrate with the water forming carbonic and (H_2CO_3). Most metals will become more soluble in water as the pH decreases. The excesses of dissolved metals in solution will negatively affect the health of the aquatic organisms. The pH value obtained from this study ranged from slightly alkaline (8.06-8.87). Most insect species such as *Agapetu halong*, *Diplectrona* spp., *Anisocentropus erichthonios* and *Ganonema* spp. are slightly affected by alkaline; whereas others are acid-sensitive. pH values recorded in the study is in agreement with the pH values reported for other fresh water systems [31].

Elevated levels of total dissolved solids (TDS) have been suggested as stressors to aquatic life in Central Appalachian streams influenced by coal mining [32], [33]. In coalfield streams, TDS is most often dominated by the dissolved ions SO_4^{2-} and HCO_3^-, with elevated concentrations (relative to reference) of Ca^{2+}, Mg^{2+}, Na^+, K^+, and Cl^- also common [33], [34]. At present here, *Ceraclea* spp. and *Marilia sumatrana* were correlated positively with sulfate. This suggests that while the number of taxa present may increase with increasing TDS, abundance of individuals within the remaining species, and perhaps overall species abundance, may remain less affected, at least within the range of TDS.

B. Caddisflies Communities and Diversity

The number of taxa (or taxa richness) is a synthetic measurement for biological structure. This structure depends on the quality and availability of habitats [35]; they reflect the impact of all investigated stressors independent of ecoregion boundaries. According to the result the highest diversity of caddisflies, species were observed in sampling site MT4 which may be due to presence of rich and undisturbed habitat structure in place, while the lowest values were observed in MK2 and MK8. Low taxa richness indicated of pollution or disturbances in environmental conditions of the streams.

The aim of this study was to investigate the diversity and structure of caddisflies communities in relation to water quality variables in order to explore the bioindication potential of caddisflies larvae for assessing water quality deterioration in northern Thailand. Surveys of this kind have been criticized for their inability to detect or interpret subtle environmental

changes leading to changes in community composition and therefore to differentiate between natural changes and those caused by pollution [36]. Since, detailed site-specific information is not usually available in developing countries; therefore, baseline surveys of the kind conducted in this study are necessary to produce a general view of the biological communities present within a particular area. The differences observed in caddisflies assemblage structure and abundance reflected the differences in location of site and distance from sources of human activities and resulting impacts (e. g. agriculture and industrial effluents).

REFERENCES

[1]   D. M. Rosenberg and V. H. Resh, "Freshwater Biomonitoring and Benthic Macroinvertebrates", New York: Chapman Hall, 1993.

[2]   M. R. Whiles and J. B. Wallace, "Leaf Litter Decomposition and Macroinvertebrate Communities in Headwater Streams Draining Pine and Hardwood Catchments", *Hydrobiologia*, 1997, 353(1-3), 107-119.

[3]   J. B. Wallace and J. R. Webster, "The Role of Macroinvertebrates in Stream Ecosystem Function", *Annual Review of Entomology*, 1996, 41, 115-139.

[4]   D. Ward, N. Holmes and P. JOSÉ, "The New Rivers and Wildlife Handbook". Bedfordshire: RSPB, NRA, The Wildlife Trusts, 1995.

[5]   R. W. Merritt and K. W. Cummins, "An Introduction to the Aquatic Insects of North America", 3rd ed. Kendall/Hunt Publishing Company, 1996.

[6]   D. F. Buss, D. F. Baptista, J. L. Nessimain and M. Egler, "Substrate Specificity, Environmental Degradation and Disturbance Structuring Macroinvertebrate Assemblages in Neotropical Streams", *Hydrobiologia*, 2004, 518(1-3), 179-188.

[7]   T. S. Woodcock and A. Huryn, "The Response of Macroinvertebrate Production to a Pollution Gradient in a Headwater Stream", *Freshwater Biology*, 2007, 52(1), 77-196.

[8]   H. B. N. Hynes HBN, "The Ecology of Running Waters", Canada: University of Toronto Press, 1970.

[9]   S. S. Roback, "Environmental Requirements of Trichoptera", In: Tarzwell CM (ed.), Third Seminar in Biological Problems in Water Pollution, pp. 118-126. No. 999-WP-25, U.S. Public Health Service, Cincinnati, Ohio. 1962.

[10] H. Malicky, "Atlas of Southeast Asian Trichoptera", Biology Department, Faculty of Science, Chiang Mai University, 2010.

[11] J. C. Morse, "Trichoptera World Checklist", http://entweb.clemson.edu/database/trichopt/index.htm, 2011.

[12] F. C. de Moor, "Regional Biogeographical Differences in Trichoptera Diversity in South Africa: Observed Patterns and Processes", In: Bueno-Soria J, Barba-Alvares R, Armitage B (eds), Proceedings of the XIIth International Symposium on Trichoptera, pp. 211-218. 2007.

[13] G. B. Wiggins, "Larvae of the North American Caddisfly Genera (Trichoptera)", 2nd edition. University of Toronto Press, 1996.

[14] V. H. Resh, "(Recent Trends in the Use of Trichoptera in Water Quality Monitoring", In: Otto C (ed.), Proceedings of the VIIth International Symposium on Trichoptera, pp. 289-291. Umea, 1992.

[15] V. H. Resh and J. D. Unzicker, "Water Quality Monitoring and Aquatic Organisms: The Importance of Species Identification", *Journal Water Pollution Control Federation, Washington*, 1975, 47, 9-19.

[16] APHA, AWWA, WPCF, "Standard Method for the Examination of Water and Wastewater", 18th ed. American Public Health Association. Washington DC, 1992.

[17] D. Dudgeon, "Tropical Asian Stream: Zoobenthos, Ecology and Conservation", Hong Kong University Press. Hong Kong, 1999.

[18] C. M. Yule and Y.H. Sen, "Freshwater Invertebrates of the Malaysian Region", Aura Productions Sdn. Bhd. Selangor, Malaysia, 2004.

[19] T. Prommi, "Taxonomy of Hydropsychidae (Trichoptera) in Mountain Streams of Southern Thailand", Unpublished Ph.D. Thesis. Prince of Songkla University, Songkhla, 2007.

[20] B. McCune and M. J. Mefford, "PC-ORD. Multivariate Analysis of Ecological Data, Version 4", MjM Software Design, Gleneden Beach, Oregon, 1999.

[21] M. Sharifinia, J. Imanpour Namin, A. Bozorgi Makrani, "Benthic Macroinvertebrrate Distribution in Tajan River Using Canonical Correspondence Analysis", *Caspian Journal of Environmental Science* 2012, 10(2), 181-194.

[22] P. C. Bispo, L. G. Oliveira, L. M. Bini and K. G. Sousa," Ephemeroptera, Plecoptera and Trichoptera Assemblages from Riffles in Mountain Streams of Central Brazil: Environmental Factors Influencing the Distribution and Abundance of Immature", *Brazil Journal of Biology* 2006, 66, 611-622.

[23] J. V. Ward, "Aquatic Insect Ecology. Biology and Habitat", John Wiley & Sons, Inc, New York, 1992.

[24] L. J. Chapman, K. R. Schneider, C. Apodaca and C. A. Chapman, "Respiratory of Microinvertebrates in a Swamp-River System of East Africa", *Biotropica*, 2004, 36, 572-585.

[25] U. Jacob and H. Walther, "Aquatic Insects Larvae as Indicators of Limiting Minimal Contents of Dissolved Oxygen", *Aquatic Insects*, 1981, 3, 219-224.

[26] H. W. Paerl, J. L. Pinckney, J. M. Fear and B. L. Peierls, "Ecosystem Responses to Internal and Watershed Organic Matter Loading: Consequences for Hypoxia in the Eutrophying Neuse River Estuary, North Carolina, USA", *Marine Ecology Progress Series*, 1998, 166, 17-25.

[27] G. Becker, "Net-Building Behaviour, Tolerance and Development of Two Caddisfly Species from the River Rhine *(Hydropsyche contubernalis* and *H. pellucidula)* in Relation to the Oxygen Content", *Oecologia*, 1987, 73, 242-250.

[28] R. W. Pennak, "Freshwater Invertebrates of the United States", 2nd Edn., John Wiley and Sons, New York, 1987.

[29] N. Zabbey and A. Z. Hart, "Influence of Some Physicochemical Parameters on the Composition and Distribution of Benthic Fauna in Woji Creek, Niger Delta, Nigeria", *Global Journal of Pure and Applied Sciences*, 2006, 12(1), 1-5.

[30] F. O. Arimoro, R. B. Ikomi and E. Erebe, "Macroinvertebrate Community Diversity in Relation to Water Quality Status of River Ase, Niger Delta. Nigeria", *Journal of Fisheries and Aquatic Science*, 2007, 2(5), 337-344.

[31] S. Sreejith, D. Padmalal and R. Mani,"Granulometric Studies of the Sediments of Sasthamkotta and Chelur Lakes, Kerala: Implications of Hydrodynamic Responses on Lacustrine Sediments", *Journal of Indian Association of Sedimentology*, 1998, Vol.17, No.2, pp. 251-262.

[32] R. Bodkin, J. Kern, P. McClellan, A. Butt and C. Martion,"Limiting Total Dissolved Solids to Protect Aquatic Life", *Journal of Soil and Water Conservation*, 2007, 62(3), 57A-61A.

[33] G. J. Pond, M. E. Passmore, F. A. Borsuk, L. Reynolds and C. J. Rose, "Downstream Effects of Mountaintop Coal Mining: Comparing Biological conditions Using Family- and Genus-Level Macroinvertebrate Bioassessment Tools", *Journal of the North American Benthological Society*, 2008, 27(3), 717–737.

[34] D. R. Mount, J. M. Gulley, J. R. Hockett, T. D. Garrison and J. M. Evans, "Statistical Models to Predict the Toxicity of Major Ions to *Ceriodaphnia dubia, Daphnia magna,* and Fathead Minnows *(Pimephales promelas)*", *Environmental Toxicology and Chemistry*, 1997, 16, 2009–2019.

[35] M. T. Barbour, J. Gerritsen, B. D. Snyder and J. B. Stribling,"Rapid Bioassessment Protocols for Use in Wadeable Streams and Rivers. *Periphyton, Benthic Macroinvertebrates, and Fish*", 2nd ed. USEPA. Washington, DC, 1999.

[36] C. F. Mason, "Biology of Freshwater Pollution", Edingbourgh: Addison-Wesley Longman Ltd, 1996.

Catalytic Wet Air Oxidation as a Pretreatment Option for Biodegradability Enhancement of Industrial Effluent

Sushma, A. K. Saroha

Abstract—Complex industrial effluent generated from chemical industry is contaminated with toxic and hazardous organic compounds and not amenable to direct biological treatment.Effectively remove many toxic organic pollutants have made it evident that new, compact and more efficient systems are needed. Catalytic Wet Air Oxidation (CWAO) is a promising treatment technology for the abatement of organic pollutants in wastewater.The main objective of this study is to use the CWAO process for converting the organics into compounds more amenable to biological treatment; complete oxidation may be too expensive. The catalysts were prepared by incipient wetness impregnation method and characterized by scanning electron microscopy (SEM), energy-dispersive X-ray spectroscopy (EDX) and BET (Brunauer, Emmett, and Teller) surface area. CWAO experiments were performed at atmospheric pressure and (30°C - 70°C) temperature conditions and the results were evaluated in terms of COD removal efficiency. The catalysts particles size was selected 50-100 nm size through optimization by catalytic experiments to avoid mass transfer limitation. The biodegradability test was performed by BOD/COD ratio for checking the toxicity of the industrial wastewater as well as for the treated water. The COD removal was achieved upto45%. The BOD/COD ratio of treated water was significantly increased and signified that the toxicity of the organics was decreased while thebiodegradability was increased, indicating the more amenability towards biological treatment.

Keywords—Catalytic wet air oxidation; Industrial organic raffinate; Alumina based Pt catalyst; COD removal efficiency; BOD/COD ratio.

I. INTRODUCTION

THE rapid increase in industrialization caused the tremendous contamination of surface waters in the last decade. Wastewaters from industries such as pulp and paper, dyeing, chemical, petrochemical, oil refining, pharmaceuticals and coking plants etc. contain hazardous and refractory organic pollutants, which can cause severe problems for the environment. Consequently, strict regulations had been made to treat these wastewaters in order to meet the specifications for discharge or for recycling in the process. In particular, chemical industries generate huge quantity of wastewater having high COD values. Beside high COD, these wastewaters are also rich in toxic compounds like ammoniacal nitrogen, pyridine, and its derivatives [1].

Since the effluents from industries contain very high organic and inorganic load and toxicity, they cannot be treated by biological wastewater treatment methods. Treatment of such high strength wastewaters containing recalcitrant compounds using advanced oxidation processes (AOPs) has proved to be very successful method [2]. The AOPs utilize the high oxidizing capacity of oxidizing agents and other strong oxidants to carry out the oxidation of high strength wastewater with toxic and refractory compounds. The AOPs include Fenton, photo-catalysis, ozonation, photo-Fenton, wet air oxidation, etc [3]. Wet Air Oxidation (WAO) employs oxidation of pollutant by highly reactive hydroxyl radicals under high pressure and temperature conditions [4]. In this process, the organic contaminants are either degraded into biodegradable compounds or completely mineralized into carbon dioxide, water and inorganic salts, which remain in the aqueous phase. To combat the requirement of extreme conditions in WAO, catalysts have been used these days in the process. It has now become possible to carry out WAO at ambient conditions with the use of suitable catalysts. Catalysts are used extensively these days in various industries like chemical, petroleum, pharmaceutical and environmental protection [5].

Catalysts can be broadly divided into two main categories: homogeneous and heterogeneous. In case of homogeneous catalyst, the reactants and the catalyst that occur in same phase while in case of heterogeneous catalyst, they occur in different phases. Homogeneous catalyst are advantageous in the respect that mass transfer limitations are minimized which results in higher reaction rates and better degradation of the pollutant [6]. The only disadvantage of the homogeneous catalyst is its separation from the reaction media after the reaction is complete. Heterogeneous catalysts are also more thermally and mechanically stable as compared to homogeneous catalysts. Therefore, heterogeneous catalysts are more desirable these days.

Catalyst selection and design is the main area of research these days for efficient operation of Catalytic Wet Air Oxidation (CWAO). Catalyst used in the process consists of the support material and the doped metal or metal oxide on it. Commonly used support materials are various forms of alumina, silica and carbon. Catalyst support may remain inert or sometime take part in the reaction. Generally, the effluents from industries contain high molecular weight compounds,

Sushma is with Department of Chemical Engineering, Indian Institute of Technology, Delhi, Hauz Khas, New Delhi–110016, India (corresponding author, phone: 011-2659-6245, e-mail: sushma.yadav4@gmail.com).
A. K. Saroha is with Department of Chemical Engineering, Indian Institute of Technology, Delhi, HauzKhas, New Delhi–110016, India.

which are unable to penetrate inside the catalyst particles due to their big sizes. So the active species on the outer surface of the catalyst is only utilized. As γ -Al$_2$O$_3$ has the advantage of high surface area, low cost, and high strength, which therefore is used as carrier often [7].

A lot of information is available on using CWAO for the treatment of synthetic solution containing single organic pollutant. But very scanty data is available for the real industrial effluent containing multi-component mixture of organic compounds. It is proposed to explore the use of CWAO for treatment of industrial effluent. Therefore efforts were made in the present study to explore the potential of alumina based Platinum (Pt) catalyst for the treatment of industrial effluent containing toxic constituents like ammonical nitrogen, pyridine etc.

II. MATERIAL AND METHODS

The industrial effluent was collected from a nearby Chemical industry and was characterized for various parameters. The industrial effluent has high COD- 3000 mg/L, high pH- 11 and high TDS- 10000 mg/L.

The alumina based Pt catalyst was prepared by incipient wetness impregnation method and was characterized for surface morphology, BET surface area analysis.

The experiments were performed in a four-neck glass reactor at ambient conditions of temperature and pressure (atmospheric pressure and ~28°C room temperature). The effect of operating parameters such as catalyst particle size, Pt loading, catalyst dosage and airflow rate was analyzed in terms of percentage COD removal. Initially the glass reactor was filled with 1 litre effluent and the known amount of catalyst was added to it. Then the airflow rate was started and the samples were withdrawn at regular time intervals. The COD of the samples were determined and analyzed by dichromate method (Open reflux, titrimetric method) [8].

Calculations:

$$COD \ (mg.l^{-1}) = \frac{(A-B) \times N}{Vol. \ of \ sample \ (ml)} \times 8000$$

where, A = Volume of FAS used for blank, ml; B = Volume of FAS used for sample, ml; N = Normality of FAS

COD removal efficiency, COD (%) was calculated by the following equation:

$$C_r(\%) = \frac{C_o - C_i}{C_o} \times 100$$

where C$_r$ is COD removal efficiency; C$_o$ is initial COD and C$_t$ is COD at a time t

III. RESULTS AND DISCUSSION

A. Characterization of Catalysts

1. BET Surface Area

The BET surface areas of the freshly prepared catalysts were determined using ASAP 2010 micro poresurface area Analyzer (Micrometrics Corporation, USA). Pure alumina has high surface area 190 m^2/g but with increase in Pt loading decreases the surface area upto 160 m^2/g for 1.5 wt%Pt catalyst. It can be noticed that BET surface area decreases with an increase in catalyst metal precursor loading because some of the surface is occupied by the loaded metal [9].

2. Scanning Electron Microscopy (SEM) Analysis

The scanning electron microscope (SEM) micrograph image (magnification: 10000X) of the freshly prepared Pt (0.1, 0.3, 0.5, 0.7 and 1 wt %) supported on Al2O3 catalysts are shown in Figures 1, 2, 3, 4, 5 and 6 respectively. It showed the morphology of the catalyst and pure alumina has more dispersed particles than others. There is not so much difference in all pictures of different wt% Pt catalyst. It can be noticed that most of the surface is covered with active sites. It is more relevant to compare these structures with used catalysts after CWAO process
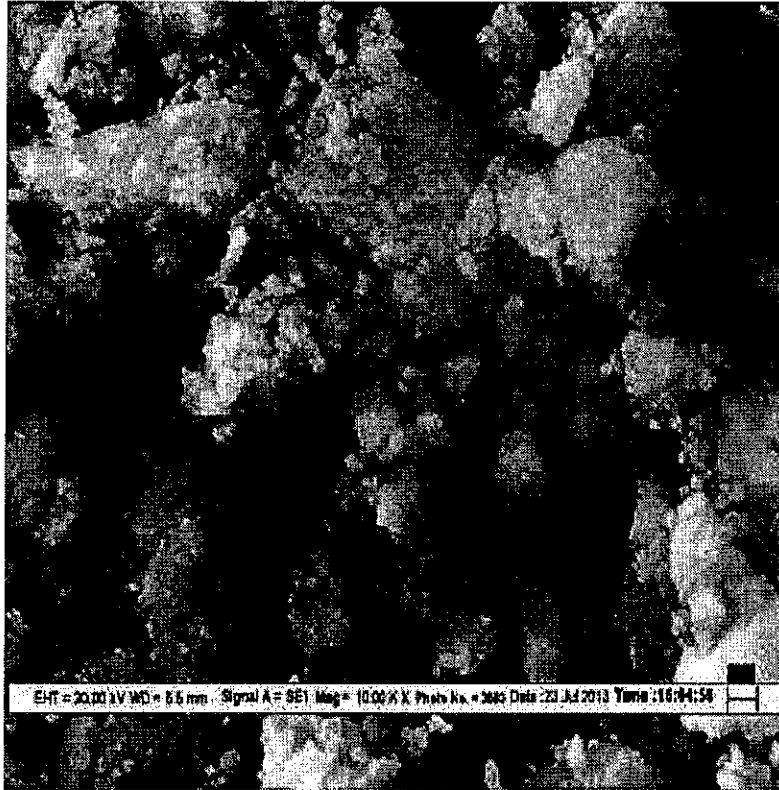
Fig. 1 SEM of Pure alumina

Fig.2 SEM of 0.1 wt%Pt/A$_{l2}$O$_3$

Fig. 3 SEM of 0.3 wt%Pt/Al$_2$O$_3$

Fig.4 SEM of 0.5 wt%Pt/Al$_2$O$_3$

Fig. 5 SEM of 0.7 wt%Pt/Al₂O₃

Fig. 6 SEM of 1 wt%Pt/Al₂O₃

3. Energy-Dispersive X-ray Spectroscopy (EDX) Analysis:

The EDX analysis was carried out for 0.1-1.5 wt%Pt/Al$_2$O$_3$ are shown in Figs. 7-12 respectively. It can be noticed the peaks for Pt, Al, O and C are observed in all the figures. It confirmed that the desired Pt content is present in the catalysts.
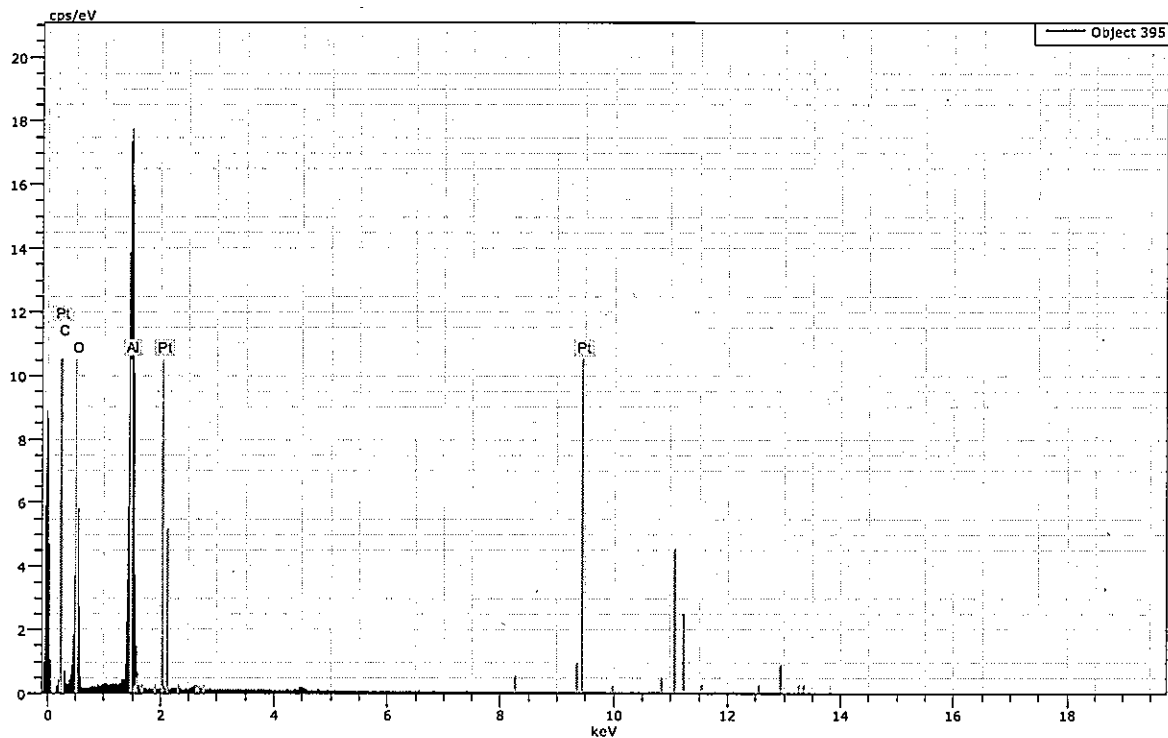

Fig. 7 EDX of 0.1 wt% Pt/Al$_2$O$_3$
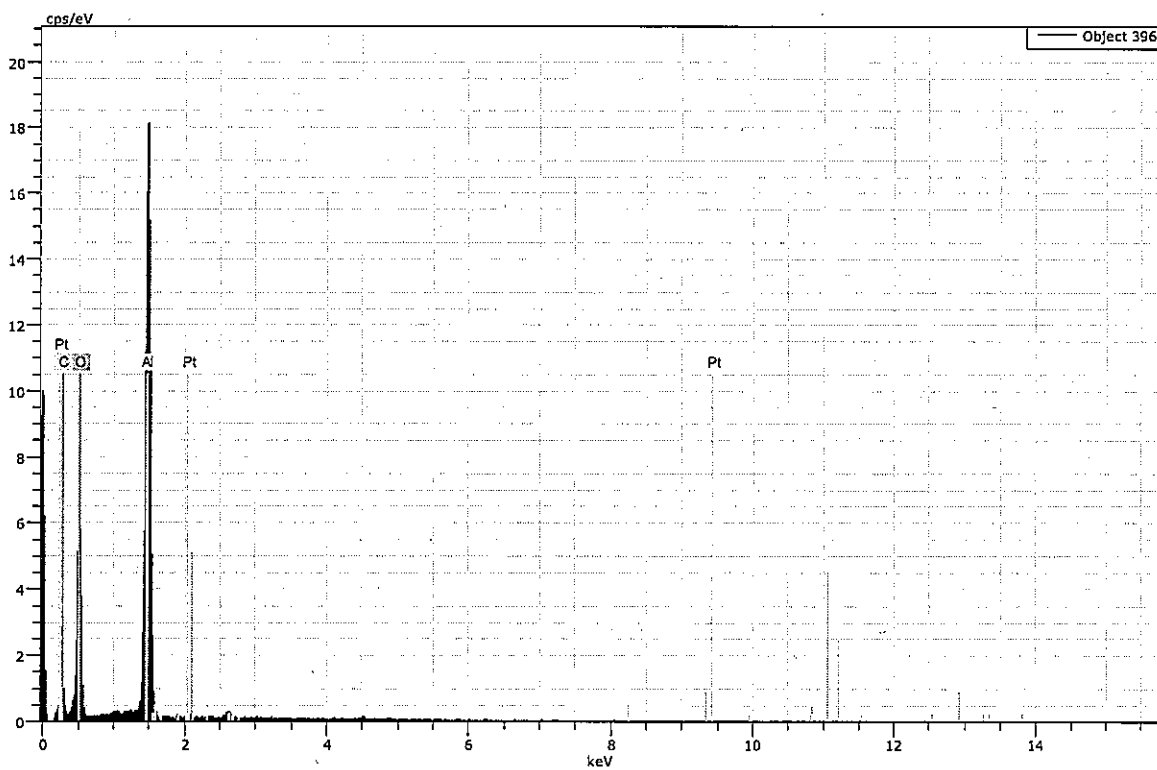
Fig. 8 EDX of 0.3 wt% Pt/Al$_2$O$_3$
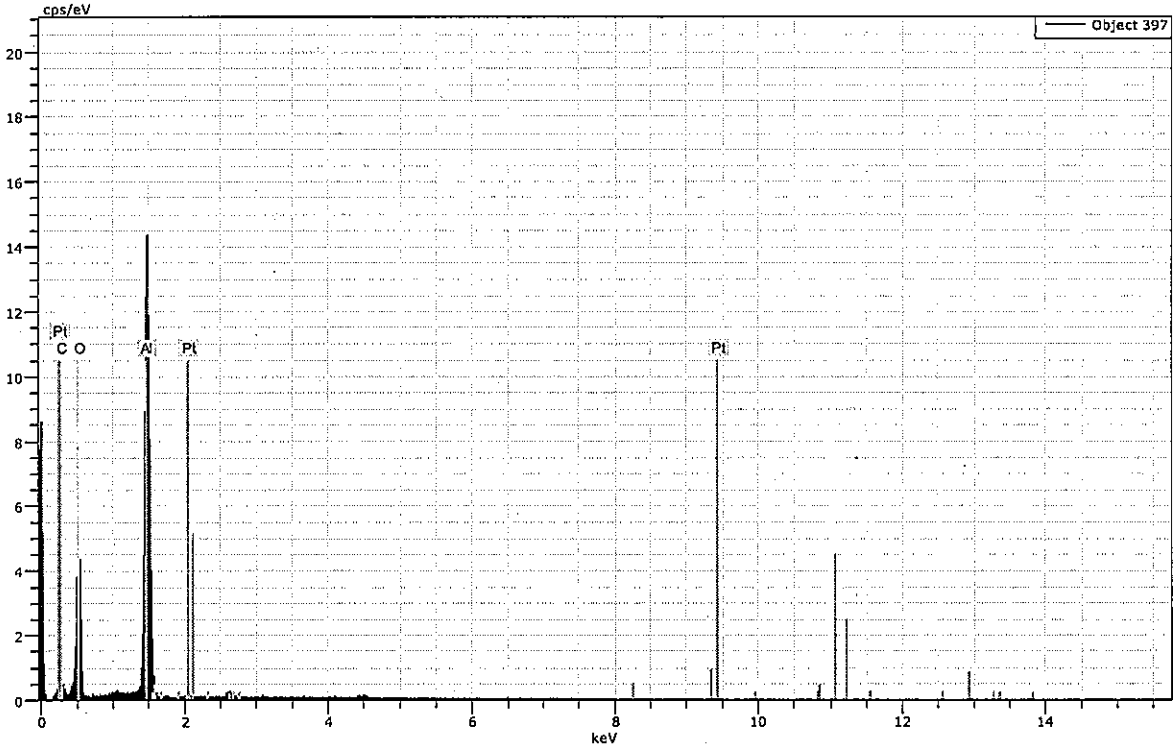
Fig. 9 EDX of 0.5 wt% Pt/Al_2O_3
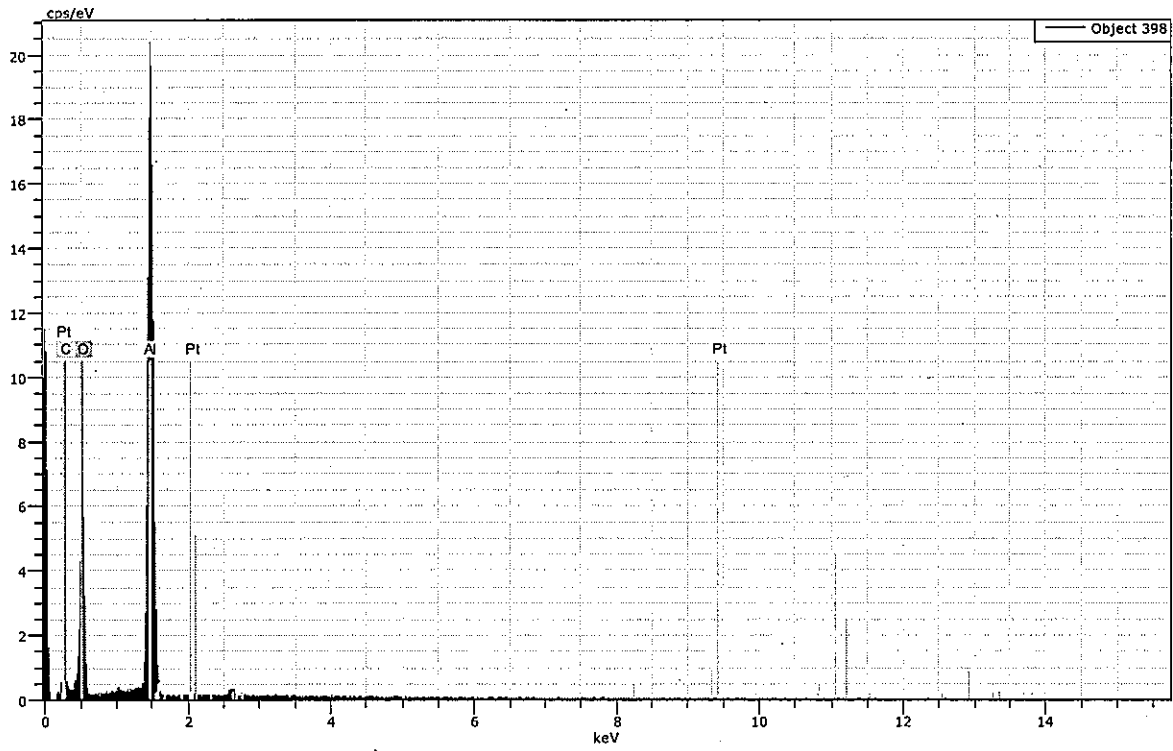
Fig. 10 EDX of 0.7 wt% Pt/Al_2O_3
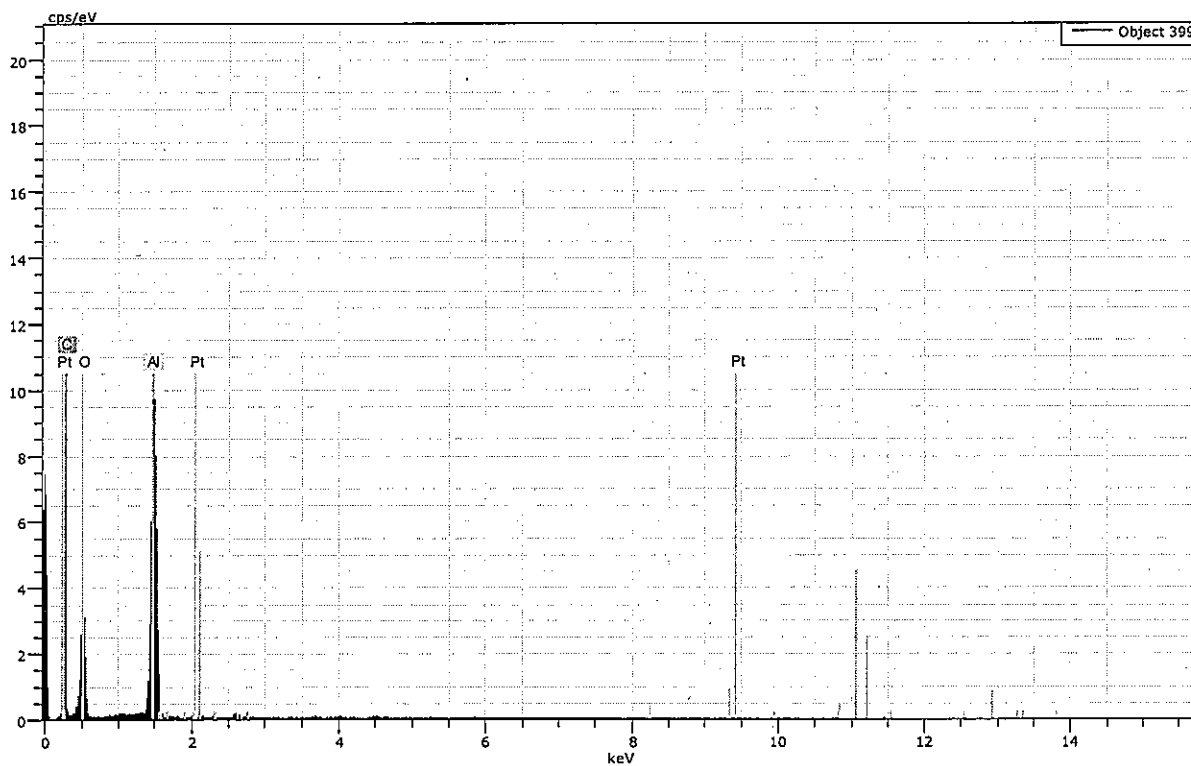
Fig. 11 EDX of 1 wt% Pt/Al$_2$O$_3$
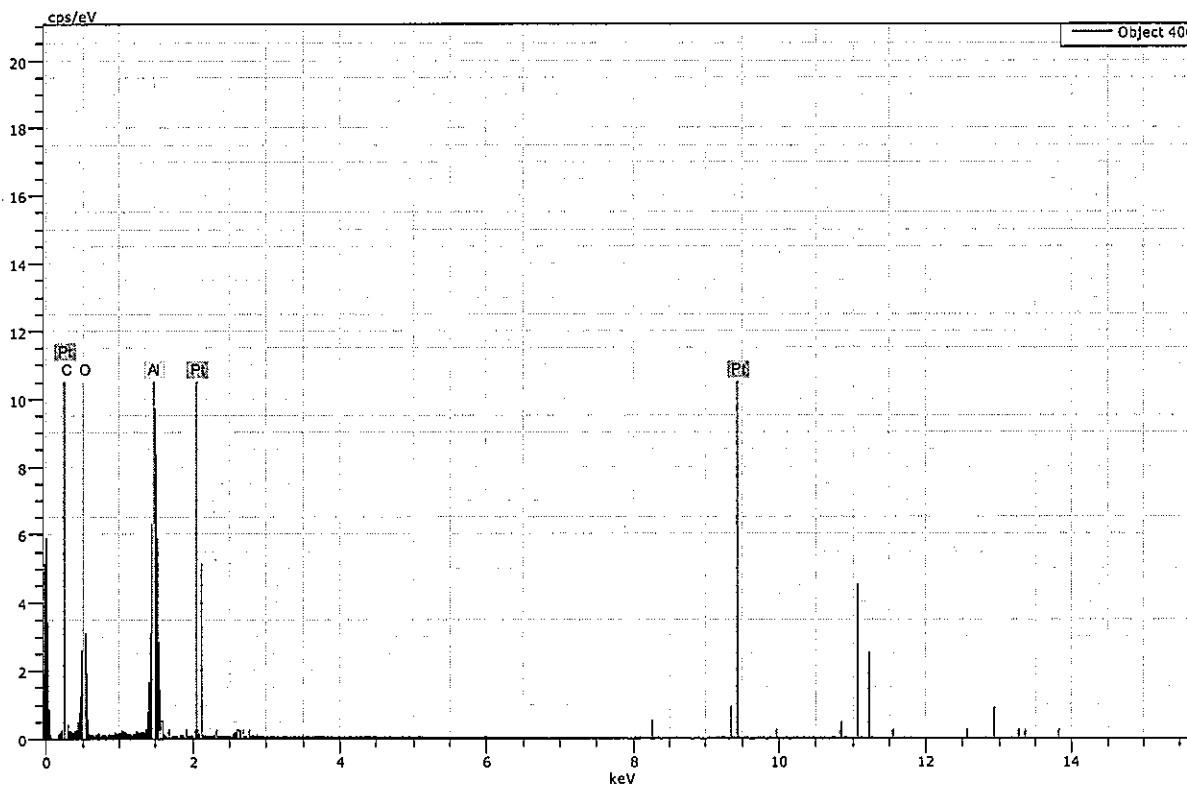
Fig. 12 EDX of 1.5 wt% Pt/Al$_2$O$_3$

B. Catalytic Activity

Experiments were conducted at predetermined optimum conditions to check the effect of temperature for COD removal. The COD removal was found to increase with an increase in reaction temperature. This is because an increase in reaction temperature leads to an increase in the value of

reaction rate constant k, resulting in an enhancement of the reaction rate. The CWAO experiments were performed at 2 L/min airflow rate, 3 g/L of 1 wt%Pt/Al$_2$O$_3$ catalysts dosage for 9 h reaction time at atmospheric pressure. The highest COD removal was obtained at 80°C temperature conditions. The BOD/COD ratio was greatly improved with increasing the temperature. It was found to be higher than 4 which confirmed that the water was completely biodegradable.
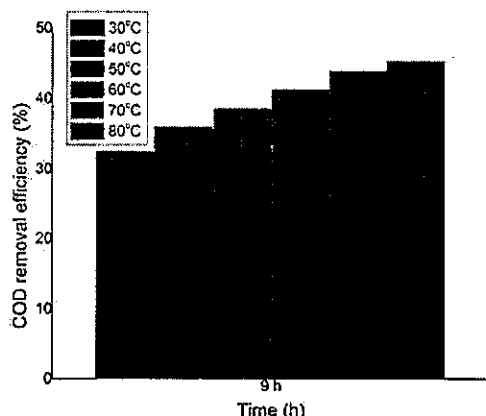
Fig. 13 C Catalytic wet air oxidation of industrial effluent at different temperature

IV. CONCLUSION

The SEM image of different wt%Pt/Al$_2$O$_3$ catalysts signified that the catalysts have rough structure and the Pt metal particles are very fine (not visualize due to very small size) which may be distributed at the surface as well as in the pores of the support. The EDX analysis confirmed that the Pt metals are present in the catalysts. The catalyst activity was expressed by COD removal as well as BOD/COD ratio. The Pt/Al$_2$O$_3$ catalysts greatly improve the biodegradability of the industrial effluent and make it completely biodegradable which can be easily used for conventional treatment method such as biological treatment.

REFERENCES

[1] V. Subbaramaiah, V. C.Srivastava, I. D., Mall, "Catalytic wet peroxidation of pyridine bearing wastewater by cerium supported SBA-15,"*J. Hazard. Mater.*, vol. 248– 249, pp. 355– 363, 2013

[2] W. H.Glaze, J. W.Kang, D. H.Chapin, "The chemistry of water-treatment processes involving ozone, hydrogen-peroxide and ultraviolet-radiation,"*Ozone-Sci. Eng.*, vol. 9, pp. 335–352,1987.

[3] V. K. Kim and S. Ihm, "Heterogeneous catalytic wet air oxidation of refractory organic pollutants in industrial wastewaters: A review," J. *Hazard. Mater., vol.*186, pp. 16-34, 2011.

[4] F. J.Zimmermann, "New waste disposal process,"*Chem. Eng. J.*, vol. 65, pp. 117–120, 1958.

[5] J. Levec and A. Pintar, "Catalytic wet-air oxidation processes: A review,"*Catal. Today, vol.* 124, pp.172-184, 2007.

[6] A.Garg, S.Saha, V.Rastogi, S.Chand, "Catalytic wet air oxidation of pulp and paper mill effluent," *Indian J. Chem. Technol.*, vol. 10, no. 3, pp. 305-310,2003.

[7] J.LevecandA.Pintar, "Catalytic oxidation of aqueous solutions of organics: an effective method for removal of toxic pollutions from waste waters,"*Catal. Today* ,vol. 24, pp. 51-58,1995.

[8] APHA, WPCF, AWWA, Standard Methods for the Examination of Water and Wastewater, 21st ed., American Public Health Association (APHA), Washington, DC, 2008.

[9] Y. Liu and D.Sun,"Effect of CeO2 doping on catalytic activity of Fe$_2$O$_3$/γ-Al$_2$O$_3$ catalyst for catalytic wet peroxide oxidation of azodyes,"J. Hazard.Mater., vol. 143, pp. 448–454, 2007.

Social Marketing–An Integrated and Comprehensive Nutrition Communication Strategy to Improve the Iron Nutriture among Preschool Children

K. Manjula, K. Chandralekha

Abstract—Anaemia is one of the world's most widespread health problems. Prevalence of anaemia in south Asia is among the highest in the world. Iron deficiency anaemia accounts for almost 85 percent of all types of anaemia in India and affects more than half of the total population. Women of childbearing age particularly pregnant women, infants, preschool children and adolescents are at greatest risk of developing iron deficiency anaemia. In India, 74 percent children between 6-35 months of age are anaemic. Children between 1-6 years in major cities are found with a high prevalence rate of 64.8 percent. Iron deficiency anaemia is not only a public health problem, but also development problem. Its prevention and reduction must be viewed as investment in human capital that will enhance development and reduce poverty. Ending this hidden hunger in the form of iron deficiency is the most important achievable international health goal. Eliminating the underlying problem is essential to the sustained elimination of the iron deficiency anaemia. The intervention programs toward the sustained elimination need to be broadly based so that interventions become accepted community practices. Hence, intervention strategies need to go well beyond traditional health and nutrition systems and based upon empowering people and communities so that they will be capable of arranging for and sustaining an adequate intake of foods with respect to iron, independent of external support. Such strategies must necessarily be multi-sectorial and integrate interventions with social communications, evaluation and surveillance.

The main objective of the study was to design a community based Nutrition intervention using theoretical framework of social marketing to sustain improvement of iron nutriture among preschool children. In order to carry out the study eight rural communities In Chittoor district of Andhra Pradesh, India were selected. A formative research was carryout for situational analysis and baseline data was generated with regard to demographic and socioeconomic status, dietary intakes, Knowledge, Attitude and Practices of the mothers of preschool children, clinical and hemoglobin status of the target group. Based on the formative research results, the research area was divides into four groups as experimental area I-III and control area. A community based, integrated and comprehensive social marketing intervention was designed based on various theories and models of nutrition education/ communication. In Experimental area I, Nutrition intervention using social marketing and a weekly iron folic acid supplementation was given to improve iron Nutriture of preschool children. In experimental area II, Social marketing alone was implemented and in experimental area III Iron supplementation alone was given.

No intervention was given in control area. The Impact evaluation revealed that among different interventions tested, the integrated social marketing intervention resulted best outcomes. The overall observations of the study state that social marketing, an integrated and functional strategy for nutrition communication to prevent and control iron deficiency. Various theoretical frame works / models for nutrition communication facilitate to design culturally appropriate interventions thus achieved improvements in the knowledge, attitude and practices there by resulting successful impact on nutritional status of the target groups.

Keywords—Anemia, Iron deficiency, social marketing, Theoretical framework.

I. INTRODUCTION

WORLDWIDE, a staggering number of people lack adequate amounts of foods that are rich in vitamins and minerals needed for health and a productive life. Hidden hunger, in the form of micronutrient deficiencies is pervasive, even where food consumption is adequate. Anaemia is one of the world's most widespread health problems. It affects more than two billion people worldwide - one third of the world's population-and is a significant public health problem throughout the developing world. In almost all developing countries, between one-third to one-half of the female and child populations are anaemic. Anaemia mainly due to iron deficiency is the most pervasive and causes 50 percent of all anaemia worldwide, affecting more than 700 million persons. In a 2002 report, the world health organization lists iron deficiency, a major cause of anaemia, as one of the top 10 risk factors in developing countries for "lost years of healthy life" [3].

Prevalence of anaemia in south Asia is among the highest in the world. About half of the world's anaemic women live in India and 88 percent of them develop anaemia during pregnancy [4]. Iron deficiency anaemia accounts for almost 85 percent of all types of anaemia in India and affects more than half of the total population including all ages and both sexes. Women of childbearing age particularly pregnant women, infants, preschool children and adolescents are at high risk of developing iron deficiency anaemia. NFHS – II data [5] reveal that 74 percent children between 6-35 months of age are anaemic. Children between 1-6 years in major cities are found with a high prevalence rate of 64.8 percent [1].

Iron deficiency anaemia has adverse health consequences for all age groups. Even mild anaemia can impair intellectual as well as physical development in infants and children, while in older children and adults; it reduces work capacity and output and impair immune function. Iron deficiency anaemia is also known to be associated with reduced reproductive

Manjula Kola is with the Sri Venkateswara University, Tirupati, Pin code 517501, AP, India (Phone: +919912366193; e-mail: manju_kola@yahoo.com).

Chandralekha K. was with the Sri Padmavathi Womens University, Tirupati pin code: 517501, AP, India, (e-mail: clekha2@rediffmail.com).

capacity. Iron deficiency anaemia is not only a public health problem, but also development problem. Its prevention and reduction must be viewed as investment in human capital that will enhance development and reduce poverty. Ending this hidden hunger in the form of iron deficiency anaemia is the most important achievable international health goal. Since 1990, outstanding progress has been made towards eliminating iodine and vitamin A deficiencies. However, during this same period, little progress has been made towards elimination of iron deficiency. Iron thus continues to remain the most 'neglected micronutrient' in spite of its greater burden on health [1]. Many control programs are currently implemented including wide spread adoption of iron folate supplementation and growing support for fortification of staple foods with iron.

The alleviation of poverty and strengthening of the national health care systems alone cannot solve the problems of iron deficiency anaemia, as it is a multi-factorial determinant. The intake is less associated with status for iron, the demand for iron varies throughout the lifecycle and the bioavailability of iron varies over a wide range because of a number of factors such as the species of iron compound, the molecular linkage, the amount of nutrient consumed in a meal, the matrix in which the nutrient is incorporated, the absorption modifiers, the nutrient status of the host, genetic factors, other host related factors and interaction among factors [7]. Eliminating the underlying problem is essential to the sustained elimination of the iron deficiency anaemia. The intervention programs toward the sustained elimination need to be broadly based so that interventions become accepted community practices. Hence, intervention strategies need to go well beyond traditional health and nutrition systems and based upon empowering people and communities so that they will be capable of arranging for and sustaining an adequate intake of foods with respect to iron, independent of external support. Such strategies must necessarily be multi-sectorial and integrate interventions with social communications, evaluation and surveillance.

Nutrition education, in the last two decades, has gone through its own development process and a dramatic change has occurred in the definition as well as in the process of nutrition education. Nutrition education has been heavily influenced in recent years by theories and models of health behavior change. There has been a move away from medical models of educating to the use of a range of strong communication channels and the use of integrated approaches by involving the community and advocating marketing principles for nutrition communication. Such an innovative approach is social marketing, an efficient communication strategy.

Social marketing is defined as the design, implementation and control of programs calculated to influence the acceptability of social ideas and involving considerations of product planning, pricing, communication, distribution and market research [19]. Social marketing is based on exchange theory. In marketing, exchange theory states that marketing does not occur unless there are two or more parties, each with something to exchange and both able to carry out

communications and distribution. Social marketing is an application of marketing and has its own uniqueness. For instance, marketing focuses on the wants and preferences of the target population and then responds by trying to satisfy them. It is also inclined to serve specific groups of people [15]. By 1995, the definition of social marketing had expanded as a strategy of understanding, identifying and satisfying the needs and wants of the target audience by placing the target population at the center of the program, not just at the beginning but throughout the process [8]. In this context, a study was carried out to design a community based Nutrition intervention using theoretical framework of social marketing to sustain improvement of iron Nutriture among preschool children.

II. METHODOLOGY

Eight rural communities in Chittoor district of Andhra Pradesh, India were selected. A formative research was carryout for situational analysis and baseline data was generated with regard to demographic and socioeconomic status, dietary intakes, Knowledge, Attitude and Practices of the mothers of preschool children, clinical and hemoglobin status of the target group. Based on the formative research results, the research area was divides into four groups as experimental area I-III and control area. In Experimental area I, Nutrition intervention using social marketing and a weekly iron folic acid supplementation was given to improve iron Nutriture of preschool children. In experimental area II, Social marketing alone was implemented and in experimental area III Iron supplementation alone was given. No intervention has given in control area.

A community based, integrated and comprehensive social marketing intervention was designed based on various theories and models of nutrition education/communication. Each theory or model offers a different perspective on the consumer and the steps leading to behavior change. The theories adopted for the current study are presenting below.

A. Social Cognitive Theory

It deals with the role of people's thoughts and judgment called cognition and how this cognition influences their health behavior [11]. It is the most frequently cited behaviorally based theory used in nutrition education [6]. At present, many techniques can be used to make thought explicit (more visible) for exploration. One of these techniques is 'cognitive mapping' which has been used largely in the social sciences as well as in operations research [17]. They define cognitive mapping as a modeling technique, which intends to portray ideas, beliefs, values, attitudes and their relationship to another in a form, which is amendable to study, and analysis.

To obtain these cognitive maps, Bougon [16] proposes a self-questioning interview technique (self-Q) in order to minimize other influences (i.e., researchers) and to allow cognitive maps to emerge as fully as possible.
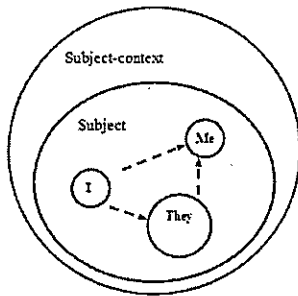
Fig.1 the Context and Perspectives Used In Self Questioning [16]

B. Social Campaign Theory

Cartwright [20] observed that a successful campaign must go through at least three important stages before it could affect individual or group behavior First, it must create a particular cognitive structure for individuals. Second, individuals must be motivated by either changing their perceived needs or by showing them how the advocated actions will meet existing needs. Lastly, the campaign needs to create a particular behavior structure to provide opportunities for individuals to enact desired behaviors at a certain time and place.

C. Stages of Change Theory

The change theory plots a continuum of five stages that individual or groups traverse as they move towards or away from adopting a behavior pattern or life style. The give stages are – Pre-contemplation (unaware, not interested in change), Contemplation (thinking about changing), Decision (being determined to change), Action (actively modifying habits and / or environments) and Maintenance (maintaining the new, healthier habits) [13]. Individuals with any population target group are diverse with respect to these stages as they move in either direction along a continuum. Understanding of the stage of individuals and groups help to determine the appropriate communication approach to move them incrementally in the direction of the desired behavior

D. Diffusion of Innovations Theory

This theory states that the adoption of an innovation (e.g. healthy eating pattern) is based on the innovation's compatibility with current beliefs, values and habits of adopters, its flexibility, relative advantage compared to current practice, reversibility or ease of returning to previous ways, cost efficiency and risk adoption of a behavior spreads through a community from opinion leaders and early adopters to later adopters [9]. Roger's model frames the process of behavior change from a different angle. According to this model, whether a new behavior is adopted depends on whether the audience:

- Perceives a benefit
- Sees it as fitting their needs and values
- Finds it easy to understand
- Can try out the behavior
- Feels that the behavior brings peer acceptance

The process that leads from recognition of an issue to behavior change has several steps. Rogers suggests that the mass media are most effective in the first three steps:

recognition, comprehension and changing attitudes. In the later stages, particularly at the point of trial or adoption of a new behavior, inter personal channels are more influential. Thus a communication strategy might use the mass media to introduce a message, provide information, influence attitudes and reinforce behavior, but use community or inter-personal interventions to teach and encourage the adoption of behavior [12].

E. Social Process Theories

Such as social influence, social comparison and convergence theories specify that one's perception and behavior are influenced by the perceptions and behavior of members of groups to which one belongs and by members of one's personal networks [18].

F. The Triple A process

The Triple A processes pioneered by UNICEF is a participatory decision making process wherein the problem of under nutrition is 'assessed', its causes 'analyzed' along with the available resources and capacity to combat it, followed by a decision on appropriate mix of 'actions'. This process is cyclical and iterative in that once the actions have been initiated; they are subsequently monitored and evaluated (reassessment) Fig. 2.
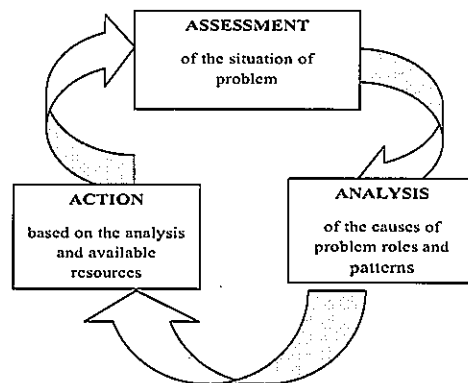

Fig. 2 The Triple A Process [14]

G. The Ecological Framework

The value of using a frame work is that it forces program planners to think about each environmental level in terms of the best opportunities to leverage change (that is, in terms of strategies) and subsequently to think about, how communication might be used to accomplish those ends (that is, what tactics to use). Strategic decisions have to do with what has to change, while tactical decisions have to do with how it will be changed. The steps involved in using ecological framework are illustrated in the Fig. 3 [2].
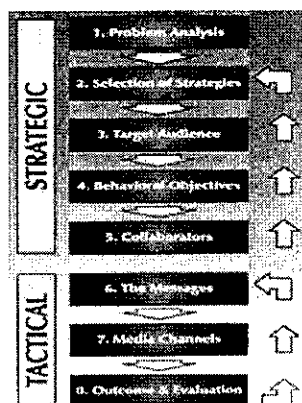
Fig. 3 Strategic Planning Process

The study attempted to integrate the above theories, models and frameworks to better understand and facilitate the health and nutritional behavior change process, particularly dietary change among preschool children.

III. RESULTS AND DISCUSSION

The outcome evaluation measures the effect of the intervention program on the target groups. It includes food and dietary intake and knowledge, attitude and practices of the selected target groups.

A. Dietary Intake of Foods with Respect to Iron

The mean iron and vitamin C intakes of preschool children after intervention were 14.0 and 29.6 mg in experimental area I and 14.6 and 30.3 mg in experimental area II respectively. The increase in both the areas was significant after the intervention period, while in experimental III and control areas where educational intervention was not carried out, no change was observed in iron intake from pre to post intervention period. Only a slight increase was seen in vitamin C intake in both the areas, which were not significant (Table I).

TABLE I
MEAN IRON AND VITAMIN C INTAKES OF PRESCHOOL CHILDREN

Mean Nutrient Intakes	Study Area			f Value	
	expt.i	expt.ii	expt.iii	control	
	Mean Iron Intake				
pre intervention	10.04±1.15	10.00±1.14	10.07±1.14	11.03±0.91	
post intervention	13.97±2.38	14.59±2.14	10.31±1.18	11.06±0.96	**18.55**
mean increase	3.93^a±2.13	4.59^a±1.85	0.24^b±0.42	0.03^b±0.73	p<0.0001
	Mean Vitamin C Intake				
preintervention	17.29±1.01	18.15±1.76	18.50±1.62	18.30±1.72	
post intervention	29.64±4.01	30.29±2.81	20.16±2.36	21.57±3.66	**31.18**
mean increase	12.35^a±4.33	12.14^a±1.16	1.66^b±1.89	3.27^b±2.31	p<0.0001

The mean percent adequacy of iron and vitamin c among the preschool children in different study areas are presented in Fig.4. After intervention period, the mean percent adequacy of iron and vitamin c intakes was improved in both experimental areas i and ii, where social marketing intervention was used for nutrition education. In experimental iii and control areas, where nutrition education was not given, a recognizable difference from pre to post intervention periods was not observed.

The primary aim of food based strategy of the current study was to increase the consumption of iron and other associated foods to improve its bioavailability through nutrition education / communication and ultimately to improve the iron status of the target groups. Implementing science for improving nutrition is not and will not be simple, especially dietary interventions because of their complexity and less impressive results (INACG, 1996). In order to hasten the situation for achieving the aim, easily available and affordable iron dense foods as well as the most palatable and culturally convenient ways of preparation methods were conveyed during communication by imparting etic perspectives in it, so that the target groups could easily adopt the idea and practice which was reflected in the outcomes of dietary intakes after intervention period.
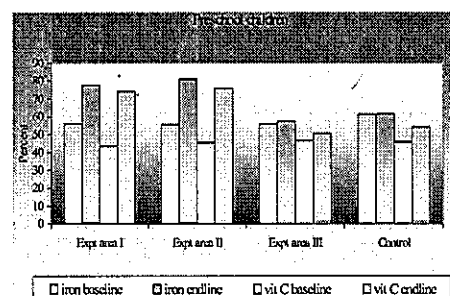

Fig. 4 Percent adequacy of Iron and Vitamin-C among Preschool Children

B. Knowledge, Attitude and Practices (KAP)

Mean scores of KAP during pre and post interventions as well as between the interventions were compared. The mean scores during pre-intervention shows not much difference between the study areas among all the Preschool children. After intervention, significant increase (P< 0.05) was observed in KAP scores of the Preschool children in experimental areas I and II, where social marketing intervention was carried out for nutrition communication (Table II).

Many studies, particularly the earlier ones, involved providing information on the assumption that the person who is exposed to new information will attend to it and gain new knowledge, leading to changes in attitude, which in turn will

result in improved dietary behavior or practices. Critical evaluation of the programs revealed that lack of 'theoretical framework' has been considered as one of the weaknesses in communication programs [10]. Hence, more recent studies targeting health promotion and disease prevention based interventions on more clearly defined theoretical frameworks, studied the various factors that were expected to contribute the effectiveness [9].

TABLE II
MEAN KAP SCORES OF MOTHERS OF PRESCHOOL CHILDREN

kap scores	study areas			
	expt i	expt ii	expt iii	control
knowledge				
baseline	6.07± 8.20	5.13± 7.59	7.73± 9.38	7.00± 8.38
endline	37.13*± 21.68	37.80*± 22.79	10.20±10.55	7.07± 8.63
mean	31.07^b± 2.83	32.67^b ±3.44	2.47^a± 0.78	0.07^a ± 0.24
attitude				
baseline	6.83± 8.04	6.00± 5.63	5.42± 5.65	5.17± 6.23
endline	26.58*± 16.51	27.00*± 14.12	6.17± 5.79	5.25± 6.27
mean	19.75^b± 2.09	21.00^b± 2.03	0.75^a±0.27	0.08^a ±0.22
practice				
baseline	12.67± 8.64	10.11± 5.71	12.11± 7.19	9.89± 5.57
endline	41.67*± 12.74	34.33*± 13.87	15.89± 7.36	10.33± 5.63
mean	29.00^c± 2.08	24.22^b± 2.15	3.78^a± 1.09	0.44^a± 0.26

* Statistically significant at p =0.05 between pre and post
Intervention periods

For instance, research suggests that some kinds of knowledge are more motivating than others. The adoption – diffusion of innovations literature refers to 'awareness' knowledge as the kind that captures people's attention, increases awareness and enhances motivation whereas 'how-to' knowledge is the kind that people need when they are already motivated. 'Motivational knowledge' is the kind of knowledge that is likely to enhance motivation to take action, while behavioral capabilities or knowledge and skills is the kind needed by people in order to act on their motivations is 'instrumental knowledge'. Both motivational and instrumental or how to knowledge, are needed for effective nutrition education designed to foster behavioral change [9].

The current study adopted the above models while introducing and disseminating new ideas and practices through integrating the knowledge, teaches the skills as how to prepare and consume the value added iron dense foods as well as how to acquire and consume iron folate supplements and motivate the mothers of Preschool children to put all these efforts in action. Due to the systematic designing and development of communication program using social marketing brings the positive change in KAP of the selected target groups in experimental areas I and II where nutrition communication interventions were carried out.

IV. CONCLUSIONS

The social marketing strategy used for nutrition communication was very effective by integrating technical information into the existing knowledge as it creates awareness, modifies attitudes, changes behaviors among the target audience. The innovative communication strategy based on theoretical framework or models helped to develop a culturally appropriate and people oriented intervention program which facilitates integration into the existing system for sustained impact.

REFERENCES

[1] U. Kapil Prevention and control of anaemia in India. A background document. National workshop on methodologies for assessment of vitamin a deficiency, iron deficiency anaemia and iodine deficiency disorders. All India Institute of Medical Sciences, New Delhi, 2004, pp. 13.

[2] J. Hyde, R. Agble and P. Nestel, The role of communication in comprehensive Anaemia control: A Framework for planning and implementing a strategic communication plan. INACG, ILSI, Washington, 2003.

[3] IASG. Anaemia Prevention and Control: What works? Part I - Programme guidance. Funded by USAID 2003.

[4] ACC/SCN. Fourth report on the world nutrition situation. ACC/SCN in collaboration with the International Food Policy Research Institute. Geneva: ACC/SCN. 2000.

[5] NFHS-II. (1998-1999). Report of National Family Health Survey- II, 1998-1999. International Institute of Population Sciences, Mumbai, India, 2000.

[6] L. A. Lytle, Eldridge Ala, K. Kotz, J. Piper, Children's interpretation of nutrition messages. Journal of nutrition education, 1997, 29: 128-136.

[7] EClive and West. Iron deficiency: The problem and approaches to its solution. Articles based on an international workshop on IDA, Food and Nutrition Bulletin.1996, Vol. 17, No.1,UNU,

[8] C.R. Lefebvre, O. Lurie, L.S. Goodman, L. Weinberg and Loughrey, Social marketing and nutrition education: Inappropriate or misunderstood. Journal of Nutrition education, 1995, 27L: 146-50.

[9] I, Contento, G. 1 .Balch, Y. L. Bronner. The effectiveness of nutrition education and implications for nutrition education policy programs and research: A review of research. Journal of nutrition education, 1995, 27: 284-418.

[10] Suttilak Smitasiri. Nutri-Action Analysis: Going beyond good people and adequate resources. Institute of nutrition, Mahidol University, Thailand 1994.

[11] K. Glanz and Eriksen M.P, Individual and community models for dietary behavior change, journal of Nutrition education, 1993, 25:80-86.

[12] Rogers Quoted in Applying health communication and social marketing to alcohol, tobacco and other drug problem prevention. 1992. http://p2001.health.org

[13] J. O Prochaska C.C Diclemente and J. C Norcoss, In search of how people change: Applications to addictive behaviors. American psychologist, 1992, 47(9): 1102-1112.

[14] UNICEF, Strategy for improved nutrition of children and women in developing countries. New York, UNICEF, 1990.

[15] D, Cornkindale, P. Balan and C.Rowe, Marketing: Making the Future Happen. Melbourne: Thomas Nelson Australia 1989.

[16] M. G. Bougon, Uncovering cognitive maps: The self-Q technique. In Morgan, G. (Ed.). Beyond Method: Strategies for Social Research. Beverly Hills: Sage Publications, 1983, pp. 173-189.

[17] C, Eden, S Jones and D. Sims, Messing About in Problems. London. Pergamon Press 1983.

[18] Rogers and Kincaid, Communication networks: A Paradigm for new research. New York, free press, 1981.

[19] P. Kotler and G. Zaltman, Social marketing: An approach to planned social change. Journal of marketing.1971, 35, 3-12.

[20] D. Cartwright, Some principles of mass persuasion. Human Relations 1949.2, 253-267.p. 92.

OLEIC ACID ENHANCES HIPPOCAMPAL SYNAPTIC EFFICACY

Rema Vazhappilly [1], Tapas Das [2]

[1] Abbott Nutrition Research and Development, 20 Biopolis Way, Singapore 138668.

[2] Abbott Nutrition Research and Development, 3300 Stelzer Road, Columbus, Ohio 43219, USA

rema.vazhappilly@abbott.com

ABSTRACT

Oleic acid is a cis unsaturated fatty acid and is known to be a partially essential fatty acid due to its limited endogenous synthesis during pregnancy and lactation. Previous studies have demonstrated the role of oleic acid in neuronal differentiation and brain phospholipid synthesis. These evidences indicate a major role for oleic acid in learning and memory. Interestingly, oleic acid has been shown to enhance hippocampal long term potentiation (LTP), the physiological correlate of long term synaptic plasticity. However the effect of oleic acid on short term synaptic plasticity has not been investigated. Short term potentiation (STP) is the physiological correlate of short term synaptic plasticity which is the key underlying molecular mechanism of short term memory and neuronal information processing. STP in the hippocampal CA1 region has been known to require the activation of N-methyl-D-aspartate receptors (NMDARs). The NMDAR dependent hippocampal STP as a potential mechanism for short term memory has been a subject of intense interest for the past few years. Therefore in the present study the effect of oleic acid on NMDAR dependent hippocampal STP was determined in mouse hippocampal slices (*in vitro*) using Multi-electrode array system. STP was induced by weak tetanic Stimulation (one train of 100 Hz stimulations for 0.1s) of the Schaffer collaterals of CA1 region of the hippocampus in slices treated with different concentrations of oleic acid in presence or absence of NMDAR antagonist D-AP5 (30 µM). Oleic acid at 20 (mean increase in fEPSP amplitude = ~135 % Vs. Control = 100%; P<0.001) and 30 µM (mean increase in fEPSP amplitude = ~ 280% Vs. Control = 100%); P<0.001) significantly enhanced the STP following weak tetanic stimulation. Lower oleic acid concentrations at 10 µM did not modify the hippocampal STP induced by weak tetanic stimulation. The hippocampal STP induced by weak tetanic stimulation was completely blocked by the NMDA receptor antagonist D-AP5 (30µM) in both oleic acid and control treated hippocampal slices. This lead to the conclusion that the hippocampal STP elicited by weak tetanic stimulation and enhanced by oleic acid was NMDAR dependent. Together these findings suggest that oleic acid may enhance the short term memory and neuronal information processing through the modulation of NMDAR dependent hippocampal short-term synaptic plasticity. In conclusion this study suggests the possible role of oleic acid to prevent the short term memory loss and impaired neuronal function throughout development.

Selected Ethnomedicinal Plants of Northern Surigao Del Sur: Their Antioxidant Activities in Terms of Total Phenolics, ABTS Radical Cation Decolorization Power, and Ferric Reducing Ability

Gemma A. Gruyal

Abstract—Plants can contain a wide variety of substances with antioxidative properties which are associated with important health benefits. These positive health effects are of great importance at a time when the environment is laden with many toxic substances. Five selected herbal plants namely, *Mimosa pudica, Phyllanthus niruri, Ceiba pentandra, Eleusine polydactyla* and *Trema amboinensi,* were chosen for the experiment to investigate their total phenolics content and antioxidant activities using ABTS radical cation decolorization power, and ferric reducing antioxidant power. The total phenolic content of each herbal plants ranges from 0.84 to 42.59 mg gallic acid equivalent/g. The antioxidant activity in the ABTS radical cation decolorization power varies from 0.005 to 0.362 mg trolox equivalent/g and the FRAP ranges from 0.30 to 28.42 mg gallic acid equivalent/g. Among the five medicinal plants, *Mimosa pudica* has been an excellent performer in terms of the 3 parameters measured; it is followed by *Phyllanthus niruri.* The 5 herbal plants do not have equivalent antioxidant power. The relative high values for *M. pudica* and *P. niruri* supports the medicinal value of both plants. The total phenolics, ABTS and FRAP correlate strongly with one another.

Keywords—ABTS, FRAP, leaf extracts, phenol.

I. INTRODUCTION

OXIDATION process is one of the routs for producing free radicals in food, drugs and even living systems [1]. It is thought that free radicals play an important role in many diseases such as chronic and degenerative disease including aging, coronary heart disease, inflammation, stroke, diabetes mellitus and cancer [2], [3]. The free radicals are formed due to environmental pollutants, radiation, chemicals, toxins, deep fried and spicy foods as well as physical stress that cause depletion of immune system antioxidants [4], [5]. Recently, a large number of researches in interest of naturally occurring antioxidants have been conducted due to their considerable multifaceted characteristic seen in their activity of providing enormous scope in correcting imbalance activity particularly treating, preventing diseases and maintaining human health [6].

For thousands of years, nature has been a source of medicinal agents. Plants as medicine have been used for years to provide health coverage for over 80% of the world's population particularly in the developing world [7]. Plants can contain a wide variety of substances with antioxidative properties which are associated to important health benefits when the environment is laden with many toxic substances. Numerous plants have been identified as having potential antioxidant activities and their consumption is recommended [8], [9].

A phenolic compound which is widely distributed in plants has been reported to exert multiple biological effects, including antioxidant, free radical scavenging abilities, anti-inflammatory and anti-carcinogenic and was also suggested to be a potential iron chelator [10]. In recent year, herbal plants are rapidly becoming popular as a source of an alternative therapy [11].

Mimosa pudica Linn. (Hibi-hibi) is a plant that belongs to family *Fabaceae*. It is a common weed widely distributed in the Philippines in open, moist and open grasslands. Traditionally, it is used for the treatment of traumatic injury, pulmonary tuberculosis, hypertension and diabetes through decoction or infusion [12].

Phyllanthus niruri (Likod) belongs to family *Euphorbiaceae*. It is an herb growing commonly in the roadside as well as in the garden as a weed. Customarily, *P. niruri* is used to treat problems related to the gastrointestinal and genitourinary tracts [13].

Trema amboinensis (Hanagdong) belongs to family *Ulmaceae*. Traditionally, the leaves are used to treat coughs, sore throats, dysenteries and hypertension and the bark is used to make a cough syrup [14].

Ceiba pentandra L. (Gapas) is a plant that belongs to family *Malvaceae* which was previously separated from the family *Bombaceae*. In West Africa, it is generally used in the treatment of diarrhea [15].

Eleusine polydactyla (Busikad) belongs to family *Cyperaceae*. Customarily it is used for cough, fever and muscle aches [16].

The search for novel natural antioxidants from plant origin has increased ever since. In the present study the aim is to determine the total phenolic content and the related total antioxidant potential in five selected ethnomedicinal plants in Surigao del Sur using ABTS radical cation decolorization power and ferric reducing activity power (FRAP).

G.A. Gruyal is with Surigao del Sur State University-Cantilan, Cantilan, Surigao del Sur, Philippines (e-mail: gemma_gruyal@yahoo.com).

II. MATERIALS AND METHODS

A. Plant Material

The samples of *M. pudica* leaf (MPL), *P. niruri* leaf (PNL), *C. pentandra* leaf (CPL), *E. polydactyla* leaf (EPL) and *T. amboinensi* leaf (TAL) were collected during the month of August, 2014 in and around the Northern part of Surigao del Sur, Philippines. These plant materials were botanically authenticated and were deposited in the herbarium at Mindanao University of Science and Technology, Cagayan de Oro City.

B. Plant Preparation

The collected MPL, PNL, CPL, EPL and TAL were sorted and washed with tap water. These plant materials were air-dried thoroughly under shade for 1-2 weeks at room temperature. The dried materials were milled into a fine particle size, place in air tight bottles and stored in the refrigerator at 4°C for subsequent analysis.

C. Chemicals

All the chemicals used for analysis were of analytical grade. Folin-Ciocalteau reagent, gallic acid, quercetin, sodium carbonate (Na_2CO_3), potassium persulfate;2,2'-azino-bis(3-ethylbenzothiazoline-6-sulphonic acid (ABTS); 6-hydroxy-2-5-7-8-tetramethylchroman-2-carboxylic acid (Trolox); potassium persulfate; sodium phosphate; potassium ferricyanide; trichloroacetic acid; Ferric chloride were purchased from Sigma Co. (St. Louis, MO, USA). Other reagents were obtained from Merck Co. (Darmstadt, Germany).

D. Plant Extract Preparation

Twenty (20) grams of each dried grounded plant samples were extracted twice (1500 ml for each sample) with 95% methanol at 20°C for 48 h and concentrated to 100 ml using a rotary evaporator (Panchun Scientific Co., Kaohsiung, Taiwan). The extracts obtained were evaporated under pressure at 50°C to a constant weight. The weight of the filtrate was then transferred to the volumetric flask and raised to 250 ml volume. The extracts were then placed into the storage bottle and placed in the refrigerator at 4°C for succeeding activities.

E. Determination of Plant Extract Yield

Twenty (20) ml of extract solution was pipetted into an aluminum dish (pre-weighed). The dish was placed in an oven to evaporate the methanol at a temperature three degrees (3°) higher than the boiling point of methanol. This was then oven dried for several hours until constant weight of the plant residues were achieved. The yield of each plant extract was calculated by dividing residue by volume of sample (20 ml).

F. Assaying Methods

1. Total Phenolic Contents Determination

The TPC of each methanolic extracts sample were determined according to the Folin-Ciocalteu method [16]. In brief, 300 μL of extract was dispensed into test tube mixed with 1.5 ml of Folin-Ciocalteu's phenol reagent. After 5 min, 1.2 ml of 7.5% (w/v) Na_2CO_3 solution was added to the mixture followed by the addition of 15 ml of dionized distilled water and mixed thoroughly and allowed to stand for 30 minutes in the dark room at room temperature, after which the absorbance was read at 765 nm. The TPC was expressed as milligrams of gallic acid equivalents (GAE) per gram of dried sample and the values are presented as means of triplicate analysis.

2. ABTS Radical-Scavenging Ability

The free radical scavenging activity of *M. pudica* leaf *(MPL)*, *P. niruri* leaf *(PNL)*, *C. pentandra* leaf *(CPL)*, *E. polydactyla* leaf *(EPL)* and *T. amboinensi* leaf *(TAL)* extracts were determined by ABTS (2,2'-azinobis (3-ethylbenzthiazoline-6-sulphonic acid) radical cation with slight modification [17]. The ABTS radical cation (ABTS+) was generated by reacting equal volume of 7 mM ABTS aqueous solution with 2.45 mM potassium persulfate ($K_2S_2O_8$) and the mixture was allowed to stand in the dark for 12-16 hrs at room temperature before use. Prior to use in the assay, the ABTS radical cation solution was diluted with 95% ethanol to an absorbance of about 0.70± 0.02 at 734nm and equilibrated at 30°C. Free radical scavenging activity was assessed by mixing 0.8 ml appropriate dilution of the plant extract was added to 8.0 ml ABTS radical cation solution and mixed thoroughly. The reactive mixture was allowed to stand at room temperature for 15 min and the absorbance was measured at 734 nm. All determinations were carried out at three trials. The antioxidant capacity based on the ABTS free radical scavenging ability of the extracts were expressed as mg Trolox equivalents per gram of the dried plant leaves.

3. Ferric Reducing Antioxidant Power (FRAP) Assay

The ferric reducing property of the plant extracts was determined using the method described by [18]. Various concentrations of each extract (2.5 ml) were mixed with 2.5 ml of 200mM, pH 6.6 sodium phosphate buffer and 2.5 ml of 1% potassium ferricyanide. The reaction mixture was incubated at 50°C for 20 min followed by addition of 2.5 ml of 10% trichloroacetic acid. The mixture was centrifuged at 650 rpm for 10 min to collect the upper layer of the solution. A volume of 5 ml supernatant was mixed with 5 ml of water and 1 ml of 0.1% (w/v) fresh ferric chloride. After 10 min reaction, the absorbance was measured at 700 nm. The ferric reducing antioxidant activity was then calculated. The higher absorbance of the reaction mixture indicates a higher reducing activity.

G. Statistical Analysis

The data were expressed as the mean ± standard deviation of triplicate separate observations and statistically analyzed using Statistical Package for Social Sciences (SPSS) version 17.

III. RESULTS AND DISCUSSIONS

A. Total Phenolic Contents

Table I shows an overview of extraction yields and total phenolic contents of methanolic extracts of *M. pudica, P. niruri, C. pentandra, E. polydactyla* and *T. amboinensi*

TABLE I
EXTRACTION YIELD AND TOTAL PHENOL CONTENT OF THE FIVE PLANT EXTRACT

Herbal Plant	Extraction Yield (mg/ml)	Total Phenolics Content (mg GAE/g)	SD
M. pudica	18.07	42.59 ±	3.11
P. niruri	9.10	24.01 ±	8.13
C. pentandra	12.97	6.04 ±	0.07
E.polydactyla	5.10	0.84 ±	0.08
T. amboinensi	11.38	9.13 ±	0.27

Results represent the mean ± standard deviation of triplicate readings. Phenolics content are expressed as Gallic acid equivalents (GAE)

There was a wide range of extraction yield and phenolic contents in methanolic plant extracts analyzed as shown in Table I. The values varied from 5.10 to 18.07 mg/ml and 0.84 to 42.59 mg GAE/g respectively. It is known that phenolic compounds derived from plants are well renowned to exhibit antioxidant activity through numerous mechanisms including free radical scavenging lipid peroxidation and chelating of metal ions [19]. Among the five selected ethnomedicinal plants only two methanolic plant extracts had phenolic content > 20 mg GAE/g: M. pudica > P. niruri. The rest of the plants extracts were < 20 mg GAE/g phenolic content. The highest phenolic content (>40 mg GAE/g) was found in M. pudica. According to [20] the antioxidant activity of phenolic compounds this is mainly due to their redox properties which can play an important role in absorbing and neutralizing free radicals, quenching singlet and triplet oxygen or decomposing peroxides.

B. ABTS Radical-Scavenging Activity

ABTS radical scavenging assay measured ability to generate a blue/green $ABTS^+$ chromophore via the reaction between ABTS and potassium persulfate. The ABTS radical cation has been often used in the evaluation of antioxidant activity of single compounds and complex mixtures of various origins like body fluids, foods, beverages, plant extracts [21].

TABLE II
ABTS RADICAL CATION DECOLORIZATION OF FIVE SELECTED ETHNOMEDICINAL PLANTS

Herbal Plant	ABTS antioxidant activity mg TE/g	SD
M P L	0.362	± 0.006
PNL	0.283	± 0.008
CPL	0.052	± 0.001
EPL	0.005	± 0.005
TAL	0.056	± 0.002

The antioxidant activity is expressed as Trolox equivalents per gram of dried leaves. Values expressed as mean ± S.D. in three replicates.
$ABTS^+$ scavenging ability reported as the Trolox equivalent

antioxidant capacity (TEAC) is presented in Table II. Results revealed that the $ABTS^+$ scavenging ability of the five herbal plants extract were significantly different ($p<0.05$) in the order of MPL>PNL>CPL> EPL >TAL. This is a clear indication that MPL, with TEAC of 0.362 mg TEAC/g dried leaves had a better $ABTS^+$ scavenging ability among other medicinal plants in the study.

C. Ferric Reducing Antioxidant Power (FRAP) Assay

FRAP assay measures the reducing ability of antioxidants present in a sample and is based on the ability of analyte to reduce the Fe^{3+} to Fe^{2+} pair. The electron donating antioxidants can be described as reductants and inactivation of oxidants by reductants can be described as redox reactions. Many studies show that the reducing power of substances is closely related to antioxidant activity [22]. Total antioxidant power can be detected using FRAP assay. The greater the reducing power the stronger the antioxidant activity.

TABLE III
FRAP ACTIVITY OF THE FIVE SELECTED ETHNOMEDICINAL PLANTS

Herbal Plant Extract	FRAP antioxidant activity mg GAE/g	SD
MPL	27.497 ±	0.806
PNL	28.417 ±	1.020
CPL	4.611 ±	0.174
EPL	0.304 ±	0.021
TAL	8.716 ±	0.194

Ferric reducing activity is expressed as Gallic acid equivalents per gram of dried leaves. Values expressed as mean ± S.D. in three replicates.

In this study the reducing power is reported as gallic acid equivalent which is presented in Table III. Results revealed that MPL, PNL, CPL, EPL and TAL were all able to reduce Fe (III) to Fe (II). Considering in this assay the following decreasing order was established: PNL>MPL>TAL>CPL>EPL. The FRAP activity of the PNL is higher than the other medicinal plant.

IV. CONCLUSION

The results of the present study revealed that the five medicinal plants do not have equivalent antioxidant powers. The relative high values for *M. pudica* (MPL) and *P. niruri* (PNL) supports the medicinal value of the two plants. The total phenolics, ABTS and FRAP correlate strongly with one another as far as the five plants are concerned.

REFERENCES

[1] F. Pourmorad, S. J., Hosseinimehr and N. Shahabimajd, "Antioxidant activity, Phenol and flavonoid contents of some selected Iranian medicinal plants", African Journal of Biotechnology, vol. 5 (11), 2006, pp. 1142-1145.
[2] L. A. Pham-Huy, H. He and C. Pham-Huy, "Free Radicals, Antioxidants

in disease and health" International Journal of Biomedical Science, 2008 June, 4(2): 89-96.

[3] G. Parameswari and M. Suriyavathana,"*In-vitro* antioxidant activity of *Chromalaena odorata* (L.) King and Robinson", International Research Journal of Pharmacy vol. 3 (11), 2012, pp. 187-192.

[4] N. C. Cook and S. Samman, "Flavonoids- chemistry, metabolism, cardioprotective effects, and dietary sources" Nutritional Biochemistry, 1996, 7: 66- 76.

[5] JT Kumpulainen and JT Salonen," Natural Antioxidants and Anticarcinogens in Nutrition, Health and Disease", The Royal Society of Chemistry, UK, 1999, pp 178- 187.

[6] B. Halliwell, JMC Gutteridge and CE Cross," Free radicals, antioxidants and human disease: where are we now? J Lab Clin Med. 1992; 119:598–620.

[7] O. O. Igbinosa, E. O. Igbinosa and O. A. Aiyegoro, "Antimicrobial activity and phytochemical screening of stem bark extracts from *Jatropha curcas* (Linn)", African Journal of Pharmacy and Pharmacology, February, 2009,Vol. 3(2). pp. 058-062.

[8] S. Y., Wang, & H. Jiao, "Correlation of antioxidant capacities to oxygen radical scavenging enzyme activities in blackberry", Journal of Agricultural and Food Chemistry, 2000, 48, 5672–5676.

[9] S. E. Lee, J. H. Hyun, J. -S., Ha, H. S., Jeong & J. H. Kim, "Screening of medicinal plant extracts for antioxidant activity" Life Sciences, (2003), 73, 167–179.

[10] I. Biskup, I. Golonka, A. Gamian and Z. Sroka, "Antioxidant activity of selected phenols estimated by ABTS and FRAP methods", Postepy Hig Med Dosw (online), 2013; 67: 958-963.

[11] S. Vinotha, I. Thabrew, S. Sri Ranjani , "*In vitro* Antioxidant Activity of Two Selected Herbal", Medicines World Academy of Science, Engineering and Technology International Journal of Medical, Health, Biomedical and Pharmaceutical Engineering, (2014) Vol:8, No:12

[12] K. Yuan, A. Jia, JL Lu, "Isolation and Identification of phenolic constituents from *Mimosa pudica*", Chin J Chin Materia Medica, 2006; 31: 1029-30.

[13] R. Karuna, S. Reddy, R. Baskar, and D. Saralakumari, "Antioxidant potential of aqueous extract of *Phyllanthus amarus* in rats," Indian Journal of Pharmacology, vol. 41, no. 2, pp. 64–67, 2009.

[14] D. N. Tchamo, G. Cartier, M.G. Dijoux-Franca, E.Tsamo, and A.M. Mariotte, Pharm. Biol., 2001;39, 3, 202–205.

[15] A. Elumalai, N. Mathangi, A. Didala, R. Kasarla, Y. Venkatesh, "A Review on *Ceiba pentandra* and its medicinal features", Asian J. Pharm. Tech. 2012; Vol. 2: Issue 3, Pg 83-86.

[16] EWC Chan, YY Lim, YL Chew, "Antioxidant activity of *Camellia sinensis* leaves and tea from a lowland plantation in Malaysia", J. food Chem, 2007; 102: 1214-1222.

[17] S. Sellappan, CC Akoh," Flavonoids and antioxidant capacity of Georgia-grown Vidalia onions", Journal of Agriculture and Food Chemistry, 2002; 50:5338-5342.

[18] M Oyaizu, "Studies on products of browning reaction: antioxidative activity of products of browning reaction prepared from glucosamine", Jpn. J. Nutri, 1986; 44:307-15.

[19] F. Shahidi, "Natural antioxidants: an overview", Chemistry, health effects and applications. Champaign, IL: AOCS 1997. Press. P. 1-.

[20] T. Osawa, "Novel natural antioxidants for utilization in food and biological systems", Biochemistry of Plant Food-Materials in the Tropics. Japan Scientific Societies Press, Tokyo, Japan, 1994, p. 241-251.

[21] V. Katalinic´, M. Milos, D. Modun, I. Music´,& M. Boban, "Antioxidant effectiveness of selected wines in comparison with (+)-catechin". Food Chemistry, (2004), 86, 593–600.

[22] X. Duan, G. Wu, Y. Jiang," Evaluation of antioxidant properties of phenolics from litchi fruit in relation to pericarp browning prevention". Molecules, 2007; 12:759-771.

Physicochemical Properties of Palm Stearin (PS) and Palm Kernel Olein (PKO$_O$) Blends as Potential Edible Coating Materials

I. Ruzaina, A. B. Rashid, M. S. Halimahton Zahrah, C. S. Cheow, M.S. Adi

Abstract—This study was conducted to determine the potential of palm stearin (PS) as edible coating materials for fruits. The palm stearin was blended with 20-80% palm kernel olein (PKOo) and the properties of the blends were evaluated in terms of the slip melting point (SMP), solid fat content (SFC), fatty acid and triacylglycerol compositions (TAG), and polymorphism. Blending of PS with PKOo reduced the SMP, SFC, altered the FAC and TAG composition and changed the crystal polymorphism from β to mixture of β and β'. The changes in the physicochemical properties of PS were due to the replacement of the high melting TAG in PS with medium chain TAG in PKOo. From the analysis, 1:1 and 3:2 were the better PSPKOo blend formulations in slowing down the weight loss, respiration gases and gave better appearance when compared to other PSPKOo blends formulations.

Keywords— Guava, palm stearin, palm kernel olein, physico-chemical.

I. INTRODUCTION

Chemical characteristics such as length of the fatty acid chain, number and position of unsaturation influence the physical properties of fats. Chemical and physical properties are fundamental factors in determining the application of oils and fats (Díaz Gamboa and Gioielli, 2003; da Silva et al., 2010). Lipids are possible materials for making coatings for fresh or further processed foods to extend their shelf life (Cocero, Martín, Ángel, Mattea, and Varona, 2009). Researchers reported that the barrier efficiency of lipids is also influenced by their solid fat content (SFC) and moisture transfer resistance of fat (Martin-Polo, Mauguin, and Voilley, 1992; Bourlieu et al., 2010).

Bourlieu et al. (2010) stated that the crystal habit of lipids (polymorphism, crystallite size and shape, spatial distribution of the network mass) may also affect their barrier efficiency. The three main polymorphic forms of triglycerides, in increasing order of thermodynamic stability and hydrocarbon chain packaging are α (hexagonal), ß' (orthorhombic) and ß (triclinic). It could be expected that the ß form which is the densest and best ordered would poses the highest moisture transfer resistance. Therefore, palm stearin which is the high-melting fraction from palm oil with ß polymorph character

istic (Shen, DeMan, and DeMan, 1990) might be need to be blend a suitable material for edible coating. However, the PS with fats have good melting properties such as palm kernel olein (PKOo) to impart plasticity. Hence, the objective of this study was to investigate the physicochemical properties of PSPKOo blends as potential material for coating of guavas.

II. MATERIALS AND METHODS

Materials

Refined, bleached and deodourised (RBD) medium-hard palm stearin (PS) (SMP 53.4°C, IV 40.3) and palm kernel olein (PKOo) (SMP 23.4, IV 24.2) were obtained from Golden Jomalina Sdn. Bhd. Klang, Malaysia and Cargill Specialty Oils and Fats Sdn. Bhd, Port Klang, Malaysia, respectively. The PS and PKOo were stored at 5°C prior to use. The chemicals used in this study were either analytical or HPLC grade. The TAG standards were purchased from SIGMA-Aldrich Co. (Missouri, USA).

Fruits

Fresh guavas were obtained from a commercial farm, Sui Yuan Fruit Trading, in Ladang Bikam, Bidor, Perak, Malaysia. The guavas with maturity index 2 were carefully selected to obtain uniform weight (approximately 400-405 g), size, shape, colour and free from injuries. The fruits were packed in small boxes and transported to the laboratory in Universiti Teknologi MARA, Shah Alam, Selangor, Malaysia. The fruits were stored for 1 hour in the chiller at 10°C prior to use.

Coating Preparation

The PS and PKOo were melted at 60°C in an oven prior to use. The PS and PKOo were mixed in the following ratios (wt/wt) as shown in Table 1.1.

Corresponding Author Ruzaina Binti Ishak from Management and Science University, , Malaysia e-mail: ruzaina_ishak@msu.edu.my

Table 1:
Palm Stearin and Palm Kernel Olein Ratios.

PS (%)	PKOo (%)	Ratios
20	80	1:4
40	60	2:3
50	50	1:1
60	40	3:2
80	20	4:1

Fruits Preparation

Guavas were prepared using the procedure described by Lerdthanangkul and Krochta (1996) with some modification. The sodium chloride was replaced by potassium sorbate for disinfection purpose. Initially, fruits were washed with a 0.5% potassium sorbate for disinfection purposes, and then rinsed with water. After rinsing, the fruits were blotted dry with paper towels. Lipid coating was applied manually on the dried guava fruits using commercial sponge of 4 cm x 4 cm x 4 cm size. Excess coating was allowed to drain off. A single layer coating was applied on the fruits. The fruits were coated with PSPKOo blends in proportions of 1:4, 2:3, 1:1, 3:2 and 4:1 and air dried at ambient temperature (20°C). These ratios were chosen base on the ability of PKOo in influencing the slip melting point (SMP) of PS as well as the mouthfeel of fat product. The uncoated guava was used as control. After coating, the fruits were stored at 20°C prior to further analysis.

Determination PSPKOo Blends Properties

Fatty Acid Composition (FAC)

Fatty acid composition in the form of fatty acid methyl esters (FAME) was determined quantitatively according to MPOB Test Method (MPOB, 2004). Analysis was conducted using Gas Chromatography System (Agilent Technologies 6890N Network) equipped with Inert Mass Selective Detector (Agilent Technologies 5973) and Agilent 7683 Series Injector. A HP-5MS capillary column (Agilent 19091S-433, 0.25 mm × 30 m × 0.25 m) was used.

The GC detection was done using an electronionisation system with ionisation energy of 70 eV in the 50–550 a.m.u. mass range. Column temperature was increased from 60°C to 315°C at the rate of 10°C/min. Initial and final times were 6 min and 10 min, respectively. Helium was used as the carrier gas, at a flow rate of 1.0 mL min in split ratio of 1:100 flow modes. Identifications were based in comparison to standard.

Triacylglycerol (TAG) Profiles

The TAG profiles of the PS and PKOo blends were analysed in a reversed-phase high-performance liquid chromatography (Gilson, Villiers-el-Bel, France). A Lichrosphere RP-18 column (250 mm x 4 mm) of 5-μm particle size (Merck, Darmstadt, Germany) with acetone/acetonitrile (75:25% v/v) as the eluent at a flow rate of 1.0 ml/min and a refractive index detector were used. Identification of TAG was done by comparison of retention times with those of TAG standards.

Slip Melting Point (SMP)

The SMP of the coating blend was determined according to MPOB Test Method (2004). At least three clean glass capillary tubes open at both ends, about 80 mm long, having an external diameter of 1.4 mm to 1.5 mm and an internal diameter of 1.0 mm to 1.2 mm were initially dipped into a completely melted oil blend to a depth of 10 mm. The tubes were then chilled until the oil blend was solidified prior to placing them in a test tube and held in a beaker of water equilibrated at 10°C for 16 h in a refrigerator (Huber, Offenburg, Germany).

The capillary tubes were subsequently removed from the test tube and attached to a thermometer with a rubber band such that the lower ends of the tubes were at the same level as the bottom of the mercury bulb of the thermometer. The thermometer was suspended in a beaker containing 400 mL of boiled distilled water. The thermometer was immersed in the water to a depth of 30-mm. The initial temperature of the thermostated water bath was adjusted to between 8 to 10°C below the expected SMP of the oil blend. The water bath was agitated using a magnetic stirrer and heat was supplied at the rate of 1°C/min and reduced to 0.5°C/min. The temperature at which the sample in the tubes started to melt and become clear is defined as the SMP. The difference between values of the measurement carried out by the same analyst on the same test sample shall not exceed 0.5°C for palm kernel olein and palm stearin. Samples were analysed in triplicates and mean values were calculated.

Solid Fat Content (SFC)

The SFC of the blend was measured using a minispec pulsed Nuclear Magnetic Resonance (pNMR) spectrometer (Bruker, Karlsruhe, Germany). The MPOB parallel test method was used. The sample in the NMR tube was first melted at 70°C for 30 mins, followed by chilling at 0°C for 90 mins and then held at each measuring temperature for 30 mins prior to measurement (MPOB, 2004). Melting, chilling and holding of samples were carried out in pre-equilibrated thermostatted water baths, accurate to 0.1°C. The % SFC was based on triplicate measurements and the value was averaged. The SFC was measured from 5 to 55°C at 5°C interval.

Iodine value (IV) by Wijs' method.

The IVs of the samples were determined according to the procedure described in the MPOB Test Method (2004). The sample (0.5 g) was diluted in 20 ml of cyclohexane and 25 ml of the Wijs' solution (Iodine monochloride) was added to halogenate the double bonds. After placing the bottles in the dark for 1 hour, the mixtures were reacted with 20 ml of potassium iodide and 100 ml distilled water. Free I_2 was measured by titration with 24.9 g/l $Na_2S_2O_3.5H_2O$ using starch (1.0 g/100 ml) as an indicator. The IV was calculated as gram I_2 absorbed per gram of sample. The iodine value of each sample was determined in triplicates. Blank and sample was titrated at the same time.

Crystal Polymorphism by X-ray Diffraction

The polymorphic forms of fat crystals in the blends were determined by X-ray diffraction, using an Enraf Nonius Model FR592 (Delft, The Netherlands). The instrument was fitted with a fine copper X-ray tube. The sample holders were flat stainless-steel plates with rectangular holes. Samples were melted at 70°C and tempered at 20°C for 30 mins. Short spacings on the X-ray film were measured with a Guinier viewer (Enraf Nonius, Delft, The Netherlands). The short spacings of the ß' forms are at 4.2 and 3.8 Å and that of the ß form is at 4.6 Å (D' Souza, deMan, and deMan, 1991). Levels of ß' and ß crystals in sample mixtures were estimated by the relative intensity of the short spacings at 4.2 and 4.6 Å.

Determination Effect of PSPKOo Coating on Guavas

Measurement of Weight Loss

Weight loss occurred due to the transfer of water vapour from the guava to the air. This was determined by weighing the guava on a digital balance (Sartorious Universal, Edgewood, New York) immediately after coating had dried. Weight loss was recorded at day 0, 1, 5, 7, 14 and 21 days of storage at 20°C. Weight loss was reported as percentage loss in weight based on the original mass.

Determination of O_2 and CO_2 Concentrations

For headspace gas analysis, guava from each treatment was placed in an individual airtight plastic container which was sealed for 2 hours just before measurement. This was to allow for equilibration of gases. The container was previously flushed with nitrogen gas within 1 minute to remove traces of O_2. The percentage concentrations of CO_2 and O_2 in the headspace of the containers were recorded using a gas analyser (MOCON Headspace Analyser, Minneapolis, USA). Three fruits per treatment were used in the analysis.

Determination of Physical Appearance

The appearance of guavas was observed and recorded using a digital camera of 12.8 megapixel (Sony, Tokyo, Japan) with the distance of 30cm from the sample. The appearance was observed at day 0, 1, 5, 7 14 and 21.

Statistical Analysis

Mean values and standard deviations were obtained using the GLM procedure in SAS Software (Release 9.0, SAS Institute Inc., Cary, NC, 2002). Significantly ($p<0.05$) different means were separated using Duncan's multiple range tests.

III. RESULTS AND DISCUSSION

Palm Stearin and Palm Kernel Olein Blends Properties

Fatty Acid Composition (FAC)

The fatty acid composition of the blends is presented in Table 3.2. The major fatty acid in PS was palmitic while the major fatty acid in PKOo was lauric acid. More palmitic acid adds hardness to blends while lauric give soft effect to the blends. However, when PS was blended with PKOo, the palmitic acid increased while lauric acid decreased with increasing PS. The major saturated fatty acids in PSPKOo blend of

Triacylglycerol (TAG) Profiles

Table 3 shows the TAG profile of different types of PSPKOo blends. The identification of the TAG peaks of the blends is based on the TAG standards. Main TAG in PS were POP, PPP and POO while in PKOo were LaLaLa, LaLaM and CaLaLa (Noor Lida et al., 2002; Bangun, 2009). In total, 4 major TAGs were detected in the PSPKOo blends namely CLaLa, CaLaLa, LaLaLa and LaLaM, whereby M, L, La, O, P and S represent myristic acid, linoleic acid, lauric acid, oleic acid, palmitic acid and stearic acid, respectively. Increasing the concentration of PS in the blends was found to significantly decrease TAGs, such as CLaLa, CaLaLa, LaLaLa, LaLaM, LaLaO, LaLaP and LaOM but increased OLL, PLL, MLP, OLO, PLO, PLP, OOO, POO, POP, PPP, SOO, POS, PPS and SOS.

Table 2:
Fatty Acid (%) Composition and Iodine Value (IV) of PSPKOo Blends.

PS: PKOo	Caproic (6:0)	Caprylic (8:0)	Capric (10:0)	Lauric (12:0)	Myristic (14:0)	Palmitic (16:0)	Stearic (18:0)	Oleic (18:1)	Linoleic (18:2)	SFA	USFA	IV
0:100	0.30±0.03^A	4.50±0.03^A	3.40±0.05^A	44.00±1.40^A	14.31±0.02^A	9.00±0.03^G	2.00±0.01^E	19.00±0.13^D	3.49±0.04^E	77.51^G	22.49^A	23.00±0.02^A
20:80	0.27±0.01^A	2.71±0.50^B	3.17±0.40^A	43.31±4.52^A	11.14±2.19^B	12.07±0.09^F	3.25±0.06^D	20.00±0.27^D	4.08±0.03^D	75.92^F	24.08^B	25.35±0.04^B
40:60	0.16±0.01^B	2.48±0.13^B	2.33±0.32^B	37.56±2.30^B	10.66±1.99^B	16.49±0.08^E	4.66±0.08^C	21.51±1.04^C	4.15±0.00^D	74.34^E	25.66^C	26.84±0.01^B
50:50	0.15±0.04^{BC}	2.31±0.13^B	2.16±0.04^B	27.43±2.69^C	9.76±2.45^C	25.13±0.33^D	5.68±0.06^C	22.14±0.09^C	5.24±0.10^C	72.62^D	27.38^D	29.47±0.01^C
60:40	0.12±0.01^{BC}	1.56±0.07^C	1.37±0.04^C	17.97±0.34^D	7.61±0.29^D	33.83±2.84^C	6.44±0.18^B	24.71±1.16^B	6.39±0.01^B	68.90^C	31.10^E	33.78±0.01^D
80:20	0.10±0.02^C	0.8±0.28^D	1.00±0.14^C	5.46±3.38^E	5.96±0.75^E	45.94±0.78^B	7.51±0.51^B	25.38±0.49^B	7.85±0.03^A	66.77^B	33.23^F	37.02±0.02^E
100:0	-	-	-	0.19±0.01^F	1.20±0.08^F	49.97±1.23^A	12.29±1.21^A	28.10±0.09^A	8.35±0.03^A	63.65^A	36.45^G	40.27±0.02^F

Note: Means with same capital letters down the columns were not significantly different (p>0.05). Means±SD were from triplicate measurements.
*SFA = saturated fatty acid, USFA = unsaturated fatty acid.

Table 3:
Triacylglycerol of PSPKOo Blends.

PS/PKOo	CLa La	CaLa La	LaLa La	La-LaM	LaLa O	LaLa P	La-OM	OLL	PLL	MLP	OLO	PLO	PLP	OOO	POO	POP	PPP	SOO	POS	PPS	SOS
0:100	9.89[A]	12.50[A]	23.31[A]	16.07[A]	8.04[A]	8.83[A]	6.94[A]	0.01[D]	0.09[F]	0.06[D]	0.22[E]	1.37[F]	2.05[F]	0.20[E]	2.60[G]	4.68[G]	2.37[G]	0.40[E]	0.38[G]	0.02[F]	0.08[B]
20:80	8.66[B]	10.55[B]	21.51[B]	12.50[B]	7.64[B]	7.66[B]	6.32[B]	0.08[C]	0.18[E]	0.07[D]	0.33[D]	1.38[F]	3.39[E]	0.49[D]	4.90[F]	7.33[F]	5.15[F]	0.45[E]	0.58[F]	1.02[E]	0.08[B]
40:60	7.23[C]	9.25[C]	20.96[C]	9.75[C]	5.75[C]	6.78[C]	5.13[C]	0.12[C]	0.22[E]	0.14[C]	0.73[C]	2.83[E]	4.45[D]	1.08[C]	8.09[E]	8.77[E]	5.85[E]	0.78[D]	1.12[E]	1.05[E]	0.08[B]
50:50	6.37[D]	9.19[D]	19.39[D]	9.33[D]	4.87[D]	5.65[D]	4.83[D]	0.14[B C]	0.32[D]	0.19[B C]	0.84[B]	3.13[D]	5.51[C]	1.13[C]	8.99[D]	9.77[D]	5.97[D]	0.86[D]	1.34[D]	2.05[D]	0.11[B]
60:40	5.61[E]	6.48[E]	18.32[E]	7.93[E]	4.57[E]	4.14[E]	4.04[E]	0.16[B C]	0.50[C]	0.21[B]	0.95[A]	3.90[C]	6.57[C]	1.19[B]	11.37[C]	11.16[C]	6.88[C]	0.98[C]	1.83[C]	3.05[C]	0.15[B]
80:20	4.14[F]	6.20[F]	14.85[F]	5.43[F]	3.32[F]	3.27[F]	2.37[F]	0.19[B]	0.60[B]	0.24[B]	0.97[A]	5.25[B]	7.60[B]	1.20[B]	13.94[B]	14.51[B]	8.38[B]	1.33[B]	2.11[B]	4.07[B]	0.15[B]
100:0	-	-	-	-	-	-	-	0.26[A]	0.73[A]	0.34[A]	0.99[A]	5.41[A]	7.71[A]	1.97[A]	15.53[A]	30.43[A]	23.41[A]	1.62[A]	5.78[A]	5.14[A]	0.72[A]

Note: Means with the same capital letters down the columns were not significantly different (p>0.05). Means±SD were from triplicate measurements. N.D is not detected. C: capric, Ca: caprylic, M: myristic acid, L: linoleic acid, La: lauric acid, O: oleic acid, P: palmitic acid and S: stearic acid.

behaviour of the fats studied. No significant increase in SMP when 40 to 50% PS was added into the blends. This related to finding in the Table 3 which shows that around that range there were no difference for unsaturated fatty acid such as caproic, caprylic and capric even 50% PS was added.

Slip Melting Point (SMP)

Slip melting point is defined as a temperature at which melting of fat starts (AOCS, 1993; Onyeka, Onuegbu, Onuoha, and Ochonogor, 2005). Blending of PS with PKOo altered the SMP of the fats. Figure 1 shows that inclusion of PS in the blend significantly elevated the SMP of fat blends. The SMP of the PSPKOo blends increased by 42.33, 43.33, 44.89 and 49.33% with the increases of 20, 40, 60 and 80% of palm stearin, respectively.

The SMP increased with an increase in the amount of PS in the blends due to the presence of high amount of high-melting TAGs, such as POP, PPP, and PPS in palm stearin as indicated in Table 4. The addition of 40% PS slowed the increasing of SMP in the blend. Blend with 80% of PKOo had SMP below body temperature. In the present study, data on SMP of the fat blends was necessary to provide information on the melting
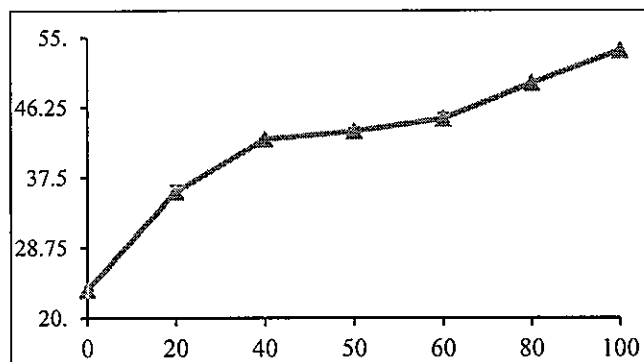
Figure 1: Slip Melting Point of PSPKOo Blends. Means±SD Were From Triplicate Measurements.

Solid Fat Content (SFC)

Figure 3 shows the SFC profiles of the PSPKOo blends as a function of temperature ranging from 5 to 55°C. The SFC increased with increasing amounts of PS in the blends. Generally, the SFC of PSPKOo blends were completely melted at 55°C. Addition of PKOo to PS lowered the SFC at all measured temperatures. The largest decline in SMP occurred at the temperature of 15 to 20°C for most of the blend. This is due to a large proportion of the TAGs liquefying and solubilising in this temperature range. The SFC of blend with 20% PS melted closed to body temperature helps to prevent gritty and waxy taste in the mouth. This was due to the presence of high amount of low and medium melting triacylglycerol such as CLaLa, CaLaLa, LaLaLa and LaLaM in the blend (Table 3).
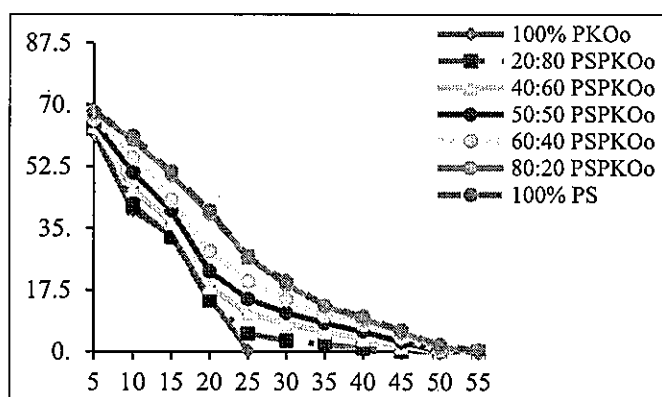
Figure 3: Percentage SFC as a Function of Temperature for PSPKOo Blends.

Iodine Value (IV)

The IV is a measure of the degree unsaturation of fat and oil. It is one of the most important parameters for measuring the quality of olein (Mamat, Nor Aini, Said, and Jamaludin, 2005). This study has shown that the IV increased significantly ($p<0.05$) with the increase of PS content and vice versa (Table 3). This might be due to the fact that PS contained higher level of unsaturated fatty acid (36.45%) than PKOo (22.49%). Palm stearin has long chain fatty acid while PKOo has short chain fatty acid. Long chain of carbon resulted as solid and single carbon atom.

Crystal Polymorphism by X-ray Diffraction

The structure, composition and polymorphic forms of fat crystal are the most important criteria for the functional properties of fats and oil. Usually ß' form is preferred in fat as it is structurally stable and maintains small to moderate crystal sizes allowing for smooth products. Simple blending had a limitation to maximize ß' crystal. The ß form exists in either a double or triple chain length configuration and orients in a more dense orthorhombic subcell structure characterised by X-ray short spacing at 3.8 and 4.2 Å.

Table 4 shows the the polymorphic forms of PSPKOo blends as determined by XRD. The PS contains 10–32% of tripalmitin, depending on the fractionation conditions. Tripalmitin is beta-tending triglyceride and has the highest melting point. The PKOo consists exclusively of the ß' crystalline form due to the presence of fatty acid of various chain lengths.

Table 3:
Polymorphic Forms of PSPKOo Blend by X-Ray Diffraction (XRD) Spectrometry.

PS:PKOo blends	Polymorphic form
0:100	β'
20:40	ß' + β
40:60	ß' + β
50:50	ß' + β
60:40	ß' + β
80:20	ß' + β
100:0	ß

The result shows that blending of PS with PKOo tempered at 20°C caused a polymorphic transition ß to mixture of ß' and ß.

These results agreed with what was reported by Timms (1990) and Norizzah et al. (2004) that PS and PKOo blend lead to mixture of ß +

ß' crystal. In coating formulation, the objective of blending is to obtain most of the fat crystals to be stabilised in the ß' polymorph.

Effect of PSPKOo Coating on Guavas

Weight Loss

Figure 4 shows that coating guavas with PSPKOo blends could slow the weight loss until day 21 of storage (20°C) as compared to uncoated fruits. Generally for all samples, the highest weight loss occurred from day 14 to 21. The guavas coated with 1:1 PSPKOo blend showed the lowest (p<0.05) weight loss with 18.41% followed by 3:2, 4:1, 2:3 and 1:4 PSPKOo blend.
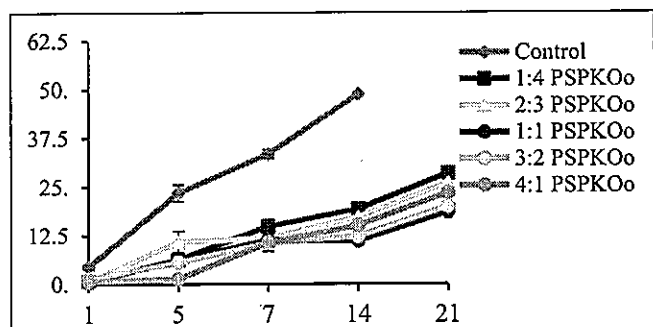
Figure 4: Weight Loss of Guava Coated With PSPKOo Blends. Means±SD Were From Triplicate Measurements.

The weight loss were 19.93, 23.34, 25.88 and 28.35% for 3:2, 4:1, 2:3 and 1:4 PSPKOo blend respectively, at day 21 of storage at ambient temperature (20°C). The control fruit however had significantly higher (p<0.05) weight loss (49%) at day 14 of storage and the fruit was spoiled. The reduction of weight loss is due to the hydrophobic nature of coating substances which were capable of forming a water-impervious structure and reduced efficiently the water transfer (Bourlieu et al., 2008).

Respiratory Gases Exchange

The oxygen (O_2) concentration decreased (Figure 3.5a) while the carbon dioxide (CO_2) concentration increased (Figure 3.5b) during storage of both coated and non-coated guavas due to the ripening genes which resulted in softening. The 1:1 and 3:2 PSPKOo blends were the most effective in lowering loss of respiration gases escaping from the internal tissue with 11.27% and 12.40% for O_2 at day 21, respectively. For CO_2, there were no difference between 1:1 and 3:2 PSPKOo blend and these two blends were most efficient in slowing the gases out from fruits. Ghosh, Jana, Ray, and Adhikar (2004) reported that the functional properties of lipid-based edible films partially explained by the lipid nature (polarity) and structure, but these parameters were always studied independently. The most hydrophobic lipids have the best barrier efficiency. Generally in this study, the PSPKOo coating blend with more than 20% PS (2:3, 1:1 and 3: 2) decreased the loss of O_2 and CO_2. Coating with higher than 60% PS (4:1) would become more brittle, which resulted in a high respiration for guava. The control and 20% (1:4) PSPKOo blend showed the highest respiration gases which lead to poor physical appearance.
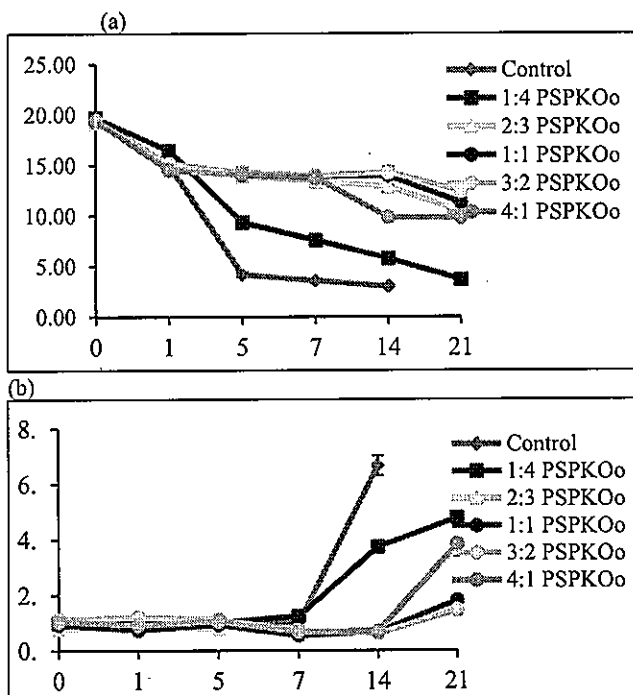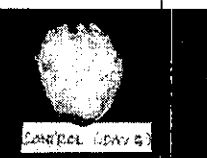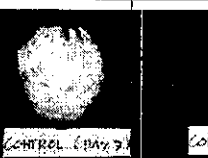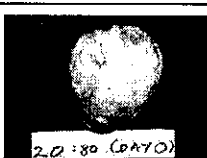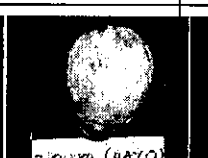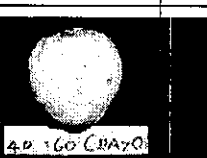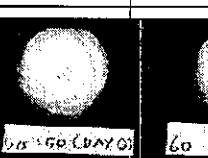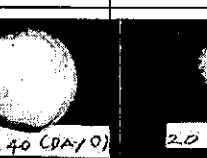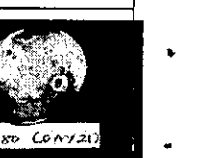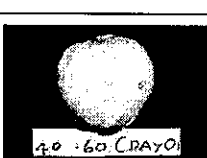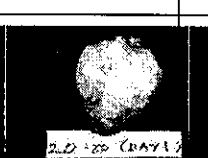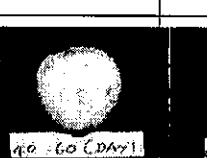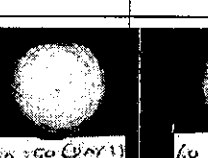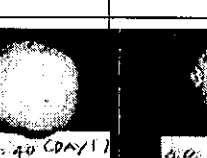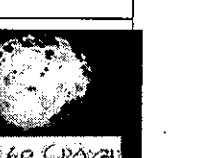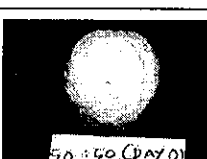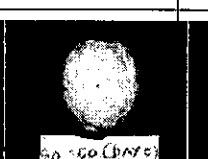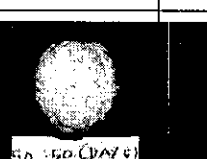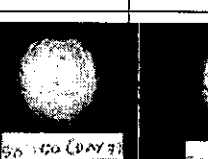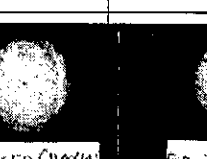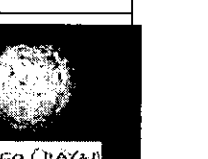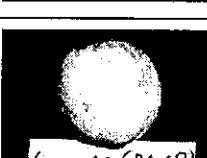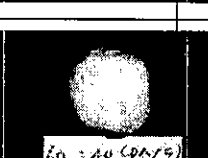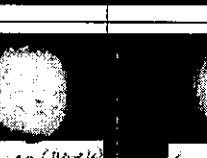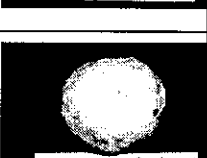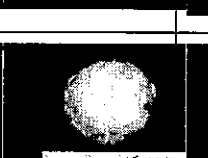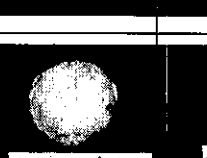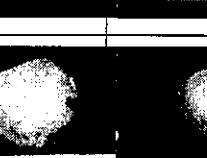

Figure 5: (a) Percent Oxygen and (b) Carbon Dioxide Concentrations in Control and Coated Guava. Means±SD Were From Triplicate Measurements.

Physical Appearance

Physical appearance is one of the most important criteria for consumer attraction. Pictures for guava coated with different PSPKOo blends showed that solid fat influenced the appearance of the fruits. At day 7 of storage, control and 4:1 PSPKOo coated guavas were observed to be soft and mouldy black spot

IV. CONCLUSIONS

Increasing the concentration of PS in the blends caused a gradual increase of the total of palmitic acid, while oleic acid gradually increased with the increasing content of PS. Increasing the concentration of PS in the blends was found to decrease TAGs, such as CLaLa, CaLaLa, LaLaLa, LaLaM, LaLaO, LaLaP and LaOM. The SMP increased with an increase in the amount of PS in the blends due to the presence of increasing amounts of high-melting TAGs, such as POP, PPP, POS and PPS in palm stearin.

PSPKOo blends	Day 0	Day 1	Day 5	Day 7	Day 14	Day 21
Control						
1:4						
2:3						
1:1						
3:2						
4:1						

Generally, the slip melting point (SMP) of PSPKOo blends was completely melted at 55°C. Blending of PKOo with PS resulted in blend with mixture of ß + ß' forms. Addition of PKOo into PS has overcome the high melting point of PS then lead to suitable coating for fruits. The guavas coated with 1:1 PSPKOo blend showed the lowest (p<0.05) weight loss with 18.41% followed by 3:2, 4:1, 2:3 and 1:4 PSPKOo blend. The 1:1 and 3:2 PSPKOo blends were the most effective in lowering weight loss while there were no different within the same formulations for CO_2. The 3:2 PSPKOo coating blend showed the best appearance for guava stored at 21 days. Therefore, 3:2 (60% PS) PSPKOo was chosen for further research due to better appearance of guava obtained.

V. ACKNOWLEDGEMENT

VI. REFERENCES

AOCS. (1993). *American Oil Chemist's Society (A.O.C.S) : Official methods and recommended practice at the American Oil Chemist Society 5th edn. Champain A.O.A.C.* (pp. 951-957). Oils and fats Official Analytical Chemists. Washington: AOAC.

Bangun, P. N. (2009). Physicochemical properties of palm stearin and mid fraction obtained by dry fractionation, AGRITECH, 29. 154-158

Bourlieu, C., Guillard, V., Vallès-Pamiès, B., Gontard, N. (2008). Edible moisture barriers for food product stabilization. New York: Springer.

Bourlieu, C., Guillard, V., Ferreira, M., Powell, H., Vallès-Pàmies, B., Guilbert, S., et al. (2010). Effect cooling rate on the structural and moisture barrier properties of high and low melting point fats. *Journal of American Oil and Chemist Society, 87*, 133-145.

Cocero, M. J., Martín, Ángel, M., Mattea, F., & Varona, S. (2009). Enapsulation and co-precipitation process with supercritical fluids: Fundamental and applications. *Journal of Supercritical Fluids, 47,* 46-555.

da Silva, C. R., Soares, D. F., Lourenço, M. B., Soares, F. A. S. M., da Silva, K. G., Gonçalves, M, I., et al. (2010). Structured lipids obtained by chemical interesterification of olive oil and palm stearin. *LWT-Food Science and Technology, 43,* 752-758.

D'Souza, V., deMan, L., & deMan, J. M. (1991). Chemical and physical properties of the high melting glyceride fractions of commercial margarine. *Journal of American Oil Chemist Society, 68,* 153-162.

Díaz Gamboa, O., Gioielli, L. A. (2003). Consistencia de lípidos estructurados a partir de aceite de pescado y grasa de palmiste. *Grasas y Aceites, 54,* 122-129.

Ghosh, R. N., Jana, T., Ray, B. C., & Adhikar. (2004). Grafting of vinyl acetate onto low density polyethylene-starch biodegradable films for printing and packaging applications. *Polymer International, 53,* 339-34.

Lerdthanangkul, S., & Krochta, J. M. (1996). Edible coating effects on postharvest quality of green bell peppers. *Journal of Food Science, 61,* 176–179.

Mamat, H., Nor Aini, I., Said, M., & Jamaludin, R. (2005). Physicochemical characteristics of palm oil and sunflower oil blends fractionated at different temperatures. *Food Chemistry, 91,* 731-736.

Martin-Polo, M., Mauguin, C., & Voilley, A. (1992). Hydrophobic films and their efficiency against moisture transfer. 1. Influence of the film preparation technique. *Journal of Agricultural and Food Chemistry, 40,* 407-412.

MPOB Test Method, (2004). A compendium of tests on palm oil products, palm kernel products, fatty acids, food-related products and others. Bangi: Malaysian Palm oil Board.

Noor Lida, H. M. D., Sundram, K., Aminah, A., & Mamot, S. (2002). TAG composition and solid fat content of palm oil, sunflower oil, and palm kernel olein blends before and after chemical interesterification. *Journal of the American Oil Chemists' Society (JAOCS), 79,* 1137-44.

Norizzah, A. R., Chong, C. L., Cheow, C. S., & Zaliha, O. (2004). Effects of chemical interesterification on physicochemical properties of palm stearin and palm kernel olein blends. *Food Chemistry, 86,* 229–235.

Onyeka, E. U., Onuegbu, N., Onuoha, N. U., & Ochonogor, F. (2005). Effect of extraction pretreatment on the composition and characteristics of seed and pulp oil of African black pear *(Dacryodes edulis). Nigerian Food Journal, 23,* 13-20.

Shen, C. F., DeMan, L., & DeMan, J. M. (1990). Effect of palm stearin and hydrogenated palm oil on the polymorphic stability of hydrogenated canola oil. *Elaeis, 2,* 143-157.

Timms, R. E. (1990). In Berger, K. G. (Ed.), *Crystallization behaviour of palm oil. Symposium proceedings: Development in palm oil.* (pp. 38–44.). Kuala Lumpur : Palm Oil Research Institute of Malaysia.

Prevalence and Risk Factors Associated With Nutrition Related Non-Communicable Diseases In a Cohort of Males in the Central Province of Sri Lanka

N.W.I.A. Jayawardana, W.A.T.A. Jayalath, W.M.T. Madhujith, U. Ralapanawa, R. S. Jayasekera, S.A.S.B. Alagiyawanna, A.M.K.R. Bandara, N.S. Kalupahana

Abstract - There is mounting evidence to the effect that dietary and lifestyle changes affect the incidence of non-communicable diseases (NCDs). This study was conducted to investigate the association of diet, physical activity, smoking, alcohol consumption and duration of sleep with overweight, obesity, hypertension and diabetes in a cohort of males from the Central Province of Sri Lanka. A total of 2694 individuals aged between 17 – 68 years (Mean = 31) were included in the study. Body Mass Index cutoff values for Asians were used to categorize the participants as normal, overweight and obese. The dietary data were collected using a food frequency questionnaire [FFQ] and data on the level of physical activity, smoking, alcohol consumption and sleeping hours were obtained using a self-administered validated questionnaire. Systolic and diastolic blood pressure, random blood glucose level were measured to determine the incidence of hypertension and diabetes. Among the individuals, the prevalence of overweight and obesity were 34% and 16.4% respectively. Approximately 37% of the participants suffered from hypertension. Overweight and obesity were associated with older age men ($P<0.0001$), frequency of smoking ($P=0.0434$), alcohol consumption level *($P=0.0287$)* and the quantity of lipid intake ($P=0.0081$). Consumption of fish ($P=0.6983$) and salty snacks ($P=0.8327$), sleeping hours ($P=0.6847$) and the level of physical activity were not significantly *($P=0.3301$)* associated with the incidence of overweight and obesity. Based on the fitted model, only age was significantly associated with hypertension ($P<0.001$). Further, age ($P< 0.0001$), sleeping hours ($P=0.0953$) and consumption of fatty foods ($P=0.0930$) were significantly associated with diabetes. Age was associated with higher odds of pre diabetes (OR:1.089;95% CI:1.053,1.127) and diabetes (OR:1.077;95% CI:1.055,1.1) whereas 7-8 hr of sleep per day was associated with lesser odds of diabetes (OR:0.403;95% CI:0.184,0.884). High prevalence of overweight, obesity and hypertension in working-age males is a threatening sign for this area. As this population ages in the future and urbanization continues, the prevalence of above risk factors will likely to escalate.

Keywords – Age, Males, Non-communicable diseases, obesity

Effects of Food Habits on Road Accidents Due to Micro-Sleepiness and Analysis of Attitudes to Develop a Food Product as a Preventive Measure

Rumesh Liyanage, S.B. Nawaratne, K.K.D.S. Ranaweera, Indira Wickramasinghe, K.G.S.C. Katukurunda

Abstract— Study it was attempted to identify effect of food habits and publics' attitudes on micro-sleepiness and preventive measures to develop a food product to combat. Statistical data pertaining to road accidents were collected from, Sri Lanka Police Traffic Division and a pre tested questionnaire was used to collect data from 250 respondents. They were selected representing drivers (especially highway drivers), private and public sector workers (shift based) and cramming students (university and school). Questionnaires were directed to fill independently and personally and collected data were analyzed statistically. Results revealed that 76.84, 96.39 and 80.93% out of total respondents consumed rice for all three meals which leads to ingest higher glycemic meals. Taking two hyper glycemic meals before 14.00h was identified as a cause of micro-sleepiness within these respondents. Peak level of road accidents were observed at 14.00 - 20.00h (38.2%)and intensity of micro-sleepiness falls at the same time period (37.36%) while 14.00 to 16.00h was the peak time, 16.00 to 18.00h was the least; again 18.00 to 20.00h it reappears slightly. Even though respondents of the survey expressed that peak hours of micro- sleepiness is 14.00-16.00h, according to police reports, peak hours fall in between 18.00-20.00h. Out of the interviewees, 69.27% strongly wanted to avoid micro-sleepiness and intend to spend LKR 10-20 on a commercial product to combat micro sleepiness. As age-old practices to suppress micro-sleepiness are time taken, modern day respondents (51.64%) like to have a quick solution through a drink. Therefore, food habits of morning and noon may cause for micro- sleepiness while dinner may cause for both, natural and micro-sleepiness due to heavy glycemic load of food. According to the study micro-sleepiness can be categorized in to three zones such as low-risk zone (08.00-10.00h and 18.00-20.00h), manageable zone (10.00-12.00h), and high- risk zone (14.00-16.00h).

Keywords— Micro-sleepiness, Food habits, Road accidents, Glycemic Load

I. INTRODUCTION

MICRO sleepiness is a temporary biological disorder, which has been a major cause of road accidents leading to physical injuries, deaths, disabilities, numbness and economic losses. Traffic accidents due to human errors cause many deaths and injuries all around the world. Especially the sleepiness simply feels after taking meals because body should gain more energy for food digestion and ultimately it may convert into micro-sleepiness, which last about 1-30 seconds. The dietary habits of a person may strongly accompanied with this biological phenomenon cause for half or full eye shutting unintentionally and wake up with unconscious mood. Also the micro- sleepiness is the main factor for sleepiness in drivers and cause one in four fatal accidents on highways.

A considerable fraction of the population does not consume a balanced diet (Jayewardena et al, 2012). Total mean carbohydrate, protein and fat intakes of Sri Lankan adults are approximately 304.4, 44.6 and 35 g and 71.2, 10.8 and 18.9% from total energy generated respectively (Jayewardena et al, 2014). Sri Lankans ingest numbers of starch sources and consume them for lunch or dinner by limiting themselves to three meals per day (Jayewardena et al, 2012). Almost 65% consumed well beyond the upper level of the references and this is principally due to the average person's meal containing three-quarters of rice with lesser amount of vegetable curry (15g), piece of meat or fish (15g) and some starchy curry as potato or dhal (Jayewardena et al, 2012). Incorporation of these types of higher glycemic loads with stresses and tiredness may eventually leads the brain towards the micro sleepiness.

The overall objective of this study was to evaluate the effect of food habits and attitudes of public on micro-sleepiness and

Rumesh Liyanage, Department of Food Science and Technology, University of Sri Jayewardenepura, Gangodawila, Nugegoda, Sri Lanka. phone:+94712958480;fax:+942802914;e-mail: rumeshprasanga@gmail.com).

S. B. Nawaratne, Department of Food Science and Technology, University of Sri Jayewardenepura, Gangodawila, Nugegoda, Sri Lanka. (e-mail: sbnawa123@yahoo.com).

K.K.D.S. Ranaweera, Director, Bandaranayake Memorial Ayurvedic Research Center Nawinna, Maharagama, Sri Lanka. (e-mail: kkdsran@yahoo.com).

Indira Wickramasinghe, Department of Food Science and Technology, University of Sri Jayewardenepura, Gangodawila, Nugegoda, Sri Lanka. (e-mail: indiraw2002@yahoo.com).

K.G.S.C.Katukurunda, Department of Food Science and Technology, University of Sri Jayewardenepura, Gangodawila, Nugegoda, Sri Lanka. (e-mail: shanakakatukurunda@gmail.com).

preventive measures with a view to develop a food product.

II. METHODOLOGY

A. Preliminary Survey

Preliminary survey was carried out to gather information on food habits and attitudes of micro- sleepiness with a pre-designed questionaries' from 250 respondents. Respondents were selected representing drivers (especially highway drivers), private and public sector workers (shift based) and cramming students (university and school). Questionnaires were directed to fill independently and personally and collected data were analyzed statistically.

B. Data Collection Pertaining To the Road Accidents.

Statistics on road accidents in Sri Lanka were collected from statistical unit of Sri Lanka Police Traffic Division, for the last ten years. And collected information were analyzed statistically.

C. Data analysis.

Collected data ware analyzed through MS Excel and Excel-stat statistical programs with a view to identify peak hours of accident occurring under Sri Lankan context.

III. RESULTS AND DISCUSSION

The occurrence of micro sleepiness of respondents were shown in Fig 1 (a) and the number of road accidents due to sleepiness in Sri Lanka is shown in fig 1 (b). Both graphs show a similar dispersion pattern. As per the graph 1 (b), large number of road accidents were occurring in between 14.00h to 20.00h (38.2%), also the highest of accidents happen in between 16.00h to 18.00h (13.43%) for last nine years (Sri Lanka Police Statistical Unit, 2015). Figure 1 (a) clearly indicates the peak intensity of micro sleepiness is occurring at 14.00-16.00h (37.36%) as a gradual increase from 10.00-16.00h and thereafter a decrease from 16.00 to 18.00h again with a slight increase from 18.00h to 20.00h. According to literature, micro-sleep is lasted for a short time due to higher glycemic load from both breakfast and lunch. This finding was further validated by the statistics of Sri Lanka Police Traffic Records, which also cited danger hours for accidents are in between 14.00h to 20.00h. Therefore, there is a strong positive co relationship between micro sleepiness and road accidents. Moreover critical hours for road accidents due to micro-sleepiness is in between 16.00h to 18.00h, reasons for these consequences are mental stress after office work, traffic jams, weather, personal matters, body itself may inadvertently tend to relax in the vehicle itself and may also cumulative influence of all of these factors
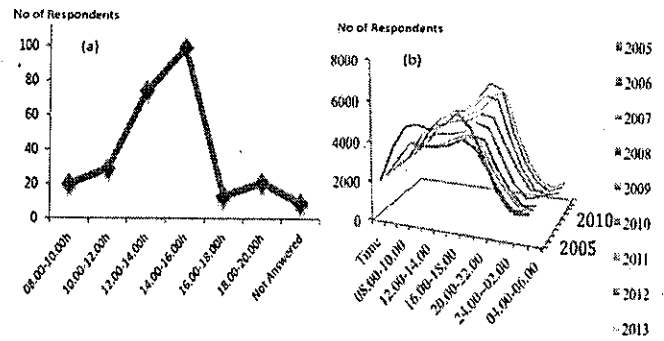

Fig 1 (a). Occurrence of Micro sleepiness of respondents (b) Number of road accidents due to sleepiness in Sri Lanka

Nevertheless the graph reveals that micro sleepiness does not become zero and it may prevail throughout the day. However human body is capable to suppress it (micro sleep) during other hours other than micro sleep hours as a result of different types of physical and mental activities. Figure 2 represents the food habits of respondents. Survey results revealed that 76.84, 96.39 and 80.93% out of total respondents consumed rice for breakfast, lunch and dinner. Since Glycemic Load (GL) of the lunch is very high, the body requires more energy to digest it. Under this condition, the person unintentionally tend to relaxations. During relaxation process of human, the metabolic activities of body are lowered and as a result of that micro-sleepiness is beginning. Therefore avoiding heavy meals with high glycemic load is advisable. Grain consumption for all 3 meals was 8.86, 1.03 and 2.06%. Trend of consuming of instant and other foods as kottu, parata etc. at dinner was observed (13.4 and 14.95%) secondly to rice. There were respondents who having no food for a single meal because of their duty shifts and many other reasons. Having two heavy glycemic meals (breakfast and lunch) before 14.00h may be a reason for micro sleepiness and occurring of accidents at that time. Since micro sleep has other numerous reasons as extreme tiredness, mental stress, traffic jams, weather conditions, personal matters and loss of proper sleep other than the higher glycemic load, this multi factorial scenario must be appropriately explored with further research.
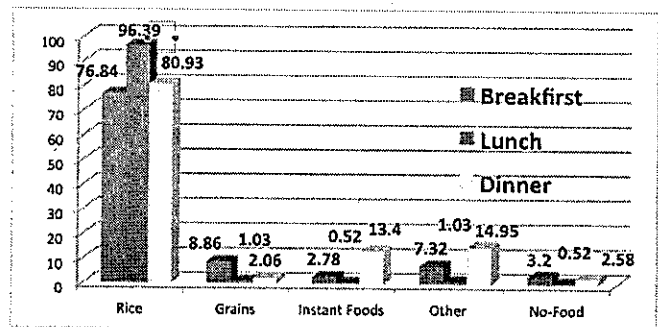

Fig 2: Food habits of respondents

When considering about the opinions of respondents regarding control of micro sleepiness, taking naps (28.95%), wash their face or/and bathing (28.07%), bite chewable food

products such as bubblegum and chew-betel(15.35%), smoke and/or take alcohol (2.19%), chewing sweet foods and toffees (9.65%) and application of ointments (0.88%) were seen respectively. Using of water (36.86%), tea (27.97%), coffee (19.25%), soft drinks (2.21%), energy drinks (6.36%) and sour drinks (1.27%) as productive solutions seen because of the belief of these drinks are capable to suppress, micro-sleepiness into a greater extent. Moreover, medical research has revealed that caffeine in coffee and tea is the active agent which can suppress micro sleepiness and sour taste substances can refresh the nerve system of the respondent.

Considering about attitudes regarding necessity and product portfolio to combat micro-sleepiness 69.27% of the respondents is willing to suppress micro-sleepiness in order to avoid negative consequences as accidents, lethargic attitudes, drowsiness, apathy etc. However 21.43% of respondents expressed lack of interest to control micro-sleepiness. The types of the products which had respondent choice were beverage (51.64%), confectionary product like toffee (19.72%), chewable food products (13.62%), pills (2.82%) and ointments (2.82%). When considering about the expected price for the product respondents proposed LKR 10-24 (58.56%), 25-39 (16.94%), 40-54 (14.9%), 55-69 (6.18%), 70-84 (2.04%) and more than LKR 85 (1.38%) respectively.

IV. CONCLUSSIONS

Food habits of public is largely responsible for micro-sleepiness, especially after taking heavy meals. Micro-sleepiness can be happen all over the day and it may especially highest in 14.00- 16.00h. However, most of respondents are willing to have a product with an affordable price along with plant based ingredients in different formulations such as in drinking, chewable, licking and ointments modes.

REFERENCES

[1] Jayawardena R, Thennakoon S, Byrne N, Soares M, Katulanda P, Hills A, 2014, "Energy and nutrient intakes among Sri Lankan adult", Int Arch Med. 2014; 7: 34.

[2] Jayawardena R, Thennakoon S, Byrne N, Soares M, Katulanda P, Hills A, "Food consumption of Sri Lankan adults: an appraisal of serving characteristics", 2012, Public Health Nutrition: 16(4), 653–658

[3] Sri Lanka Police Traffic Division statistical reports on road accidents, 2015.

[4] Philip A, Hans P.A, Gerard A, *Human sleep and cognition part I: clinical and applied research*, 2011.

[5] Rivera M, Salas L, Monitoring of micro sleep and sleepiness for the drivers using EEG signals, 2013.

[6] National Highway Traffic Safety Administration. U.S. Department of Transportation, November1994